Multi-TASTE Phase F

Multi-Mission Technical Assistance to ESA Validation by Sounders, Spectrometers and Radiometers

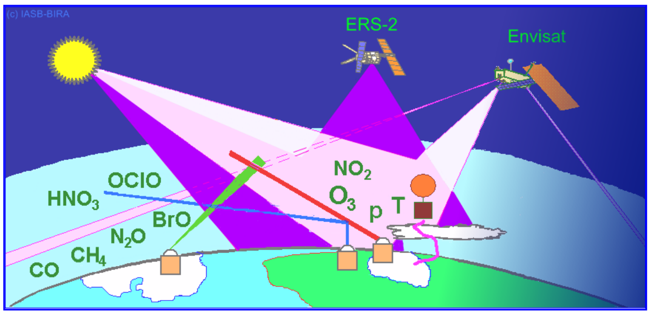

Validation report

MIPAS ORM 8.22 profiles of T, altitude, O_3, CH_4, HNO_3 and N_2O

authors | auteurs D. Hubert, A. Keppens, J. Granville and J.-C. Lambert (BIRA-IASB)

reference | référence TN-BIRA-IASB-MultiTASTE-Phase-F-MIPAS-ORM8-Iss1-RevB
date of issue | date d'édition 18 December 2020
issue | édition 1
revision | révision B
ESA contract Nr | contrat ESA No 4000112093/14/I/LG/CCN1

title | titre	Multi-TASTE Phase F Validation Report / Ground-based validation of MIPAS ESA operational products (ORM 8.22) : T, altitude, O3, CH3, HNO3 and N2O
reference | référence	TN-BIRA-IASB-MultiTASTE-Phase-F-MIPAS-ORM8-Iss1-RevB
date of issue | date d'édition	18 December 2020
issue | édition	1
revision | révision	B
status | état	Final
document type | type de document	Validation Report
ESA contract Nr | contrat ESA No	4000112093/14/I/LG/CCN1
prepared by | préparé par	D. Hubert, A. Keppens, J. Granville and J.-C. Lambert (BIRA-IASB)

document change record | historique du document

Issue	Rev.	Date	Section(s)	Description of Change
1	A	11.12.2020	all	First version
1	B	18.12.2020	all	Incorporation of comments by MIPAS QWG

Executive summary

This validation report has two objectives. The first is to document the quality of six primary ORM 8.22 Level-2 vertical profile data products for the entire MIPAS mission (July 2002 – April 2012). And secondly, to compare their quality to that of preceding operational processor chains. The validation results presented are consolidated and serve as feedback to the MIPAS Quality Working Group and to the users of MIPAS operational data products. Table 1 and the paragraphs below give an overview of our main observations and conclusions.

This report presents the results of detailed validation analyses of the operational MIPAS ORM 8.22 Level-2 data and compares these to results for earlier operational MIPAS processors (ML2PP 7.03, ML2PP 6.0 and IPF 5.05/5.06). The quality of six Level-2 data products (vertical profiles of temperature, altitude, O3, CH4, HNO3 and N2O) retrieved for the entire MIPAS mission (~35000 orbits) were evaluated through extensive comparison to correlative observations of reference collected from ground-based instruments certified for WMO's Global Atmosphere Watch (https://woudc.org) and contributing networks like NDACC (http://ndacc.org) and SHADOZ (https://tropo.gsfc.nasa.gov/shadoz). The list of reference instruments includes radiosondes, ozonesondes, stratospheric temperature and ozone lidars, ozone microwave radiometers and FTIR spectrometers.

Table 1 on the next page summarises our main observations and conclusions. **We conclude that the quality of all considered ORM 8.22 data products is at least as good if not better than the ML2PP 7.03 data release.** For a few products and in specific regions of the atmosphere the quality of V8 is worse for one or more indicators than for V7. These are exceptions, however, since most observed changes improve the agreement with ground-based reference measurements, in terms of bias or of dispersion of the comparisons, or their dependence on geophysical parameters (latitude, pressure, season, and year). **Most observed changes are consistent with what is anticipated from the changes in the operational Level-1 and Level-2 processors.**

Considerable improvements are found in the temperature product. Version 8 temperatures are generally warmer than V7 which leads to a better agreement with ground-based data. Also the temporal stability improved, even substantially. The long-term drift in the OR period (2005-2012) is reduced in the lower and middle stratosphere and it is less altitude-dependent. The amplitude of the seasonal cycle in the comparisons at least twice smaller than in earlier data releases, which improves the observed spread in the comparisons. The only degradation with respect to V7 is found in the UT/LS where the V8 data are cooler, resulting in a larger negative bias. Improvements in the temperature record lead to a **slightly improved altitude product**, although the agreement of V7 and reference data was already well within most user requirement. **The ozone profile record has a smaller bias in the tropical UT/LS and mid-latitude LS.** Version 8 ozone mixing ratios are smaller than for V7 which reduces the positive bias found across the stratosphere. Otherwise the temporal, vertical and latitudinal patterns are unchanged. Version 8 volume mixing ratios for CH4, HNO3 and N2O are generally a few percent larger than for V7, leading to a **smaller negative bias for the HNO3 product and larger positive biases for the CH4 and N2O products during the OR period.** The stability of the V8 data record is similar to that of V7 for HNO3 and N2O, and slightly better for CH4.

Table 1: Overview of the validation of operational MIPAS Level-1-to-2 processor ORM 8.22 (2002-2012 data) and changes relative to the previous operational processor ML2PP 7.03. The Full Resolution (FR) and Optimised Resolution (OR) measurement periods cover, respectively, 2002-2004 and 2005-2012. Layers in the atmosphere are abbreviated: upper troposphere (UT), lower/middle/upper stratosphere (LS/MS/US), lower mesosphere (LM).

	Correlative data sets	Coverage validation	Main conclusions V8 data quality	V8 changes relative to V7
Temperature (Sect. III.1)	• 85 radiosondes • 9 stratospheric T lidars	• Representative pseudo-global sample. • Troposphere up to lower mesosphere.	• Negative bias, about 0.5-1 K or more, dependent on pressure and latitude. • Dispersion 1-1.5 K in LS+MS and 3-4 K in LM. • FR/OR discrepancy: offsets of 0.5 K dependent on altitude; FR data usually more noisy than OR. • No or weak temporal bias patterns: peak-to-peak amplitude seasonal cycle less than 0.5-1 K; long-term drift at most +0.4 K/dec. during OR phase in LS+MS.	Overall reasonably similar in all indicators, with several improvements • V8 negative bias is 0.3-0.6 K smaller than for V7 in large part of atmosphere, but 0.9 K larger in UT/LS. • Substantially reduced annual cycle, this reduces the dispersion as well (by 0.2-0.5 K). • V8 drift changes in UTLS (by >+1.5 K/dec.) and in MS (by -0.5 K/dec.) clearly improving long-term stability.
Altitude (Sect. III.2)	85 radiosondes	• Representative pseudo-global sample. • Troposphere up to ~30 km.	• Bias < 50-100 m. • Dispersion < 50-100 m. • FR/OR discrepancy: FR data slightly more noisy. • No signs of temporal dependences (amplitude annual cycle < 50 m, long-term drift < 50 m/dec.)	V8 quality is quasi-identical yet slightly better than V7 due to its smaller annual cycle, dispersion and overall bias. Differences are almost negligible for most use cases.
O_3 (Sect. III.3)	• 85 ozonesondes • 12 stratospheric O_3 lidars • 4 O_3 MWRs	• Representative pseudo-global sample. • Troposphere up to lower mesosphere.	• Positive bias, about 5% in MS+US, +5-10% in LS. • Dispersion around 4-5% or better in MS and large part of US. • FR/OR discrepancy: bias differs by ~5% (FR ozone > OR in LS; FR ozone < OR in MS and US). • No clear temporal pattern in bias (seasonal cycle, long-term drift), except for an overestimated depletion of Antarctic ozone hole.	Overall within ~1-2% in all indicators, except for two regions • 5-10% reduction in bias for V8 in mid-latitude LS and tropical UT/LS. • 5% reduction in V8 dispersion in Antarctic LS during the FR period.
CH_4 (Sect. III.4)	9 FTIRs	• Representative sample in NH only • Between 9-60 km (3 subcols.)	• Positive bias, about 3-10 %. • Dispersion 2-10 % (below 30 km). • No clear difference between FR & OR phase.	• V8 bias a few % larger than for V7 in OR period, but 5-10 % smaller in FR period. • V8 drift smaller than the (statistically insignificant) 5 %/dec. negative drift found for V7.
HNO_3 (Sect. III.5)	9 FTIRs	• Representative sample in NH only • Between 12-30 km (1 subcol.)	• Negative bias, less than 5 %. • Dispersion 10 %. • Clear vertical and seasonal dependence of bias. • No significant long-term drift.	V8 has negative bias that is a few % smaller than V7 (which was 5-10 %).
N_2O (Sect. III.6)	8 FTIRs	• Representative sample in NH only • Between 9-30 km (2 subcols.)	• Positive bias, about 5-10 %. • Dispersion 5-10 %. • No clear difference between FR & OR phase. • No significant seasonal cycle or long-term drift.	V8 bias is a few % larger than for V7 in OR period, but a few % smaller than V7 in FR period.

Table of contents

Introduction

This document reports on the ground-based validation of the MIPAS operational Level-2 processor ORM 8.22. Six Level-2 profile data products (T, altitude, O3, CH4, HNO3 and N2O), retrieved for the entire mission, were evaluated through extensive comparison to correlative observations of reference collected from ground-based instruments certified for WMO's Global Atmosphere Watch and contributing networks like NDACC and SHADOZ (sonde, lidar, microwave radiometers and FTIR spectrometers). This work was requested by the MIPAS Quality Working Group (QWG) and ESA, and carried out by the validation team at BIRA-IASB in the frame of the TASTE MIPAS Phase-F project.

There are two main objectives of this report. The first is to report the quality of six primary ORM 8.22 Level-2 vertical profile data products for the entire MIPAS mission (Jul 2002 – Apr 2012). And secondly, to compare their quality to that of preceding operational processor chains. The validation results presented hereafter are consolidated and serve as feedback to the MIPAS QWG and to the users of MIPAS operational data products.

The structure of this document is as follows. Section I presents the MIPAS data sets under investigation, and is followed a description of the methodology of the different validation analyses (Sect. II). Section III contains concise evaluations of the geophysical data quality of each Level-2 product, differentiated by pressure and latitude where sensible and feasible. Specific attention is given to the evolution of ORM 8.22 relative to earlier MIPAS data releases. Each section concludes by a summary table. References and acronyms can be found in Sects. V and VI respectively. The concluding Appendix contains graphics that illustrate the evolution in data quality of operational MIPAS Level-1-to2 processors, complementing the material in Sect. III.

I MIPAS data sets

The quality of the Level-2 data products retrieved by the operational Level-1-to-2 processor ORM 8.22 is the main subject of this report. It is compared to that of earlier operational processor chains.

Level-2 processor	Input data (Level-1b)	Period	# orbits
ORM 8.22	IPF 8.03	Aug 2002 – Apr 2012	35060
ML2PP 7.03 (W)	IPF 7.11	Aug 2002 – Apr 2012	34929
ML2PP 6.0 (U)	IPF 5.05 & 5.06	Aug 2002 – Apr 2012	35043
IPF 5.05 (R) & 5.06 (R)	IPF 5.05 & 5.06	Aug 2002 – Apr 2012	34437

The Level-2 ORM 8.22 data set was retrieved from an updated Level-1 data set. So, changes in the Level-1 processor may impact Level-2 data quality, in addition to the algorithm changes in the Level-2 processor. More details on processor upgrades can be found in the respective Product Readme Files prepared by the MIPAS Quality Working Group.

Also, the Level-2 data format was completely revised and now follows the netCDF CF conventions, rendering the V8 data products more user-friendly than earlier MIPAS product versions. The validation results reported here were obtained from analyses of the simplified ORM 8.22 data products (filename identifier *_2PS_*). However, these results are applicable to the extended products (filename identifier *_2PE_*) as well since the simplified and extended products are identical in all primary variables.

Applicable documentation related to processor upgrades and data format changes is available at https://earth.esa.int/web/sppa/mission-performance/esa-missions/envisat/mipas/products-and-algorithms/products-information.

For the Level-1 processor

- *MIPAS Level 1B IPF 5.06 products Disclaimer*, ENVI-GSOP-EOGD-QD-11-105, issue 1.1, https://earth.esa.int/documents/700255/707722/MIP_NL_1P_Disclaimers.pdf/17ae8d2b-f1ee-49a8-ade3-1bda7a7c1d7c, 22 Jun 2011;
- *Product Quality Readme File for MIPAS Level 1b IPF 7.11 products*, ENVI-GSOP-EOPGD-QD-15-0130, issue 1.1, https://earth.esa.int/documents/700255/707722/RMF_0130+MIP_NL__1P_issue1.1_final.pdf, 23 Dec 2015;
- *Product Quality Readme File for MIPAS Level 1b IPF 8.03 products*, ESA-EOPG-EBA-TN-1, issue 1.1, https://earth.esa.int/documents/700255/3711375/Read_Me_File_MIP_NL__1PY_ESA-EOPG-EBA-TN-1+issue1.1.pdf/e989ac1e-83b5-485d-8e25-b208891d84bf, 8 Sep 2019;

and for the Level-2 processor

- *MIPAS Level 2 IPF 5.06 Readme*, ENVI-GSOP-EOGD-QD-11-0111, issue 2.0, https://envisat.esa.int/handbooks/availability/disclaimers/MIP_NL_2P_README_V5.pdf, 18 Oct 2011;
- *MIPAS Level 2 ML2PP Version 6 Readme*, ENVI-GSOP-EOGD-QD-12-0116, issue 1.1, https://earth.esa.int/documents/700255/707722/MIP_NL_2P_README_V6.0.pdf/1a6c6de8-35f3-400b-abd0-8ca8c0640453, 5 Jun 2012;
- *Product Quality Readme File for MIPAS Level 2 version 7.03 products*, ENVI-GSOP-EOGD-QD-16-0141, issue 1.0, https://earth.esa.int/documents/700255/2635669/RMF_0141+MIP_NL__2P_issue1.pdf/59beb833-5ad4-4301-8422-f41001da36d4, 7 Sep 2016;
- *Product Quality Readme File for MIPAS Level 2 version 8.2 products*, ESA-EOPG-EBA-TN-5, issue 1.0, 2020.

The first step in the Level-2 retrieval scheme is the simultaneous retrieval of the pressure and temperature profile (pT). This information is then used to retrieve, sequentially, the volume mixing ratio (VMR) profiles of the trace gases: first H2O, then O3, HNO3, CH4, N2O, etc… As a consequence, the quality of the trace gas profiles depends on the quality of the pT retrievals. And they can depend on the quality of previous trace gas retrieval(s) as well, if the latter contribute(s) to the radiance signal in the retrieval microwindows.

MIPAS observations have been carried out in several modes determined by the spectral and the spatial sampling of the instrument (Raspollini *et al.*, 2013). MIPAS was operated at full spectral resolution (FR) between June 2002 and March 2004, and in an optimised spectral resolution (OR) mode from January 2005 to April 2012. Besides its nominal vertical scan sequence (constituting >70% of measurements), alternative sequences were routinely active and focused either on UTLS, middle atmosphere, upper atmosphere, aircraft emissions and noctilucent clouds. Unless specified otherwise below, a distinction is made in the validation analyses between the FR and OR phase of the mission, but not for the different vertical scan modes.

In this report, shorter notations for the processor versions can be used: V5, V6, V7 and V8. These refer to the Level-2 processor.

II Validation methodology

II.1 Comparison to sonde, lidar and microwave radiometer

MIPAS temperature, altitude and ozone profile data from the latest operational processor (ORM 8.22) and earlier versions (ML2PP 7.03, ML2PP 6.0 and IPF 5.05/5.06) are compared to co-located observations by sonde (radiosonde, ozonesonde), lidar (Rayleigh temperature or DIAL ozone) or ozone microwave radiometer (MWR) instruments contributing to GAW and affiliated networks NDACC and SHADOZ. The correlative data records sample a variety of atmospheric regions and states from the Arctic to the Antarctic and from the ground up to the upper stratosphere or lower mesosphere.

Table 2, Table 3 and Table 4 summarise the adopted validation methodology for, respectively, vertical profiles of temperature, altitude and ozone. It is identical to that used in earlier Multi-TASTE reports (Hubert *et al.*, 2012, 2016bc) and was published in Hubert *et al.* (2016a). The three analysis set-ups differ in the use of absolute (T, altitude) rather than relative (O3) differences, or in the application of MIPAS vertical AK (T and O3) or not (altitude, MWR) to smoothen correlative profiles.

The smoothing of correlative profiles with MIPAS vertical AK can introduce artificial features if the raw data do not cover a sufficiently large part of the vertical AK distribution. This is typically the case at the top or bottom of the ground profile for ozone data. In addition, ozonesonde data are increasingly biased low towards the top of the profile (pressures smaller than ~15 hPa). As a result, MIPAS ozone minus sonde bias profiles will systematically tend to more positive values in this altitude range. This behaviour should hence not be interpreted as a feature in the MIPAS ozone data set.

Table 2: Validation methodology for temperature profiles.

1. Correlative data	NDACC/GAW/SHADOZ radiosonde and NDACC stratospheric T lidar; Troposphere to lower mesosphere
2. Data screening	MIPAS: QWG recommendation in README files; Correlative data: standard procedure (Hubert *et al.*, 2016a)
3. Co-location MIPAS-GND	<500km from station and < ±6h (and only closest MIPAS-GND pair)
4. Profile representation	Temperature on fixed pressure levels
5. Vertical smoothing	Correlative data smoothed with co-located MIPAS AK
6. Quality indicators	Statistical properties of distribution $\Delta T = T_{MIPAS} - T_{GND}$ (K); including median difference ("bias"), half-width 68% interpercentile ("dispersion") and slope of linear regression ("drift") of ΔT difference time series

Table 3: Validation methodology for altitude profiles.

1. Correlative data	NDACC/GAW/SHADOZ radiosonde (i.e., attached to ozonesonde); Troposphere to 10 hPa (~30 km)
2. Data screening	MIPAS: QWG recommendation in README file; Correlative data: standard procedure (Hubert *et al.*, 2016a)
3. Co-location MIPAS-GND	<500km from station and < ±6h (and only closest MIPAS-GND pair)
4. Profile representation	Altitude on fixed pressure levels
5. Vertical smoothing	Correlative profile data regridded, but not explicitly smoothed
6. Quality indicators	Statistical properties of distribution $\Delta z = z_{MIPAS} - z_{GND}$ (m); including median difference ("bias") and half-width 68% interpercentile ("dispersion")

Table 4: Validation methodology for ozone profiles.

1. Correlative data	NDACC/GAW/SHADOZ ozonesonde, NDACC stratospheric O3 lidar and O3 microwave radiometer; Troposphere to lower mesosphere
2. Data screening	MIPAS: QWG recommendation in README files; Correlative data: standard procedure (Hubert *et al.*, 2016a)
3. Co-location MIPAS-GND	<500km from station and < ±6h (and only closest MIPAS-GND pair)
4. Profile representation	Ozone VMR on fixed pressure levels
5. Vertical smoothing	Sonde and lidar data smoothed with co-located MIPAS AK, MWR data are regridded, but not explicitly smoothed
6. Quality indicators	Statistical properties of distribution $\Delta O3 = 100*(O3_{MIPAS} - O3_{GND}) / O3_{GND}$ (%); including median difference ("bias"), half-width 68% interpercentile ("dispersion") and slope of linear regression ("drift") of ΔO3 difference time series

II.2 Comparison to ground-based FTIR

The comparative validation methodology for ENVISAT/MIPAS profiles is based on Vigouroux et al. (2007) (for HNO3 and N2O) and Payan et al. (2009) (for CH4 and N2O):

- **Each MIPAS profile is degraded to the lower vertical resolution of the ground-based FTIR profile** following Rodgers and Connor (2003). As a result, "[...] the vertical smoothing error (Rodgers, 2000), one of the larger FTIR error sources, which comes from the fact that the FTIR retrievals cannot see the real vertical fine structure of the atmosphere, can be neglected in the uncertainties that are to be considered in the comparison results." (Vigouroux et al., 2007)
- Satellite-ground **co-location settings are 300 km and 3 hours (Payan et al., 2009) at the MIPAS nominal tangent height around 30 km**. This is in disagreement with Vigouroux et al. (2007) where the coincidence criteria were less strict, which was compensated by the use of the data assimilation system BASCOE. Data assimilation is however not considered here.
- "Another requirement to be considered for intercomparison of polar winter measurements has been a recommended **maximum potential vorticity difference [smaller than] 15 %**." (Payan et al., 2009)
- "**The upper altitude limit for the comparisons is chosen taking into account the ground-based FTIR sensitivity which is reasonable [> 0.5] up to around 30 km** [...] at all stations." (Payan et al., 2009) "[T]he sensitivity [...] must be larger than 0.5, which means that the retrieved profile information comes for more than 50 % from the measurement, or, in other words, that the a priori information influences the retrieval for less than 50 %." (Vigouroux et al., 2007)
- "[...] **in all cases, the DOFS are lower than [about 3], thus these profile comparisons should not be over-interpreted.** The detailed shapes of the profile comparisons will strongly depend on the individual FTIR averaging kernel shapes and thus on the FTIR retrieval parameters." (Vigouroux et al., 2007)
- "**The means of the statistical comparisons (i.e., the biases) are compared to the 3σ standard errors on the means (SEM) to discuss their statistical significance.** The SEMs are calculated as $3\times STD/\sqrt{N}$, N being the number of coincidences, and STD the standard deviation of the differences. **The precision of the instruments will also be discussed by comparing the STD with the random error on the difference** MIPAS-FTIR. The random error covariance matrix of the difference of the profiles MIPAS-FTIR has been evaluated, using the work of Rodgers and Connor (2003) for the comparison of remote sounding instruments and of Calisesi et al. (2005) for the [pseudo-inverse] re-gridding between the MIPAS and FTIR data, as done in Vigouroux et al. (2007)." (Payan et al., 2009)

- "To avoid the need to extrapolate MIPAS profiles beyond the altitude limits for which retrieved VMR values are provided, while keeping a statistically relevant data set, **we have restricted the considered MIPAS data set to the scans for which the lower altitude limit is smaller than or equal to 12 km** […]."(Vigouroux et al., 2007)

As a result, difference statistics are calculated for three subcolumns integrated between 9 and 12 km, 12 and 30 km, and 30 and 60 km (integration in the pressure or altitude domain has been tested not to make any difference, so the former has been applied here). Only those subcolumns with sensitivity larger than 0.5, which are expected have up to one degree of freedom in the retrieval, are considered in the validation analysis. The median (bias) and 68 % interpercentile (spread) of the 12-30 km profile differences are calculated as well, whereby the MIPAS profiles are vertically smoothed using the coincident FTIR averaging kernel matrices.

Next to the data restrictions prompted by the outlined MIPAS validation methodology, additional filtering recommendations are taken from Tables 3 and 4 in the MIPAS L2 V8 Readme file (MIPAS QWG, 2020). An overview of all satellite data screening is provided in Table 5 and Table 6.

Table 5: Overview of general MIPAS profile data screening based on Vigouroux et al. (2007) and Payan et al. (2009).

Source	Constraint	Application (yes/no)
(Payan et al., 2009)	Max. PV difference < 15 %	Yes
(Vigouroux et al., 2007)	Lower altitude limit ≥ 12 km	Yes

Table 6: Overview of MIPAS profile data filtering, as recommended in the Level-2 V8 Readme file (MIPAS QWG, 2020, Table 3-4).

Field name	Description	Threshold
chi2	Final chi_square	chi2 smaller than chi2_Threshold
lambda_marq	Final Marquardt lambda	lambda Marquardt smaller than lambda_Threshold
Profile_error	Error of the retrieved profile	maximum error smaller than max_err_Threshold
conv_id	It provides information on convergence of the retrieval. Possible values: 0, convergence reached 1, maximum number of macro-iterations exceeded 2, maximum number of micro-iterations exceeded 3, maximum run-time exceeded 4, retrieval failed 5, convergence reached and final matrix singular 6, maximum number of macro-iterations exceeded and final matrix singular 7, maximum number of micro-iterations exceeded and final matrix was singular	0 or 5

An overview of the 15 NDACC FTIR stations providing CH4, HNO3, or N2O reference profile data is shown by their global distribution in Figure 1 and by listing in Table 7. This table moreover contains each station's operational time span within the Envisat lifetime and the number of profile co-locations (hence comparisons) with Envisat MIPAS instrument observations (note that the number of subcolumn comparisons can be different because of vertical integration constraints). Data of questionable quality, marked in red, have not been considered in the validation analysis.

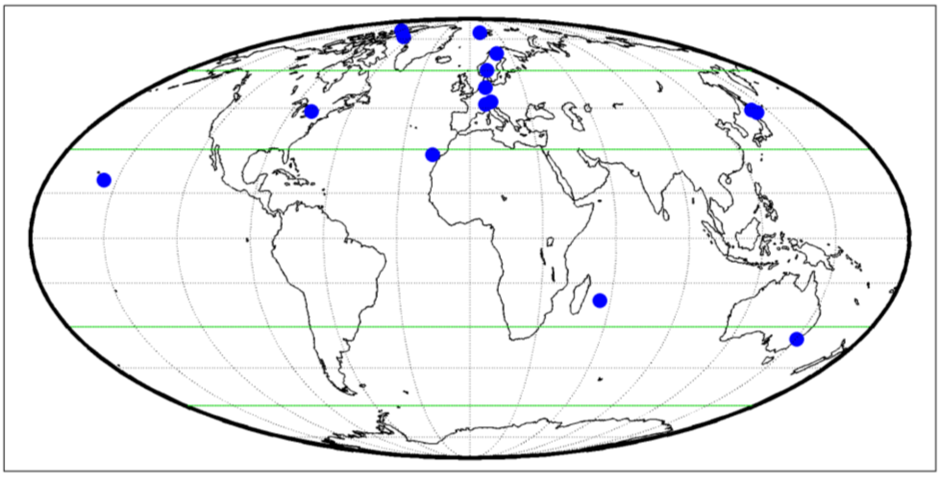

Figure 1: Global distribution of the 15 NDACC FTIR stations providing CH4, HNO3, or N2O reference profile data. Green lines mark the edges of the latitude bands considered in Table 7.

Table 7: List of 15 NDACC FTIR stations (sorted north to south) providing CH4, HNO3, or N2O reference profile data. The number of co-locations (and hence comparisons) for the MIPAS profile retrieval datasets has been provided for each station and species for the full mission V8 processing. Questionable FTIR data are marked in red and have not been considered in the validation analysis.

Station	Lat.	Lon.	Period	CH4	HNO3	N2O
Eureka	79.99	-85.93	2007-2009	878	1552	665
Ny-Ålesund	78.93	11.93	2002-2012	164	147	/
Thule	76.53	-68.74	2002-2011	208	193	300
Kiruna	67.84	20.41	2002-2012	93	105	78
Harestua	60.20	10.80	2002-2012	93	/	/
Bremen	53.10	8.80	2004-2012	81	/	/
Zugspitze	47.42	10.98	2002-2012	326	/	612
Jungfraujoch	46.55	7.98	2002-2012	117	137	86
Moshiri	44.40	142.30	2002-2007	/	3	/
Toronto	43.78	-79.47	2006-2011	137	67	286
Rikubetsu	43.50	143.80	2002-2009	/	8	/
Izaña	28.30	-16.50	2002-2012	326	126	171
Mauna Loa	19.53	-155.58	2003-2010	17	7	20
St Denis	-20.90	55.50	2004-2010	160	133	18
Wollongong	-34.41	150.88	2002-2008	414	/	388

III Validation results

III.1 Temperature

III.1.1 Results ORM 8.22

The vertical profile of the MIPAS temperature quality indicators are shown further below: overall bias (Figure 8) and dispersion (Figure 7) for the FR and OR periods and in five latitude bands; and the drift over the 2005-2012 period averaged over the ground networks (Figure 6). But we start with a discussion of the smoothed difference time series (12-month moving window) for the radiosonde (Figure 2) and temperature lidar (Figure 3) comparisons at selected pressure levels and in different latitude bands. Supplementary graphics showing results for earlier releases of MIPAS operational data (IPF 5.05+5.06, ML2PP 6.0, ML2PP 7.03) can be found in Appendix VII.1.

Generally, we observe that MIPAS ORM 8.22 temperature retrievals are too cool relative to sonde and lidar observations in a large part of the stratosphere & lower mesosphere and most of the time. The magnitude of the negative median difference depends on space (pressure, latitude) and time (month, year). The MIPAS QWG has put a lot of effort in reducing possible discrepancies resulting from the change in spectral resolution. However, while clear improvements are seen with respect to earlier versions V5 and V6 (Sect. III.1.2), the quality of the ORM 8.22 temperature data remains dependent on the spectral resolution mode. Therefore, we separate the full resolution (FR) and optimised resolution (OR) results in the following.

DISCREPANCY BETWEEN FR AND OR PHASE

The time series in Figure 2 and Figure 3 and the bias results in Figure 8 illustrate the differences between the FR (2002-2004) and OR periods (2005-2012). It is difficult to identify a clear spatial pattern in sign or magnitude of the difference in bias. MIPAS temperature data during the FR period are typically warmer than during the OR period at the lower end of the profile (pressure >100-200 hPa, ~1-1.5 K) and between 10-50 hPa (~0.5 K). In contrast, the FR data are cooler (~0.5 K) than during OR between 50-100 hPa. It is unclear whether the larger deviations (~1.5-2 K) noticed in the lower mesosphere at NH mid-latitudes and in the lower stratosphere at SH mid-latitudes are due to MIPAS or due to larger sampling uncertainty at these locations. Overall, the FR and OR period averages differ less than 0.5-1 K. The structure of the FR/OR discrepancy in dispersion (i.e., the spread in the comparisons) is very similar although the FR data are slightly more noisy than OR data (but no more than 0.5 K) in several regions of the atmosphere.

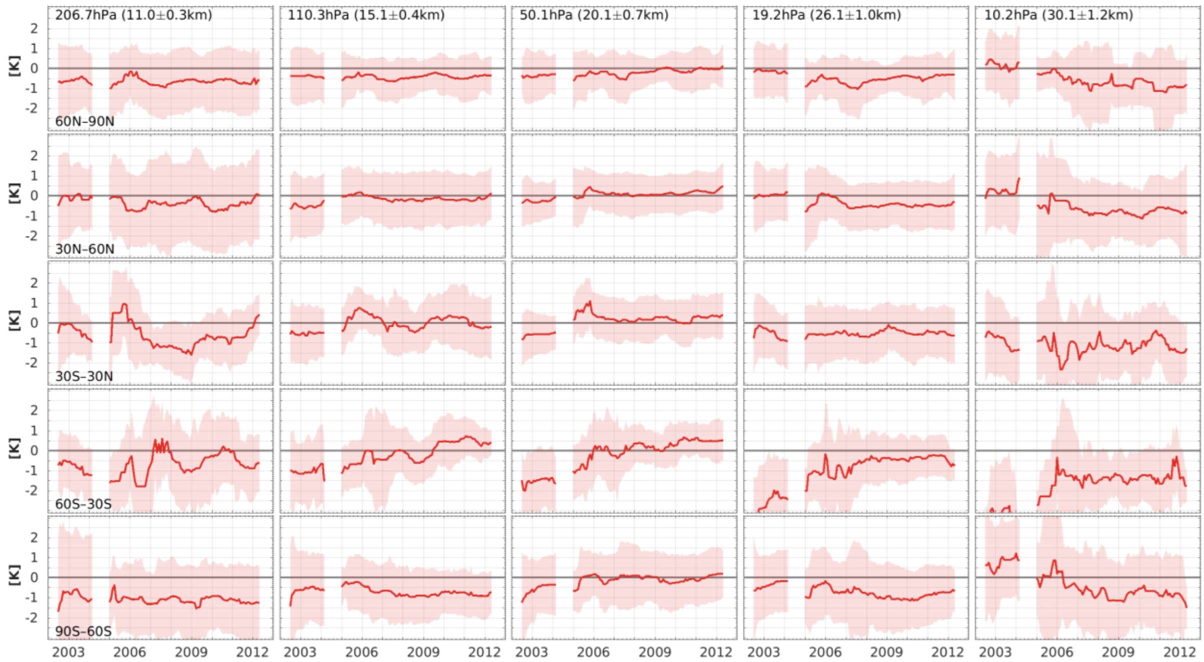

Figure 2: Absolute difference time series of co-located MIPAS ORM 8.22 and radiosonde temperature profiles in different latitude zones (top to bottom) and at different pressure levels (left to right; approximate altitude is labelled in first row). Each graph shows the median (solid line) and 1σ spread (shaded area) in 12-month moving windows. Positive values indicate too warm MIPAS temperature relative to correlative data. Results obtained for previous MIPAS data versions are shown in Figure 29.

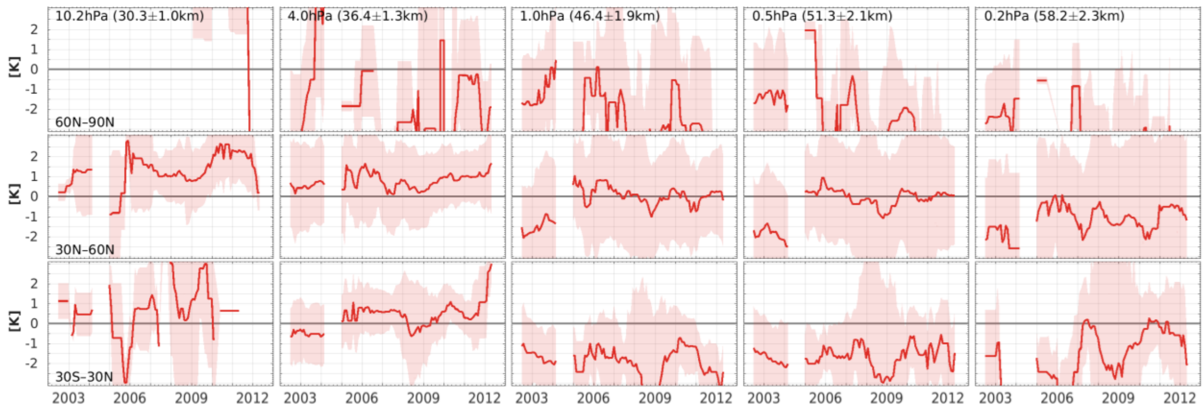

Figure 3: As in Figure 2, but for the comparisons to temperature lidar. Results obtained for previous MIPAS data versions are shown in Figure 30.

SEASONAL CYCLE

A second candidate pattern in the temporal structure of MIPAS comparison data is a seasonal cycle. Figure 4 and Figure 5 show no signs of a strong cycle in the ORM 8.22 results. Peak-to-peak variations across the year typically remain less than 0.5-1 K over most of the atmosphere. We speculate that the consideration of horizontal gradients by the V8 retrieval algorithm reduces the seasonal structure in the comparison time series which was clearly seen for all previous MIPAS data releases (Sect. III.1.2).

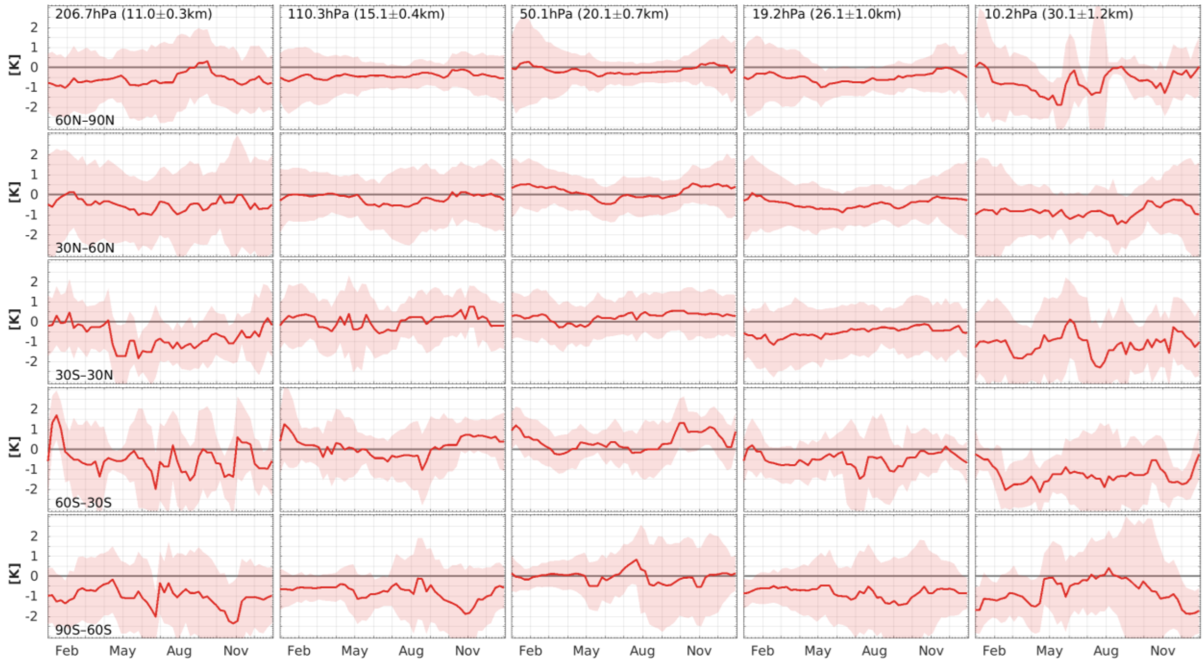

Figure 4: Seasonal dependence of the absolute difference of co-located MIPAS ORM 8.22 and radiosonde temperature profiles in different latitude zones (top to bottom) and at different pressure levels (left to right; approximate altitude is labelled in first row). Each graph shows the median (solid line) and 1σ spread (shaded area) in one-month moving windows. Positive values indicate too warm MIPAS temperature relative to correlative data. Results obtained for previous MIPAS data versions are shown in Figure 25.

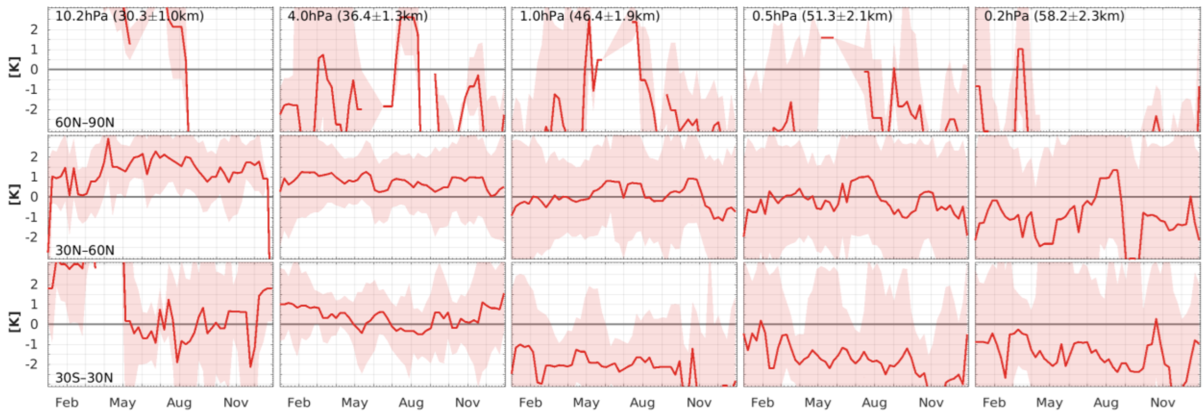

Figure 5: As in Figure 4, but for the comparisons to temperature lidar. Results obtained for previous MIPAS data versions are shown in Figure 26.

LONG-TERM EVOLUTION

A third possible temporal pattern is that of a long-term evolution in the bias. A simple linear model was fitted to the absolute difference time series at each site using a robust regression technique, then averaged (variance-weighted) over the entire ground-network. Only the 2005-2012 period was considered, hereby avoiding a possible step change between the FR and OR periods. The addition of a breakpoint in the regression model would have allowed us to regress the entire time series, but was out of scope for this report. Comparison time series differ by latitude band (Figure 2): the largest slope is found at mid-latitude SH between 20-100 hPa, in other bands it is smaller but positive almost everywhere in the lower and middle stratosphere. The network-averaged drift of MIPAS temperature relative to radiosonde is small (+0.4 K/dec.) but statistically significant drift (2σ) between 15-70 hPa

(Figure 6). There is no vertical structure in the drift profile between 5-500 hPa. Estimates change sign around the stratopause and become negative but insignificant in the lower mesosphere (-1.2 K/dec.).

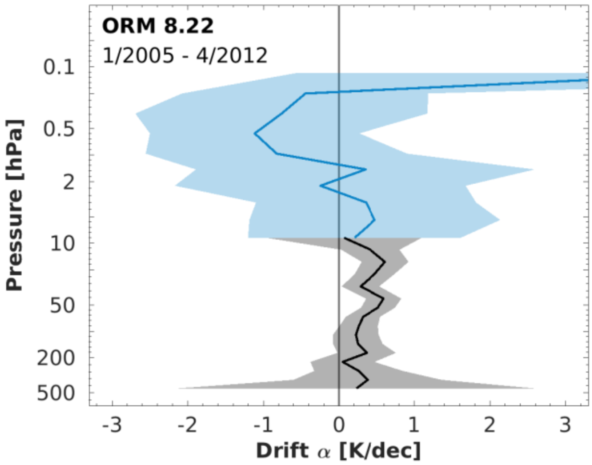

Figure 6: Ground-network averaged linear drift (K per decade) during the 2005-2012 period of MIPAS ORM 8.22 temperature relative to radiosonde (black) and lidar (blue). Positive values indicate that MIPAS T increases relative to correlative data. The shaded areas represent the 95% confidence interval for the drift estimates. Results obtained for previous MIPAS data versions are shown in Figure 33.

EPISODIC CHANGES

Several episodic changes are clearly superimposed on the long-term evolution of the bias. Such changes happen over various time scales at various pressure levels in all latitude bands. For instance, around 1 hPa in the mid NH there are four occurrences of 0.5-1.5 K changes in the bias over several months time. Also, MIPAS NH temperature systematically bumped up and down by at least 0.5 K relative to radiosonde over the course of 2005 and 2006 between 20 and 100 hPa. More examples can be found. Again, it is not known at the moment what causes these transient bias events. They might be due to temporal inhomogeneities in the ground-based records (especially radiosonde). But if similar features are seen at the same time in different latitude bands, then these are most likely not related to uncertainties in the correlative data.

GENERAL : DISPERSION

In the following, we disregard temporal features and discuss the average behaviour of bias and dispersion. MIPAS underestimates temperature in most of the atmosphere, but the magnitude depends on latitude and pressure. In the next paragraph we present the bias results per latitude region. Here we discuss dispersion (Figure 7), or the spread in the comparisons (1σ equivalent), whose structure is somewhat simpler than that of bias. Minimal values are typically between 1-1.5 K at pressures between 20-100 hPa. At altitudes above 10 hPa the observed spread is at least 1.5-2 K and rises to 3-4 K at 0.2 hPa. Similarly, the spread is larger in the UT/LS (up to 2-3 K) than in LS/MS (1-1.5 K). The vertical dependence of the observed spread is similar for different latitudes. The FR comparisons are a bit more noisy (at most 0.5 K) than OR data in some regions of the atmosphere. MIPAS precision is not necessarily the main contributor to dispersion, since sometimes non-negligible random uncertainties are expected due to co-location mismatch and due to the precision of the correlative measurements. These contributions depend on altitude as well.

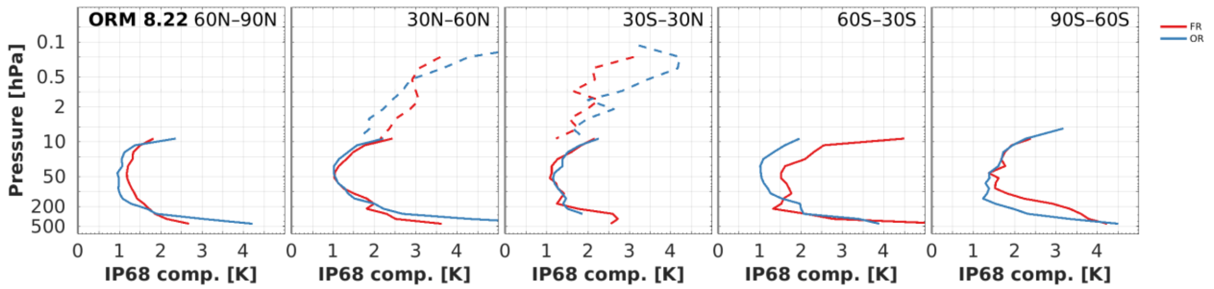

Figure 7: Dependence on MIPAS spectral resolution scanning mode of the spread in the comparisons of MIPAS ORM 8.22 temperature to lidar (dashed line) and radiosonde (solid line). FR stands for Full Resolution (2002-2004), OR for Optimised Resolution (2005-2012). Results obtained for previous MIPAS data versions are shown in Figure 34.

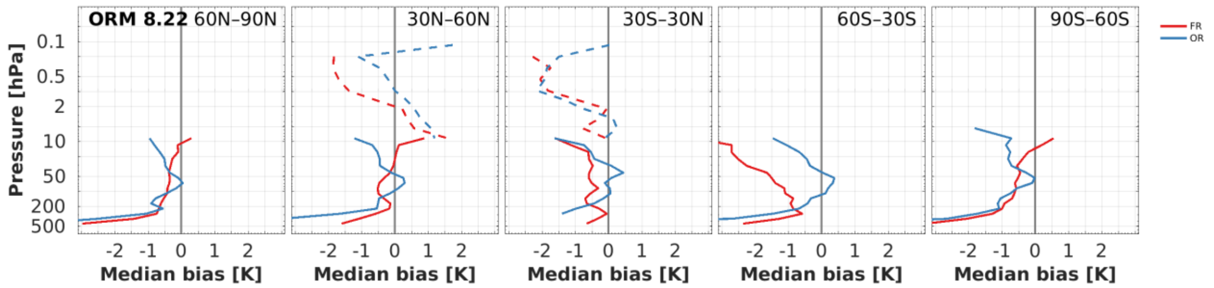

Figure 8: As in Figure 7, but for the median of the absolute differences. Positive values indicate that MIPAS ORM 8.22 retrievals overestimate correlative measurements. Results obtained for previous MIPAS data versions are shown in Figure 35.

GENERAL : BIAS

MIPAS temperature data are generally too cold with respect to ground-based data. The negative bias is less than 0.5-1 K in the middle/upper stratosphere and at most 1.5-2 K in the lower mesosphere and lowermost stratosphere. The vertical structure of the OR bias is coherent across all latitude bands: a positive vertical gradient is present between tropopause and 50-100 hPa, followed by a negative vertical gradient up to around 0.5 hPa, and finally changing back to a positive gradient at the top of the profile. A bump of +0.5 K is noted around 50-100 hPa which results in a positive bias. The comparisons in the mid-latitude SH are peculiar, with a much larger offset between FR and OR than noted in other latitude bands. Incidentally, the temporal structure is peculiar as well (Figure 2). The representativeness of the analysis results may be less good in this latitude zone since there are fewer ground stations.

III.1.2 Changes relative to earlier versions

Appendix VII.1 repeats all figures shown earlier this section for four operational MIPAS Level-2 data records (ORM 8.22, ML2PP 7.03, ML2PP 6.0 and IPF 5.05/5.06) processed using identical validation methods and reference data. The MIPAS V8 quality indicators exhibit a vertical-latitudinal structure that is often similar to that of its predecessors. However, there are various regions where V8 data quality notably differs. We focus mainly on the changes with respect to V7, earlier versions are included to complete the historic picture (V5 and V6 data are very comparable in all aspects of data quality).

MIPAS V8 temperature data (Figure 35) are warmer than the V7 data in the stratosphere (+0.3 K) and in the lower mesosphere as well during the FR period (+0.6 K), thereby partially removing the negative bias of V7. In contrast, V8 data are cooler than V7 data in the UT/LS (-0.9 K) which were already biased negative.

A second clear improvement in V8 data is that the seasonal cycle in the bias is reduced substantially and almost entirely eliminated (Figure 25 to Figure 28). All previous MIPAS data versions had a clear seasonal cycle in the middle stratosphere and part of the upper stratosphere, which increases the overall dispersion in the comparisons. The improvement is especially visible at mid-latitudes and in Antarctica. The introduction of horizontal gradients in the V8 retrieval algorithm scheme may be the main reason for this.

The overall spread in the V8 comparisons is 0.2-0.5 K smaller than for V7 at mid and high latitudes (Figure 34). The elimination of the seasonal cycle in the bias reduces the dispersion and may, in fact, be the main driver for tighter constraints on the MIPAS precision in these regions of the atmosphere. No clear differences were found in the tropics or in the upper stratosphere. In the upper troposphere the V8 dispersion is slightly larger than that of V7.

Last but not least, there is a clear improvement in drift for V8 in the UT/LS up to the middle stratosphere (Figure 33). It seems that the persistent, large negative drift of earlier versions at the lower end of the profile is now removed. In the middle stratosphere, the small positive drift of V8 is 0.4 K/dec. less than that of V7, but still larger than that of V5 and V6. The temporal structure at smaller time scales appears unchanged, most episodic events occur for earlier processor versions as well (Figure 29 and Figure 32).

III.1.3 Summary table

Table 8: Absolute differences between MIPAS ORM 8.22 temperature profile (full mission) and ground-based instruments (radiosonde, T lidar). The statistics are separated for Full Resolution (2002-2004; left) and Optimised Resolution (2005-2012; right) periods. Positive bias values imply that MIPAS temperature is larger than correlative measurements.

ORM 8.22	Full Resolution (2002-2004)					Optimised Resolution (2005-2012)				
	60N-90N	30N-60N	30N-30S	30S-60S	60S-90S	60N-90N	30N-60N	30N-30S	30S-60S	60S-90S
Median bias (K)										
> 200 hPa	-1.5†	-0.8†	-0.4	-1.3†	-1.8†	-2.3†	-2.9†	-1.1	-1.5†	-2.0†
100-200 hPa	-0.5	-0.4	-0.6	-1.0	-0.7	-0.7	-0.4	-0.3	-0.3	-0.9
50-100 hPa	-0.4	-0.4	-0.5	-1.4	-0.6	-0.2	+0.2	+0.1	+0.3	-0.4
20-50 hPa	-0.3	-0.1	-0.6	-2.1†	-0.4	-0.4	-0.3	0.0	-0.1	-0.6
10-20 hPa	-0.1	+0.1	-1.0	-2.8	0.0	-0.7	-0.6	-0.7	-0.9	-0.8
5-10 hPa		+0.8†	(-0.4)				+1.1	(0.0)		
2-5 hPa		+0.4	(-0.3)				+0.7	(-0.3†)		
1-2 hPa		-0.7†	(-1.0†)				+0.3	(-1.5†)		
0.5-1 hPa		-1.6	(-1.9)				-0.1	(-2.0)		
0.2-0.5 hPa		-1.8	(-1.9)				-0.6	(-1.7)		
Dispersion (1σ, K)										
> 200 hPa	2.0	2.4†	2.1†	2.5†	3.7†	2.5†	3.4	1.6	2.8†	2.8†
100-200 hPa	1.4	1.8	1.4	1.6	2.3	1.2	1.7	1.4	1.5	1.4
50-100 hPa	1.3	1.2	1.3	1.7	1.6	1.0	1.2	1.3	1.2	1.3
20-50 hPa	1.3	1.2	1.2	1.7	1.7	1.0	1.1	1.3	1.1	1.5
10-20 hPa	1.4	1.7†	1.7	2.6†	1.9	1.4	1.6	1.7	1.5	1.8
5-10 hPa		2.3	1.5				1.7	1.7		
2-5 hPa		2.6	1.7				2.0	2.0		
1-2 hPa		3.0	1.9				2.4	2.3		
0.5-1 hPa		3.0	1.9				2.8	3.2		
0.2-0.5 hPa		3.2	2.5				3.7	4.0		
Network-averaged drift (K/decade)										
> 200 hPa	Time series too short						+0.3			
100-200 hPa							+0.3			
50-100 hPa							+0.4			
20-50 hPa							+0.4			
10-20 hPa							+0.4			
5-10 hPa							(+0.4)			
2-5 hPa							(+0.2)			
1-2 hPa							(-0.2)			
0.5-1 hPa							(-0.8)			
0.2-0.5 hPa							(-0.7)			

Comments

- All MIPAS measurement modes included; screening procedure as described in ORM 8.22 Readme file.
- Quoted values represent central values of each pressure-latitude bin. A dagger symbol (†) indicates where the range of values in the bin is larger than 1 K.
- Estimates between brackets () are potentially subject to larger sampling uncertainties due to the sparsity of the ground-based network. These values should therefore be considered with care.
- Weak annual cycle : peak-to-peak amplitude typically less than 0.5-1 K.

III.2 Altitude

Two different altitude profile products can be read from the MIPAS Level-2 data files: corrected altitude and ECMWF-corrected altitude (introduced in ML2PP V7). Both products use MIPAS-retrieved pressure and temperature information to compute the altitude increments between subsequent retrieval levels from the hydrostatic equation. These increments are hence –by construction– identical. The products differ in the choice of altitude of the reference level, which determines the absolute vertical registration of the altitude profile. This leads to a profile-dependent offset between the corrected and ECWMF-corrected altitude products. It is important to be aware of this difference, since it determines the quality of the altitude data.

The MIPAS QWG recommends the ECWMF-corrected altitude profiles for ORM V8 and ML2PP V7. Earlier MIPAS data records do not include the ECMWF anchor in which case the corrected altitude profiles is recommended over the engineering altitude scale (the latter is not discussed here). Supplementary graphics showing results for earlier releases of MIPAS operational data (IPF 5.05+5.06, ML2PP 6.0, ML2PP 7.03) can be found in Appendix VII.2.

III.2.1 Results ORM 8.22

Figure 9 shows the time series of 12-month moving median and spread of ORM 8.22 minus radiosonde. The agreement between both data sets is remarkably good at all pressure levels and for all latitude zones. Several space-time patterns are seen in the absolute difference time series but they are not pronounced and therefore likely not a limiting factor in many analyses. Generally, the 12-month moving median difference remains less than 50 m and increases slightly (to at most ~100 m) from the lower to the middle stratosphere or from the tropics to the poles. There is virtually no annual cycle in the altitude differences (Figure 10), with a peak-to-peak amplitude that is typically less than 50 m and at most 100 m. The dispersion in the difference time series is generally less than 50-100 m, the FR altitude comparison data are slightly more noisy (20-40 m) than the OR data (Figure 11). The long-term stability is very good as well (Figure 9): the ECMWF-corrected altitude data drifts less than 50 m per decade away from the radiosonde data. Again –as with overall bias– the drift values are a bit larger in the polar regions and around 10 hPa, but not more than 100 m per decade. Finally, the discrepancy in bias and short-term variability between the FR and OR data are small if not negligible (Figure 12). Typically the OR data are of higher quality.

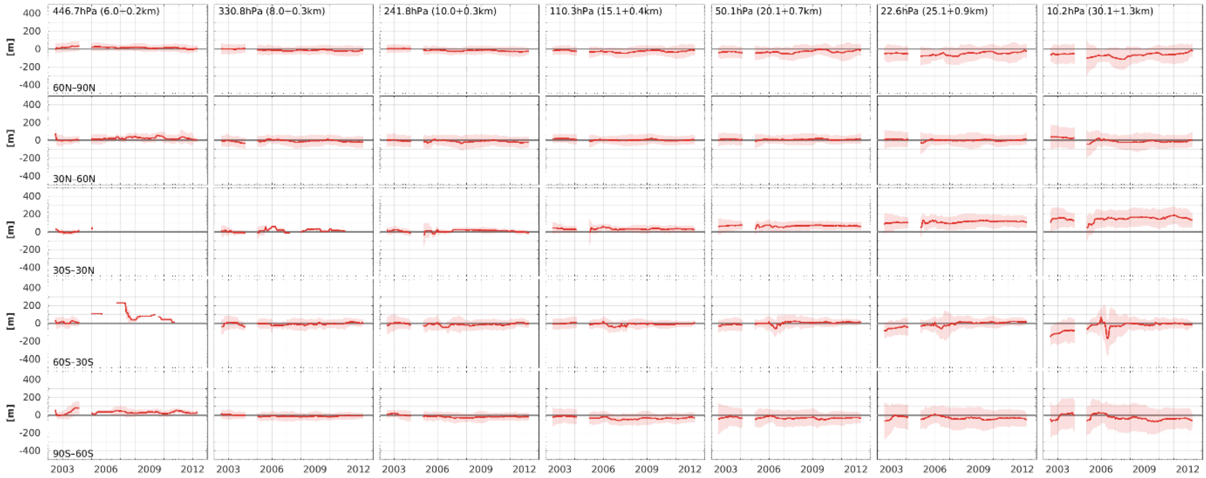

Figure 9: Absolute difference time series of co-located MIPAS ORM 8.22 and radiosonde altitude profiles in different latitude zones (top to bottom) and at different pressure levels (left to right; approximate altitude is labelled in first row). Each graph shows the median (solid line) and 1σ spread (shaded area) in 12-month moving windows. Positive values indicate too high MIPAS altitude relative to correlative data. Results obtained for previous MIPAS data versions are shown in Figure 38.

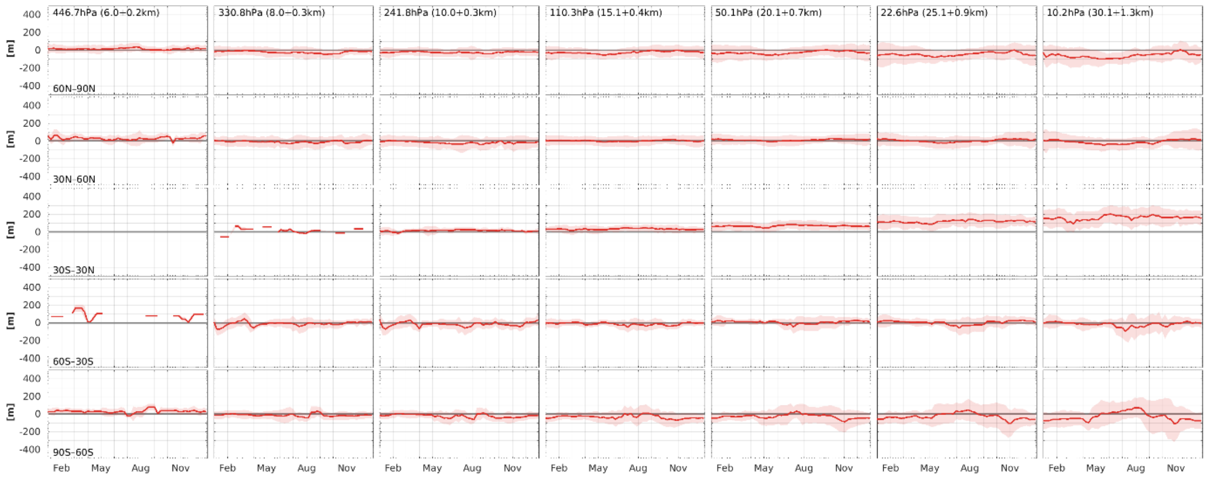

Figure 10: Seasonal dependence of the absolute difference of co-located MIPAS ORM 8.22 and radiosonde altitude profiles in different latitude zones (top to bottom) and at different pressure levels (left to right; approximate altitude is labelled in first row). Each graph shows the median (solid line) and 1σ spread (shaded area) in one-month moving windows. Positive values indicate too high MIPAS altitude relative to correlative data. Results obtained for previous MIPAS data versions are shown in Figure 36.

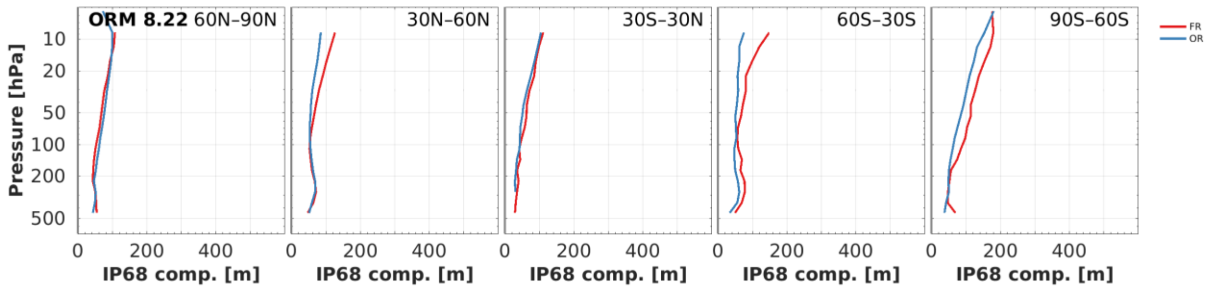

Figure 11: Dependence on MIPAS spectral resolution scanning mode of the spread in the comparisons of MIPAS ORM 8.22 altitude to radiosonde. FR stands for Full Resolution (2002-2004), OR for Optimised Resolution (2005-2012). Results obtained for previous MIPAS data versions are shown in Figure 40.

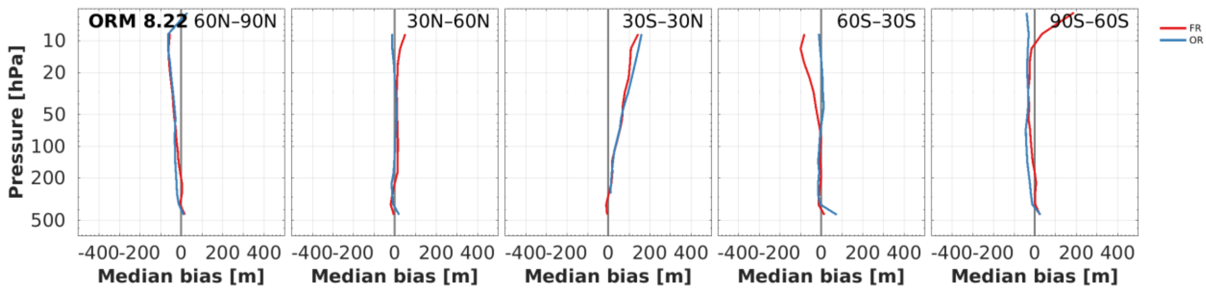

Figure 12: As in Figure 11, but for the median of the absolute differences. Positive values indicate that MIPAS ORM 8.22 retrievals overestimate correlative measurements. Results obtained for previous MIPAS data versions are shown in Figure 41.

III.2.2 Changes relative to earlier versions

Appendix VII.2 repeats all figures shown earlier this section for four operational MIPAS Level-2 data records (ORM 8.22, ML2PP 7.03, ML2PP 6.0 and IPF 5.05/5.06) processed using identical validation methods and reference data. The altitude scale differs however for MIPAS V7/V8 ("ECMWF-corrected altitude") and V5/V6 ("corrected altitude"), see the information at the start of this section. Both altitude scales are sensitive in an identical way to uncertainties in MIPAS retrieved temperature. These accumulate with height and are more easily detectable higher up in the altitude profile.

Below, we summarise the main differences in quality between ORM 8.22 and ML2PP 7.03 ECMWF-corrected altitudes. The ECMWF-corrected scale uses a more reliable anchor point than the corrected scale and is therefore recommended by the MIPAS QWG. The figures in Appendix corroborate this clearly: V5/V6 altitude data quality is inferior in all aspects to V7/V8 data.

The seasonal cycle in bias of V8 altitude is smaller than that of V7 and virtually negligible. This is clearly visible at the highest probed altitude level (10 hPa). It is a direct consequence of the elimination of the seasonal cycle in the MIPAS V8 temperature data. For this same reason the dispersion in the V8 altitude results is also reduced with respect to V7 (by at most 20-40 m). On average the V8 altitudes are identical to or slightly larger (<20-40 m at 10 hPa) than the V7 data. This leads to an insignificant improvement in the bias versus radiosonde at mid and high latitudes, and an insignificant degradation in bias in the tropics. No clear change is seen in the long-term stability between V7-V8.

III.2.3 Summary table

Table 9: Data quality indicators of the MIPAS ORM 8.22 ECMWF-corrected altitude profile product based on comparisons to radiosonde. Quoted values represent central values of each pressure-latitude bin. Positive bias values imply that MIPAS altitude is larger than correlative measurements.

ORM 8.22	60°N-90°N	30°N-60°N	30°N-30°S	30°S-60°S	60°S-90°S
Median bias (m)					
500-200 hPa	-10	< 10	< 10	< 10	-20
200-100 hPa	-20	< 10	+30	< 10	-30
100-50 hPa	-30	< 10	+50	< 10	-40
50-20 hPa	-40	< 10	+80	-20	-30
20-10 hPa	-50	< 10	+120	-20	-30
Dispersion (1σ, m)					
500-200 hPa	50	60	30	50	40
200-100 hPa	60	60	40	50	50
100-50 hPa	70	60	40	50	70
50-20 hPa	80	70	60	60	100
20-10 hPa	100	80	80	60	120
Comments					
• FR/OR discrepancy : negligible (bias) or differences less than 20-40 m (dispersion) • Amplitude annual cycle : typically less than 50 m, at most 100 m. • Long-term drift : typically less than ±50 m per decade.					

III.3 Ozone

III.3.1 Results ORM 8.22

The vertical profile of the MIPAS ozone quality indicators are shown further below: overall bias (Figure 21) and dispersion (Figure 20) for the FR and OR periods and in five latitude bands; and the drift over the 2005-2012 period averaged over the ground networks (Figure 19). But we start with a discussion of the smoothed difference time series (12-month moving window) for the ozonesonde (Figure 13), ozone lidar (Figure 14) and microwave radiometer (Figure 15) comparisons at selected pressure levels and in different latitude bands. Supplementary graphics showing results for earlier releases of MIPAS operational data (IPF 5.05+5.06, ML2PP 6.0, ML2PP 7.03) can be found in Appendix VII.3.

We observe that MIPAS ORM 8.22 ozone retrievals are generally too high relative to all ground-based reference observations in the stratosphere and most of the time. The magnitude of the positive median difference depends on space (pressure, latitude) and to some extent on time as well. The MIPAS QWG has put a lot of effort in reducing possible discrepancies resulting from the change in spectral resolution. However, the quality of the ORM 8.22 ozone data remains dependent on the spectral resolution mode, as for earlier versions (cf. Sect. III.3.2). Therefore, we separate the FR and OR results in the following. We also reflect on the possible impact of the retrieved temperatures on the ozone data quality.

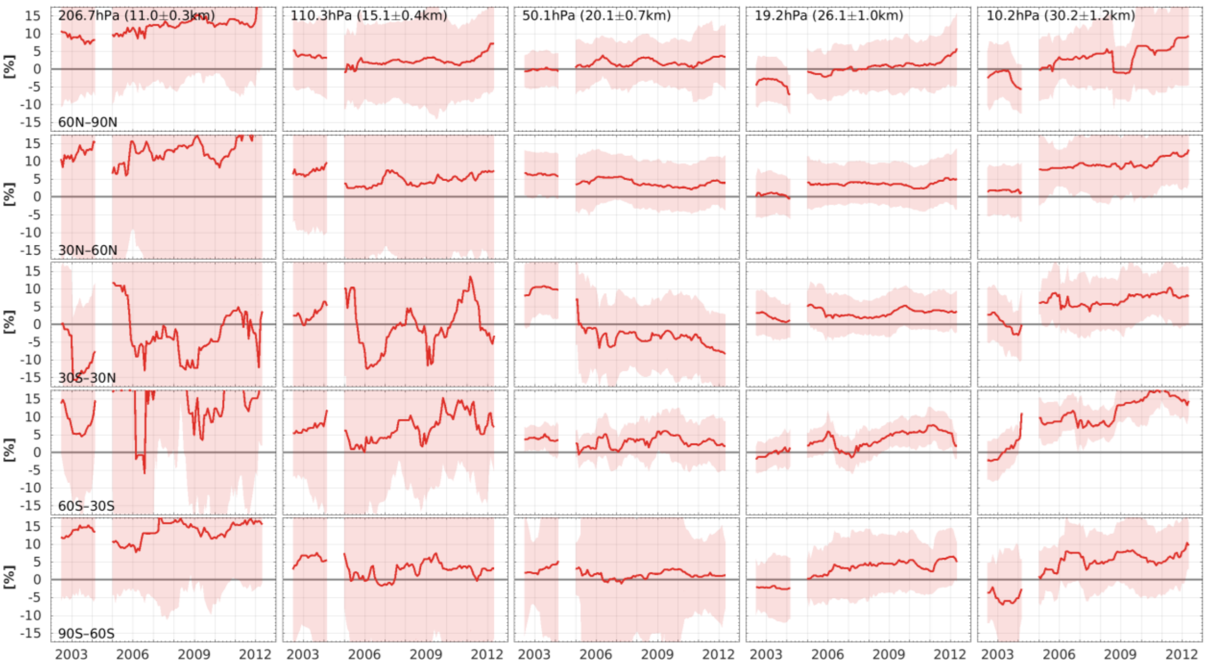

Figure 13: Relative difference time series of co-located MIPAS ORM 8.22 and ozonesonde ozone profiles in different latitude zones (top to bottom) and at different pressure levels (left to right; approximate altitude is labelled in first row). Each graph shows the median (solid line) and 1σ spread (shaded area) in 12-month moving windows. Positive values indicate too high MIPAS ozone relative to correlative data. Results obtained for previous MIPAS data versions are shown in Figure 48.

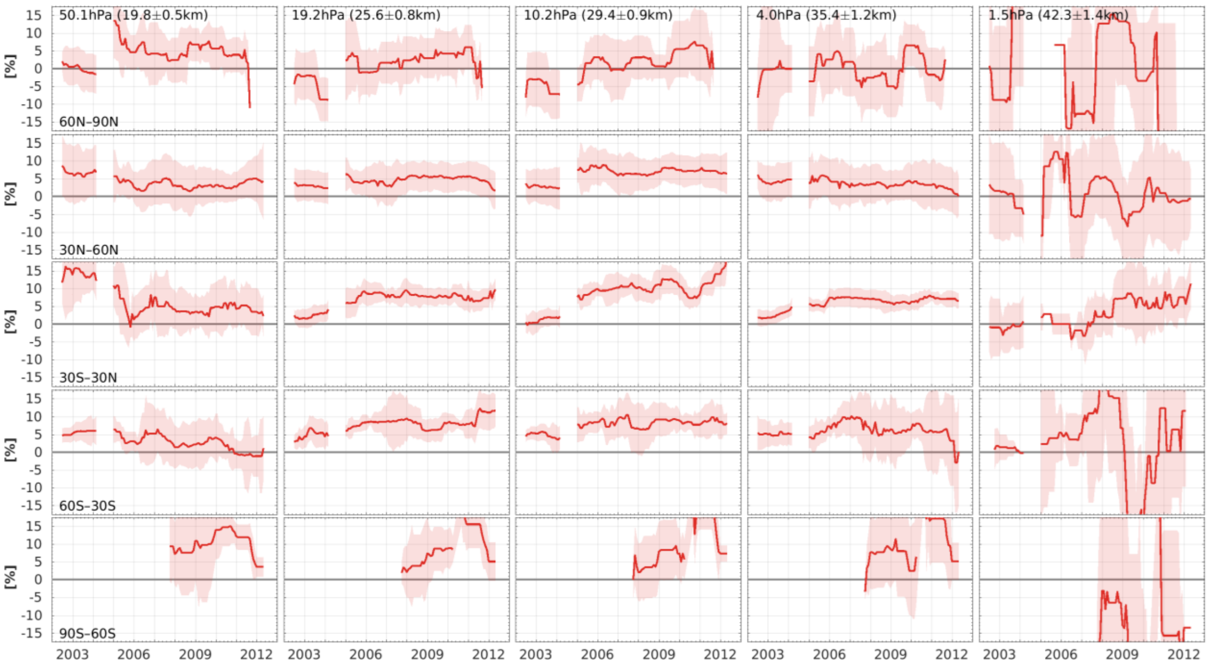

Figure 14: As in Figure 13, but for the comparisons to ozone lidar. Results obtained for previous MIPAS data versions are shown in Figure 49.

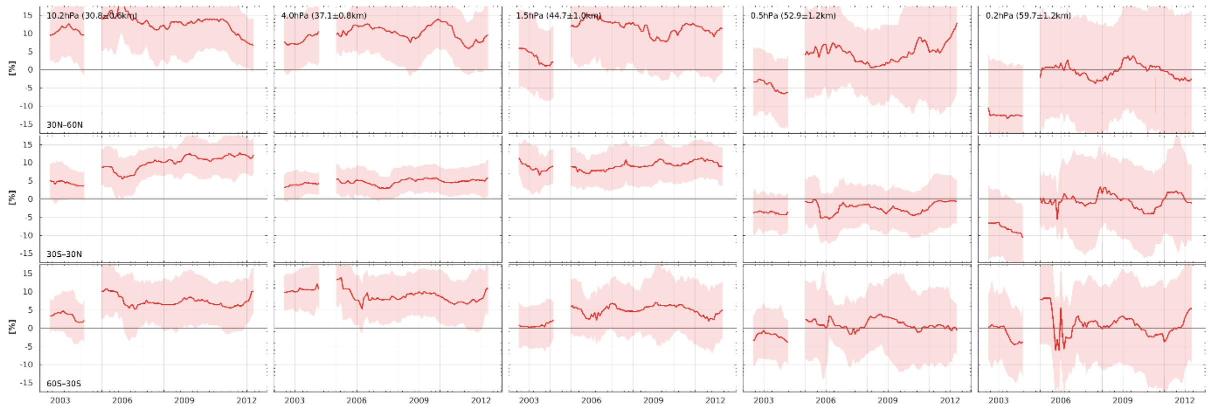

Figure 15: As in Figure 13, but for the comparisons to ozone microwave radiometer. Results obtained for previous MIPAS data versions are shown in Figure 50.

Discrepancy between FR and OR phase

Figure 13 to Figure 15 show signs of a discontinuity in the transition from the FR to the OR phase, especially in the tropics. The discrepancy is clearer in the time-averaged results (Figure 21) and exhibits a vertical pattern that is consistent for the comparisons all types of ground-based instruments. In the LS, the MIPAS FR bias relative to sonde is more positive –generally by less than 5% and in the tropics by 10%– than the OR bias. The discrepancy has opposite sign in the MS and US, here, FR data have about 4% smaller positive bias than OR measurements. The sign change occurs several km above the tropopause, around 20 hPa in the tropics and 50-100 hPa at high latitude). The bias discrepancy vanishes almost entirely at the bottom of the profiles (for pressure > 100-200 hPa). Figure 20 does not indicate a clear change in precision, although the FR comparisons are consistently a little less noisy (not more than 1-3%) than the OR data at most considered altitudes.

SEASONAL CYCLE AND ANTARCTIC OZONE HOLE

Figure 16 to Figure 18 show no clear coherent picture of a seasonal cycle in the ozone bias. The observed seasonal patterns generally vary with pressure, latitude, and also with the type of correlative instrument. Latter inconsistency can not solely be explained by different time-dependent co-location mismatch uncertainties, e.g., because the diurnal ozone cycle is very weak in the MS.

There are signs of a seasonal cycle in ozone bias in the mid-latitude Northern hemisphere in the middle and upper stratosphere (4-50 hPa). The cycle has a peak-to-peak amplitude of at most 3-5% and a maximum/minimum in local summer/winter (JJA/DJF). It is unclear whether this ozone bias cycle is linked to the annual cycle in MIPAS temperature bias that can be noticed in radiosonde comparisons in the middle stratosphere of this latitude band (Figure 4). The temperature cycle has opposite phase of that of ozone (maximum/minimum in local winter/summer).

A clear annual pattern in Figure 16 occurs during the Antarctic ozone hole season. MIPAS overestimates LS ozone by 5-15% during JJA, and underestimates relative to sonde by 10-20% during SON. Hence, the amount of ozone depletion is overestimated on average by up to 30%. This pattern is not seen at altitudes above the 50 hPa level. Previously quoted values should not be taken at face value, since the co-location mismatch error budget is not taken into account in the analysis. Mismatch errors (systematic and random) can be large, especially for co-location pairs situated in large spatial gradients of the ozone field, such as the polar vortex. This is why we disregard the Antarctic lidar results for this part of the analysis.

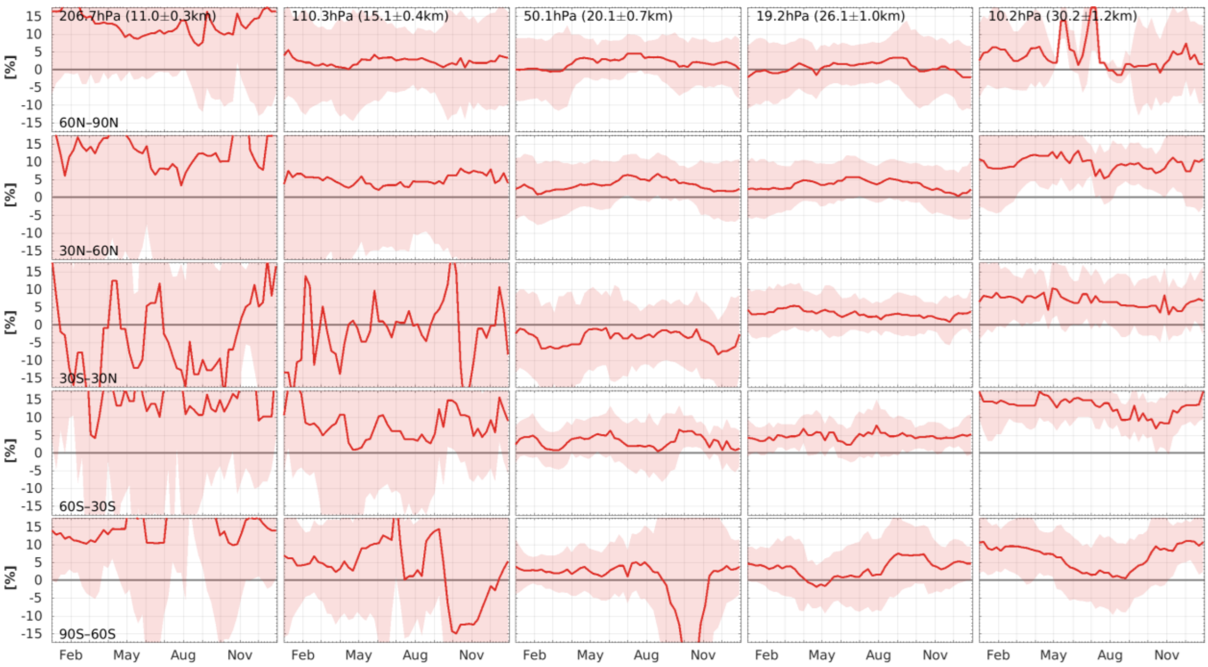

Figure 16: Seasonal dependence of the relative difference of co-located MIPAS ORM 8.22 and ozonesonde ozone profiles in different latitude zones (top to bottom) and at different pressure levels (left to right; approximate altitude is labelled in first row). Each graph shows the median (solid line) and 1σ spread (shaded area) in one-month moving windows. Positive values indicate too high MIPAS ozone relative to correlative data. Results obtained for previous MIPAS data versions are shown in Figure 42.

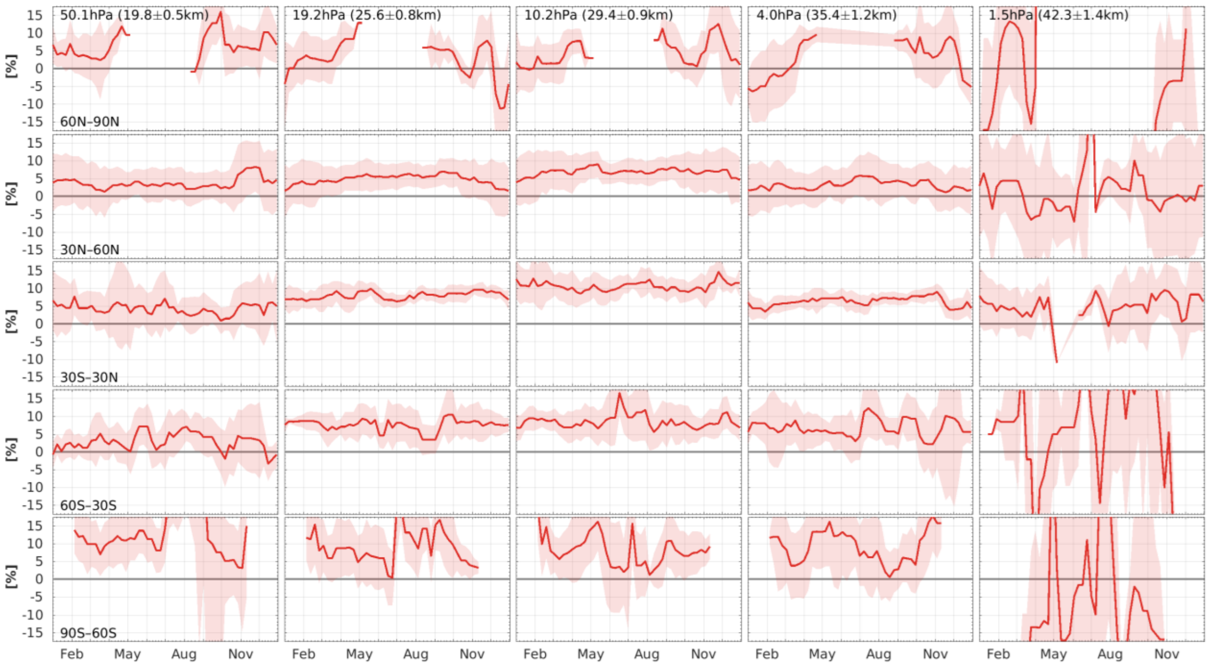

Figure 17: As in Figure 16, but for the comparisons to ozone lidar. Results obtained for previous MIPAS data versions are shown in Figure 43.

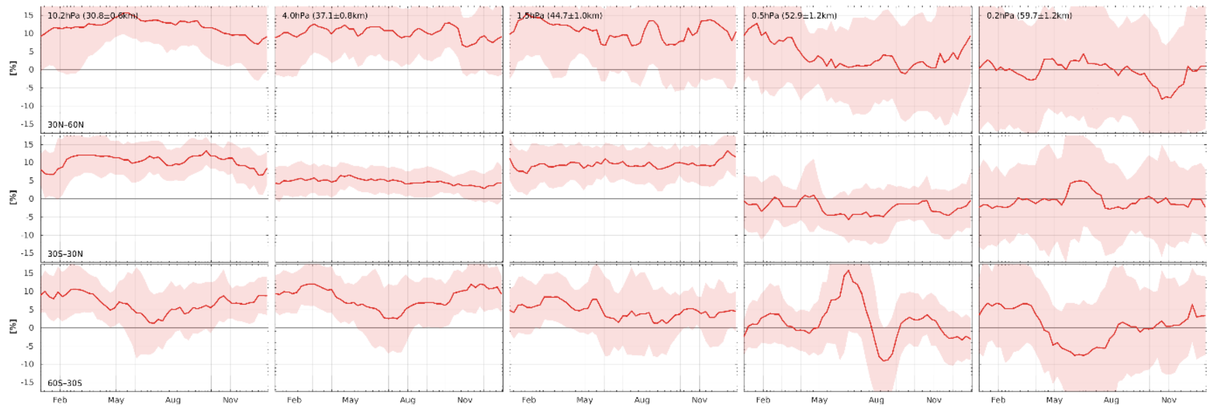

Figure 18: As in Figure 16, but for the comparisons to ozone microwave radiometer. Results obtained for previous MIPAS data versions are shown in Figure 44.

LONG-TERM EVOLUTION

A linear regression analysis of the relative difference time series for 2005-2012 shows that there is no statistically significant evidence of a long-term drift of MIPAS ozone relative to the ozonesonde, lidar or microwave radiometer networks. Only the 2005-2012 period was considered, hereby avoiding a step change between the FR and OR periods. The addition of a breakpoint in the regression model would have allowed us to regress the entire time series, but was out of scope for this report.

The regressed slope values lie around zero in the LS and slightly above zero in the MS and US, but these remain less than 3% per decade over most of the stratosphere (Figure 19). A small region around 10 hPa displays a positive drift that is statistically significant, here estimates are +4-5 % per decade relative to all ground-based instruments. Around the stratopause drift estimates turn negative, but remain statistically insignificant mainly due to the small number of MWR instruments in the network.

There is a reasonably good coherence in the vertical dependence of the drift profile for the different types of reference instruments. Local minima are found around 50 hPa and 3-4 hPa, and a local maximum at 10 hPa. Drift estimates are generally not statistically significant, but the coherence of the results builds confidence in the presence of such a vertical pattern.

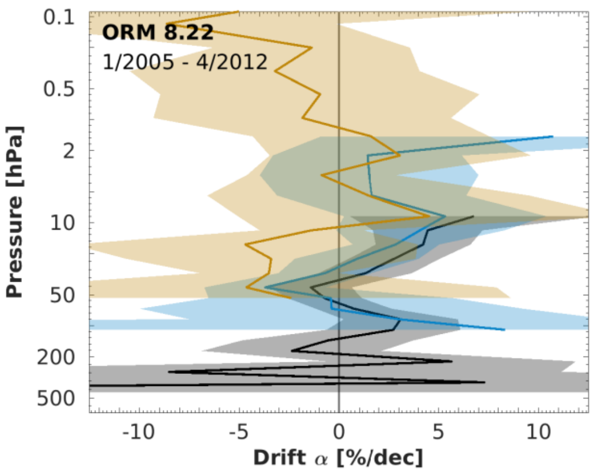

Figure 19: Ground-network averaged linear drift (% per decade) during the 2005-2012 period of MIPAS ozone relative to ozonesonde (black), lidar (blue) and microwave radiometer (orange). Positive values indicate that MIPAS O3 increases relative to correlative data. The shaded areas represent the 95% confidence interval for the drift estimates. Results obtained for previous MIPAS data versions are shown in Figure 54.

EPISODIC CHANGES

The time series in Figure 13 to Figure 15 exhibit several features at time scales of weeks or months. However, there is no consistent pattern in the location, timing, sign and amplitude of episodic changes in the comparisons. For instance, the 50 hPa lidar comparison time series show a clear increase of about 5% around 2007 in three latitude bands at low and mid-latitudes, but this is not seen in the ozonesonde comparisons. This illustrates that short-term features could be caused by spatial and temporal inhomogeneities in the correlative data records as well.

CORRELATION OF OZONE QUALITY WITH THAT OF TEMPERATURE

MIPAS ozone retrievals anti-correlate with retrieved temperature, through the temperature-dependent ozone cross sections. Too cool retrieved temperatures should lead to too high retrieved ozone. Can this be seen in the comparisons to ground-based measurements? In this respect, it is important to realise that differences in spatial and temporal sampling of the co-located MIPAS-ground profile pairs contributes to the differences seen in the T and O3 analyses. Especially for the lidar analyses since the T and O3 measurements are done by different physical instruments at different locations and times. The sonde analyses are more helpful to answer this question, although we note that no effort was done to select identical MIPAS-ground pairs for the T and O3 analyses.

The overall sign of the temperature bias (negative) and the ozone bias (positive) is consistent with expectations. Otherwise there are not clear signs of a correlation between the quality of temperature data (Sect. III.1.1) and ozone data, except for the anti-correlated annual cycle in T and O3 bias in the middle stratosphere at NH mid-latitudes (Figure 4 and Figure 16). For instance, most episodic changes in temperature (Figure 2) do not seem to induce large changes in ozone (Figure 13). Even the long-term dependence of the ozone bias is not strongly linked to that of temperature. The drift of ORM 8.22 relative to correlative data is positive in the MS for both temperature and ozone data, while an opposite sign would be expected if all other effects play no significant role. Hence, these observations suggest that other factors than temperature co-determine the characteristics of the ozone profiles.

GENERAL : DISPERSION

In the following, we ignore temporal features and discuss the average behaviour of bias and dispersion. Here, we discuss the dispersion of the comparisons (Figure 20), which has a simpler structure than the bias. Between 5-50 hPa the spread typically straddles 3-6%, with the smaller values for the lidar comparisons (more precise reference measurements) or at low latitudes (lower co-location mismatch error due to lower natural variability). At higher altitudes the observed spread increases to 10-15% at the stratopause. The spread increases rapidly in the UT/LS, up to 30-40% around the tropopause. FR comparisons are generally a bit less noisy (by ~1-3%) than OR data. As implicitly mentioned above, MIPAS precision is not necessarily the main contributor to dispersion, since sometimes non-negligible random uncertainties are expected due to co-location mismatch and due to the precision of the correlative measurements. These contributions depend on altitude and latitude.

GENERAL : BIAS

MIPAS overestimates ozone in most of the stratosphere with a magnitude that depends mildly on latitude and pressure (Figure 21). The exception is the rapid increase in percentage bias in the **lower stratosphere** (altitudes below the 100 hPa level) as a result of the lower ozone concentrations and the larger natural variability. The overestimation easily becomes 10-15% around the tropopause. In the MS and US, the vertical dependence of bias is not very pronounced, varying by just a few %.

In the **Arctic**, the bias is positive during the OR period and the FR period for altitudes below the 20-50 hPa level. The agreement with correlative data is perhaps slightly better than at other latitudes, with biases not more than about 3-4% (except in the UT/LS region). The FR and OR comparison results for sonde lie within less than 5%.

At **mid-latitudes** (North and South) the overestimation lies around +5% and exhibits excursions to 0% or 7% at some pressure levels. The difference between FR and OR data is quite clear, and amounts to up to 4%. FR ozone is high compared to OR data in the LS, and the other way round for pressures smaller than 30 hPa. As mentioned before, the apparent increase in positive bias from 20 hPa to 10 hPa is considered an artefact due to the larger sonde bias and due to an incomplete profile for smoothing.

The positive bias and its vertical dependence and FR/OR discrepancy is most pronounced in the **tropics**, especially in the US and LS. The larger disagreement with ground-based data can at least partially be ascribed to the lower ozone concentrations and the larger vertical gradient in the ozone field. OR ozone is about 4% larger than FR data in the US. On the other hand, OR data are biased low by ~7% relative to the FR measurements in the LS.

The bias of **Antarctic** data is overall similar to that found at mid-latitudes, with a general positive bias of about 5% and ~5% differences between FR and OR phase. However, the evolution of bias depends strongly on season in the LS (Figure 16). MIPAS-ground differences change by up to 30% around September: there is a large positive bias in JJA, and large negative values in SON. Again, the large percentage values are in part due to the lower absolute ozone concentrations.

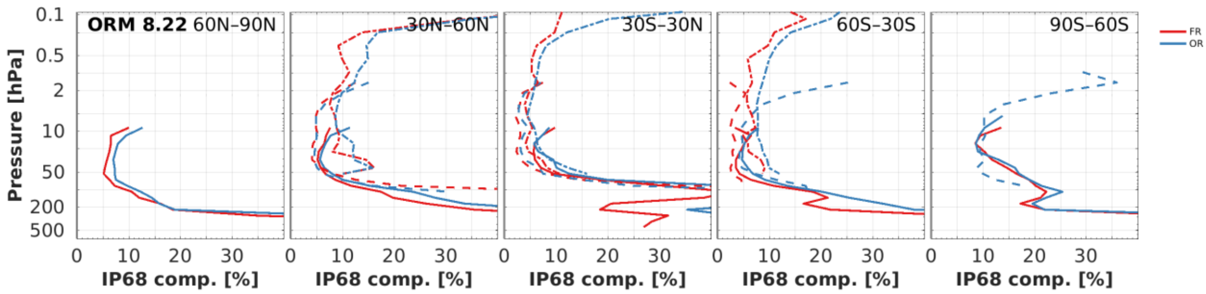

Figure 20: Dependence on MIPAS spectral resolution scanning mode of the spread in the comparisons of MIPAS ORM 8.22 ozone to microwave radiometer (dash-dotted line), lidar (dashed line) and ozonesonde (solid line). FR stands for Full Resolution (2002-2004), OR for Optimised Resolution (2005-2012). Results obtained for previous MIPAS data versions are shown in Figure 55.

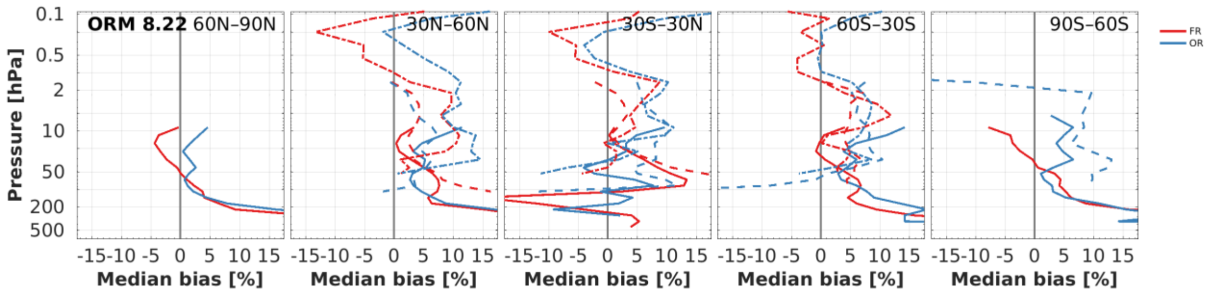

Figure 21: As in Figure 20, but for the median of the relative differences. Positive values indicate that MIPAS ORM 8.22 retrievals overestimate correlative measurements. Results obtained for previous MIPAS data versions are shown in Figure 56.

III.3.2 Changes relative to earlier versions

Appendix VII.3 repeats all figures shown earlier this section for four operational MIPAS Level-2 data records (ORM 8.22, ML2PP 7.03, ML2PP 6.0 and IPF 5.05/5.06) processed using identical validation methods and reference data. The MIPAS V8 quality indicators exhibit a vertical-latitudinal-temporal structure that is often similar to that of its predecessors. However, there are various regions where V8 data quality differs notably. We focus mainly on the changes with respect to V7, earlier versions are included to complete the historic picture (V5 and V6 data are very comparable in all aspects of data quality).

The clearest change between V8 and V7 occurs in the UT/LS bias. Here, V8 ozone mixing ratios are about 3-5% lower than for V7 at mid-latitudes and about 10% lower in the tropics (Figure 56). This reduces the positive bias with respect to ozonesonde. In the Antarctic lower stratosphere a 5% reduction is seen in the dispersion of FR comparisons, but not in the OR period (Figure 55). The temporal structure (annual cycle, long-term change) of MIPAS V7 and V8 is nearly identical (Figure 54).

III.3.3 Summary table

Table 10: Relative differences between MIPAS ORM 8.22 ozone profile (full mission) and ground-based instruments (ozonesonde, lidar and microwave radiometer). The statistics are separated for Full Resolution (2002-2004; left) and Optimised Resolution (2005-2012; right) periods. Positive bias values imply that MIPAS ozone is larger than correlative measurements.

ORM 8.22	Full Resolution (2002-2004)					Optimised Resolution (2005-2012)				
	60N-90N	30N-60N	30N-30S	30S-60S	60S-90S	60N-90N	30N-60N	30N-30S	30S-60S	60S-90S
Median bias (%)										
> 200 hPa	> +15†	> +15†	+2†	> +15†	> +15†	> +15†	> +15†	-4	> +15†	> +15†
100-200 hPa	+5	+7	-8†	+6	+7	+5	+7	+1	+10	+7†
50-100 hPa	+2	+7	+12	+5	+4	+2	+3	+3	+4	+3
20-50 hPa	-2	+3	+6†	+3	-1	+2	+4	+2	+7	+7
10-20 hPa	-3	+2	+1	+3	-4	+3	+7	+7	+6	+6
5-10 hPa		+4	(+2)	(+2)			+5	(+8)	(+8)	(+7)
2-5 hPa		+4	(+3)	(+5)			+3	(+7)	(+7)	(+8)
1-2 hPa		(+3)	(+5)	(0)			(+11)	(+7)	(+4)	(-10†)
0.5-1 hPa		(-3)	(-3)	(-4)			(+7)	(+1)	(0)	
0.2-0.5 hPa		(-8)	(-7)	(-3)			(+2)	(-2)	(0)	
Dispersion (1σ, %)										
> 200 hPa	> 40†	> 40†	28†	> 40†	> 40†	> 40†	> 40†	> 40†	> 40†	> 40†
100-200 hPa	13†	21†	35†	18	20	14	28†	> 40†	35†	22†
50-100 hPa	7	8	20†	8	19	9	11†	30†	10†	16
20-50 hPa	6	5	4	3	13	7	5	5	5	10
10-20 hPa	7	5	3	3	10	9	5	4	5	10
5-10 hPa		5	3	3			5	4	6	10
2-5 hPa		6	4	4			8	4	8	18†
1-2 hPa		10	6	6			12	6	9	
0.5-1 hPa		10	5	6			14	7	10	
0.2-0.5 hPa		11	7	9			16	9	12	
Network-averaged drift (%/decade)										
> 200 hPa	Time series too short						-2†			
100-200 hPa							+1			
50-100 hPa							+1			
20-50 hPa							+1			
10-20 hPa							+4			
5-10 hPa							+3			
2-5 hPa							+2			
1-2 hPa							(0)			
0.5-1 hPa							(-2)			
0.2-0.5 hPa							(-2)			

Comments

- All MIPAS measurement modes included; screening procedure as described in ORM 8.22 Readme file.
- Quoted values represent central values of each pressure-latitude bin. A dagger symbol (†) indicates where the range of values in the bin is larger than 10% or 5% per decade.
- Estimates between brackets () are potentially subject to larger sampling uncertainties due to the sparsity of the network. These values should therefore be considered with care.
- There is no clear evidence for a seasonal cycle in the bias or dispersion, except perhaps in the middle stratosphere at NH mid-latitudes. Another, notable exception is in the Antarctic LS during the ozone hole season (on average, a +5-15% bias is seen in late August and a –(10-15)% bias in October).

III.4 Methane

Using co-location criteria of 300 km and 3 hours, 2767 unique CH4 profile measurements from nine FTIR stations have been found to coincide with the MIPAS L2 V5 to V8 observations (note that the number of subcolumn comparisons can be different because of vertical integration constraints). Time series of the yearly relative MIPAS CH4 bias and spread with respect to these measurements are plotted in Figure 22. The bias is calculated as the weighted median relative difference, while the spread equals the 68 % interpercentile of the set of relative differences. For each FTIR instrument, these difference statistics are shown for three subcolumns integrated between 9 and 12 km, 12 and 30 km, and 30 and 60 km, which each contain roughly one degree of freedom in the retrieval. The median (bias) and 68 % interpercentile (spread) of the 12-30 km profile differences are added as well, whereby the individual MIPAS profiles have been vertically smoothed using the coincident FTIR averaging kernel matrices. Within each plot, all four MIPAS CH4 retrieval products under consideration are overplotted for intercomparison. Subcolumn difference statistics for all nine FTIR stations, subdivided over five latitude bands, are moreover collected for MIPAS CH4 L2 V8 in Table 11. The following observations can be made:

- The CH4 comparison results show a globally (without the Antarctic) and vertically consistent MIPAS V8 positive bias of about 3 to 10 % and a similar spread below 30 km, increasing above due to decreasing concentrations and appearance of fluctuations in the comparisons, especially in the first years of the MIPAS instrument operation. This means that median differences are at the edge of being significant. For all four product versions, a consistent 5 to 10 % positive bias and a 10 to 15 % interpercentile spread are observed.
- Despite the typically smaller number of comparisons for the lowest subcolumn (9-12 km), which is due to the FTIR instrument measurement range not always reaching below 9 km, the comparison statistics are similar to those of higher subcolumns. This indicates that the bias and spread values are also vertically consistent (although a smaller number of comparisons typically increases the dispersion).
- At all stations and for all three subcolumns the ORM V8 typically shows an observable bias reduction (5-10 %) in the MIPAS full resolution sensing period w.r.t. V7, yet apparently at the cost of a small bias increase (order of a few percent only) in the optimised resolution period. As a result, the MIPAS CH4 bias becomes more consistent throughout the entire mission time range (2002-2012). The order of 5 % per decade negative drift for the CH4 subcolumns that was estimated for the V7 processing, although statistically insignificant, therefore is clearly reduced in V8.
- The 12-30 km difference profile shape looks in agreement with the MIPAS balloon comparisons (at Kiruna, see MIPAS QWG, 2020), with a small vertical dependence, being mostly constant above 18 to 20 km, while going down to lower values below.

Table 11: CH4 subcolumn difference statistics for MIPAS ORM 8.22 retrievals versus coincident FTIR measurements, subdivided over five latitude bands.

ORM 8.22	# stats.	# comps.	bias [%]	spread [%]	bias [%]	spread [%]	bias [%]	spread [%]
			9-12 km		12-30 km		30-60 km	
60N-90N	4	1385	+6.5	5.9	+7.4	6.1	+3.1	19.1
30N-60N	3	664	+5.0	7.7	+4.0	6.8	+6.3	15.5
30N-30S	1	358	+6.5	6.5	+4.5	6.3	+13.0	6.5
30S-60S	1	360	+10.5	3.3	+7.0	5.8	+18.5	10.5
60S-90S	0	0						

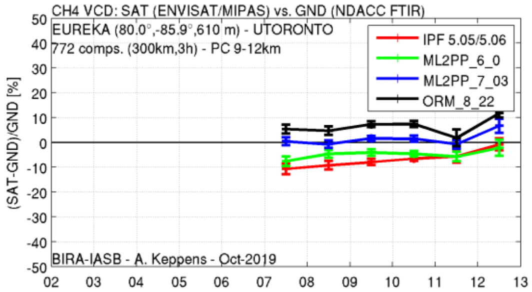
CH4 VCD: SAT (ENVISAT/MIPAS) vs. GND (NDACC FTIR)
EUREKA (80.0°,-85.9°,610 m) - UTORONTO
772 comps. (300km,3h) - PC 9-12km
IPF 5.05/5.06
ML2PP_6_0
ML2PP_7_03
ORM_8_22
(SAT-GND)/GND [%]
BIRA-IASB - A. Keppens - Oct-2019

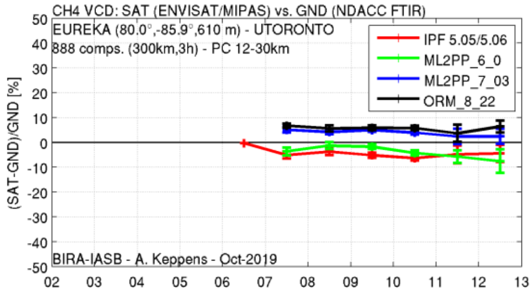
CH4 VCD: SAT (ENVISAT/MIPAS) vs. GND (NDACC FTIR)
EUREKA (80.0°,-85.9°,610 m) - UTORONTO
888 comps. (300km,3h) - PC 12-30km
IPF 5.05/5.06
ML2PP_6_0
ML2PP_7_03
ORM_8_22
(SAT-GND)/GND [%]
BIRA-IASB - A. Keppens - Oct-2019

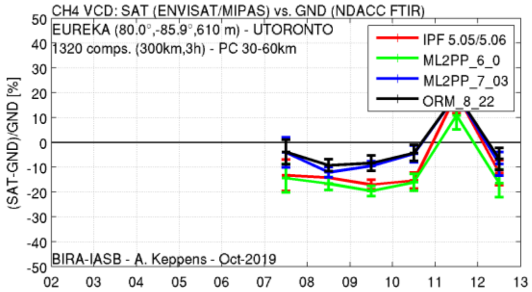
CH4 VCD: SAT (ENVISAT/MIPAS) vs. GND (NDACC FTIR)
EUREKA (80.0°,-85.9°,610 m) - UTORONTO
1320 comps. (300km,3h) - PC 30-60km
IPF 5.05/5.06
ML2PP_6_0
ML2PP_7_03
ORM_8_22
(SAT-GND)/GND [%]
BIRA-IASB - A. Keppens - Oct-2019

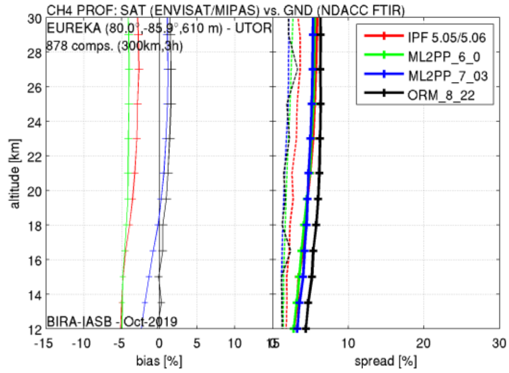
CH4 PROF: SAT (ENVISAT/MIPAS) vs. GND (NDACC FTIR)
EUREKA (80.0°,-85.9°,610 m) - UTOR
878 comps. (300km,3h)
IPF 5.05/5.06
ML2PP_6_0
ML2PP_7_03
ORM_8_22
altitude [km]
bias [%]
spread [%]
BIRA-IASB - Oct-2019

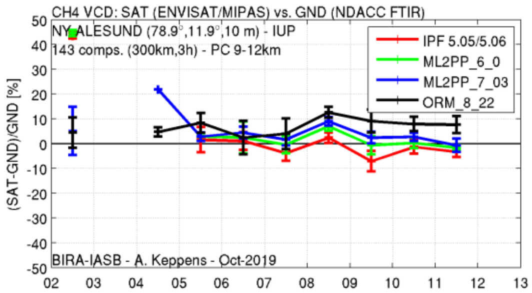
CH4 VCD: SAT (ENVISAT/MIPAS) vs. GND (NDACC FTIR)
NY ALESUND (78.9°,11.9°,10 m) - IUP
143 comps. (300km,3h) - PC 9-12km
IPF 5.05/5.06
ML2PP_6_0
ML2PP_7_03
ORM_8_22
(SAT-GND)/GND [%]
BIRA-IASB - A. Keppens - Oct-2019

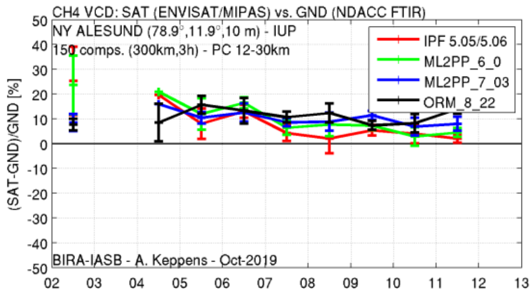
CH4 VCD: SAT (ENVISAT/MIPAS) vs. GND (NDACC FTIR)
NY ALESUND (78.9°,11.9°,10 m) - IUP
150 comps. (300km,3h) - PC 12-30km
IPF 5.05/5.06
ML2PP_6_0
ML2PP_7_03
ORM_8_22
(SAT-GND)/GND [%]
BIRA-IASB - A. Keppens - Oct-2019

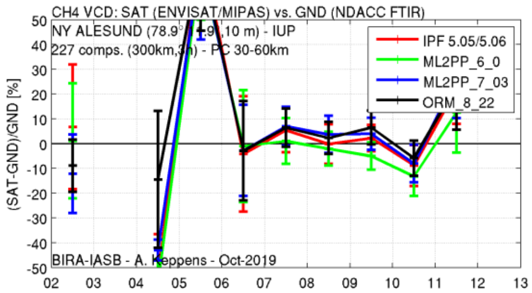
CH4 VCD: SAT (ENVISAT/MIPAS) vs. GND (NDACC FTIR)
NY ALESUND (78.9°,11.9°,10 m) - IUP
227 comps. (300km,3h) - PC 30-60km
IPF 5.05/5.06
ML2PP_6_0
ML2PP_7_03
ORM_8_22
(SAT-GND)/GND [%]
BIRA-IASB - A. Keppens - Oct-2019

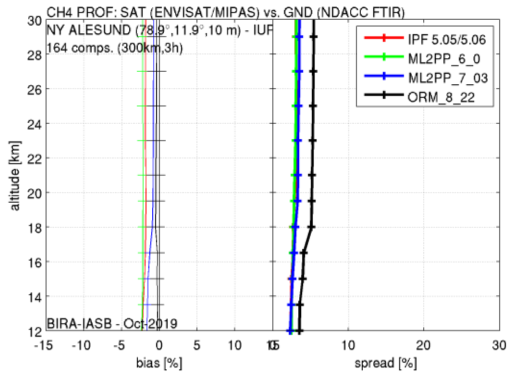
CH4 PROF: SAT (ENVISAT/MIPAS) vs. GND (NDACC FTIR)
NY ALESUND (78.9°,11.9°,10 m) - IUP
164 comps. (300km,3h)
IPF 5.05/5.06
ML2PP_6_0
ML2PP_7_03
ORM_8_22
altitude [km]
bias [%]
spread [%]
BIRA-IASB - Oct-2019

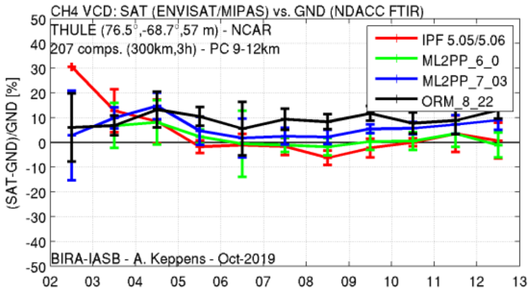
CH4 VCD: SAT (ENVISAT/MIPAS) vs. GND (NDACC FTIR)
THULE (76.5°,-68.7°,57 m) - NCAR
207 comps. (300km,3h) - PC 9-12km
IPF 5.05/5.06
ML2PP_6_0
ML2PP_7_03
ORM_8_22
(SAT-GND)/GND [%]
BIRA-IASB - A. Keppens - Oct-2019

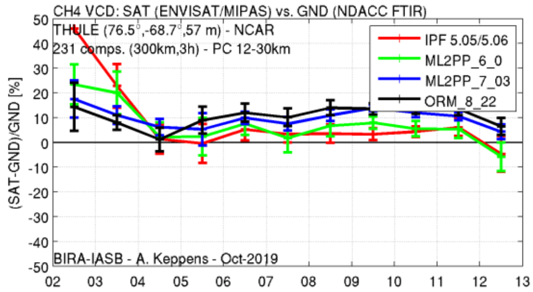
CH4 VCD: SAT (ENVISAT/MIPAS) vs. GND (NDACC FTIR)
THULE (76.5°,-68.7°,57 m) - NCAR
231 comps. (300km,3h) - PC 12-30km
IPF 5.05/5.06
ML2PP_6_0
ML2PP_7_03
ORM_8_22
(SAT-GND)/GND [%]
BIRA-IASB - A. Keppens - Oct-2019

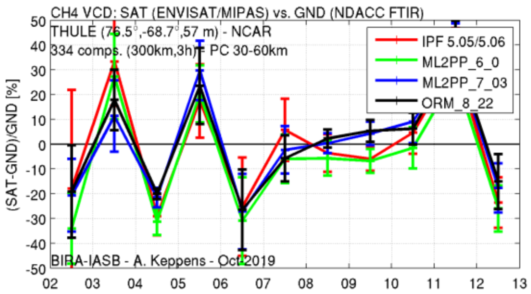
CH4 VCD: SAT (ENVISAT/MIPAS) vs. GND (NDACC FTIR)
THULE (76.5°,-68.7°,57 m) - NCAR
334 comps. (300km,3h) - PC 30-60km
IPF 5.05/5.06
ML2PP_6_0
ML2PP_7_03
ORM_8_22
(SAT-GND)/GND [%]
BIRA-IASB - A. Keppens - Oct-2019

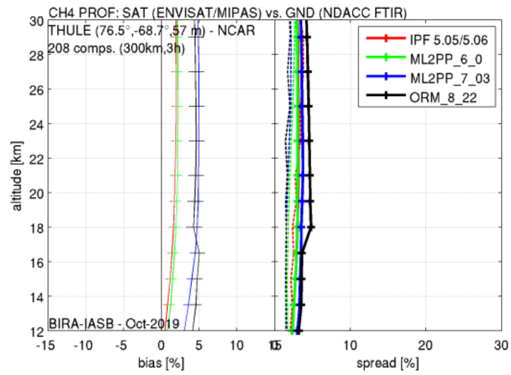
CH4 PROF: SAT (ENVISAT/MIPAS) vs. GND (NDACC FTIR)
THULE (76.5°,-68.7°,57 m) - NCAR
208 comps. (300km,3h)
IPF 5.05/5.06
ML2PP_6_0
ML2PP_7_03
ORM_8_22
altitude [km]
bias [%]
spread [%]
BIRA-IASB - Oct-2019

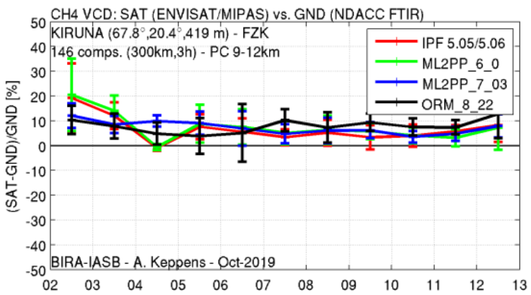
CH4 VCD: SAT (ENVISAT/MIPAS) vs. GND (NDACC FTIR)
KIRUNA (67.8°,20.4°,419 m) - FZK
146 comps. (300km,3h) - PC 9-12km
IPF 5.05/5.06
ML2PP_6_0
ML2PP_7_03
ORM_8_22
(SAT-GND)/GND [%]
BIRA-IASB - A. Keppens - Oct-2019

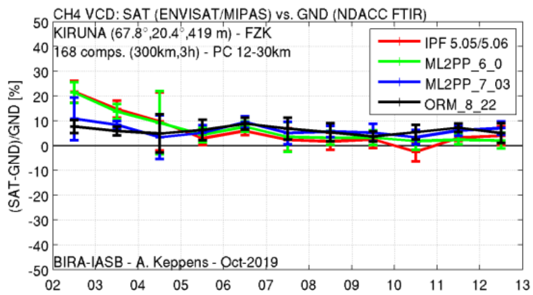
CH4 VCD: SAT (ENVISAT/MIPAS) vs. GND (NDACC FTIR)
KIRUNA (67.8°,20.4°,419 m) - FZK
168 comps. (300km,3h) - PC 12-30km
IPF 5.05/5.06
ML2PP_6_0
ML2PP_7_03
ORM_8_22
(SAT-GND)/GND [%]
BIRA-IASB - A. Keppens - Oct-2019

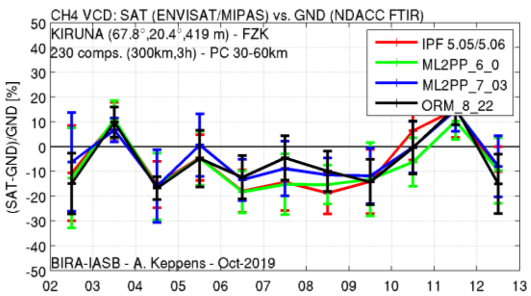
CH4 VCD: SAT (ENVISAT/MIPAS) vs. GND (NDACC FTIR)
KIRUNA (67.8°,20.4°,419 m) - FZK
230 comps. (300km,3h) - PC 30-60km
IPF 5.05/5.06
ML2PP_6_0
ML2PP_7_03
ORM_8_22
(SAT-GND)/GND [%]
BIRA-IASB - A. Keppens - Oct-2019

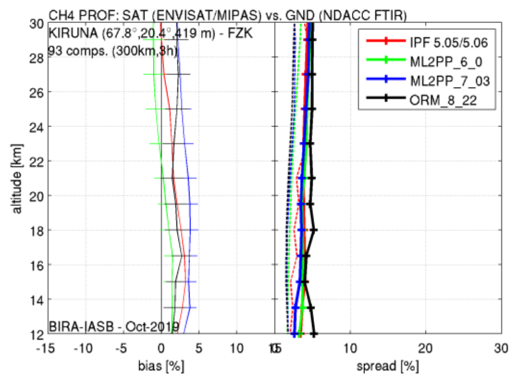
CH4 PROF: SAT (ENVISAT/MIPAS) vs. GND (NDACC FTIR)
KIRUNA (67.8°,20.4°,419 m) - FZK
93 comps. (300km,3h)
IPF 5.05/5.06
ML2PP_6_0
ML2PP_7_03
ORM_8_22
altitude [km]
bias [%]
spread [%]
BIRA-IASB - Oct-2019

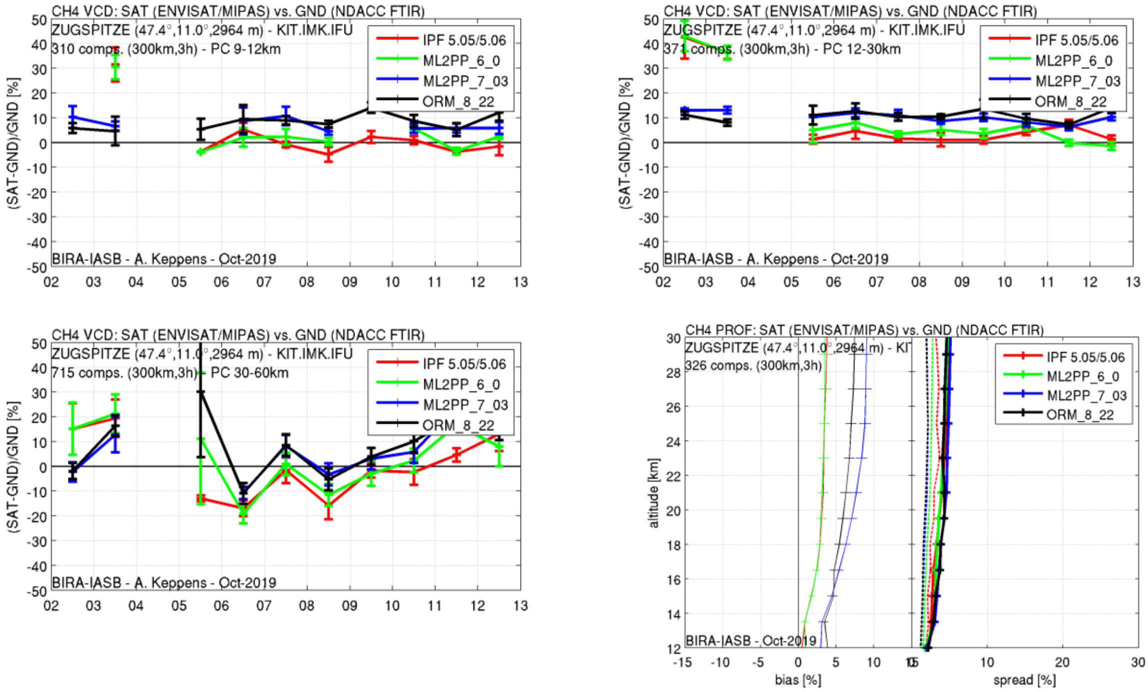
CH4 VCD: SAT (ENVISAT/MIPAS) vs. GND (NDACC FTIR)
ZUGSPITZE (47.4°,11.0°,2964 m) - KIT.IMK.IFU
310 comps. (300km,3h) - PC 9-12km
371 comps. (300km,3h) - PC 12-30km
715 comps. (300km,3h) - PC 30-60km
CH4 PROF: SAT (ENVISAT/MIPAS) vs. GND (NDACC FTIR)
326 comps. (300km,3h)
IPF 5.05/5.06
ML2PP_6_0
ML2PP_7_03
ORM_8_22
(SAT-GND)/GND [%]
altitude [km]
bias [%]
spread [%]
BIRA-IASB - A. Keppens - Oct-2019

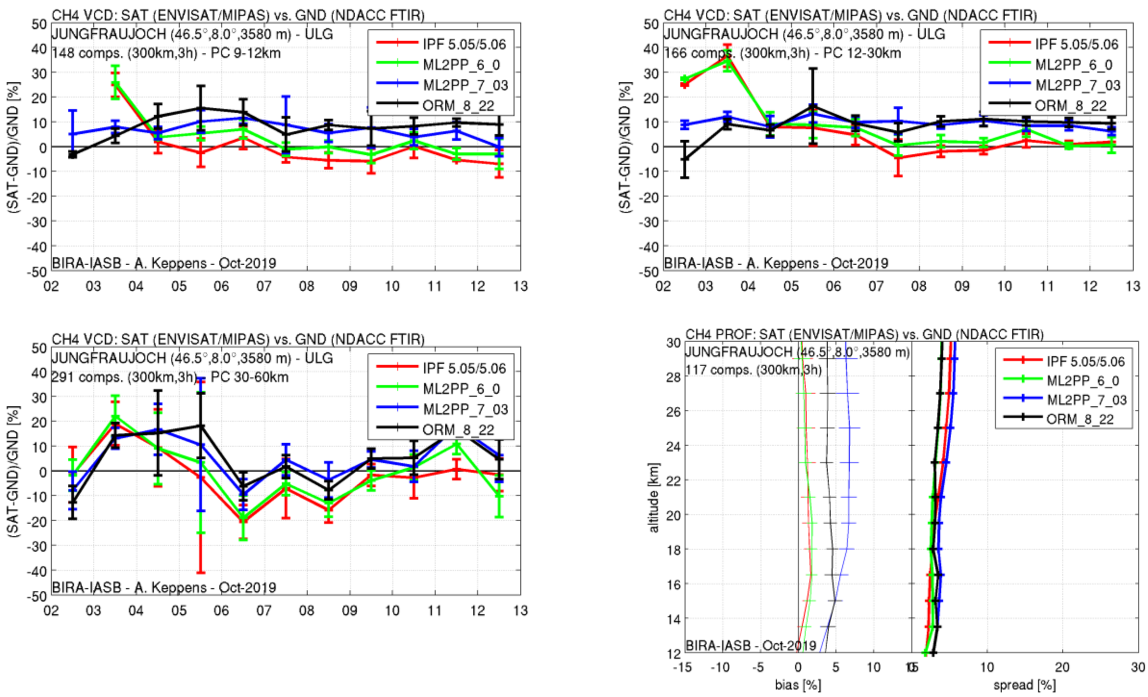
CH4 VCD: SAT (ENVISAT/MIPAS) vs. GND (NDACC FTIR)
JUNGFRAUJOCH (46.5°,8.0°,3580 m) - ULG
148 comps. (300km,3h) - PC 9-12km
166 comps. (300km,3h) - PC 12-30km
291 comps. (300km,3h) - PC 30-60km
CH4 PROF: SAT (ENVISAT/MIPAS) vs. GND (NDACC FTIR)
117 comps. (300km,3h)
IPF 5.05/5.06
ML2PP_6_0
ML2PP_7_03
ORM_8_22
(SAT-GND)/GND [%]
altitude [km]
bias [%]
spread [%]
BIRA-IASB - A. Keppens - Oct-2019

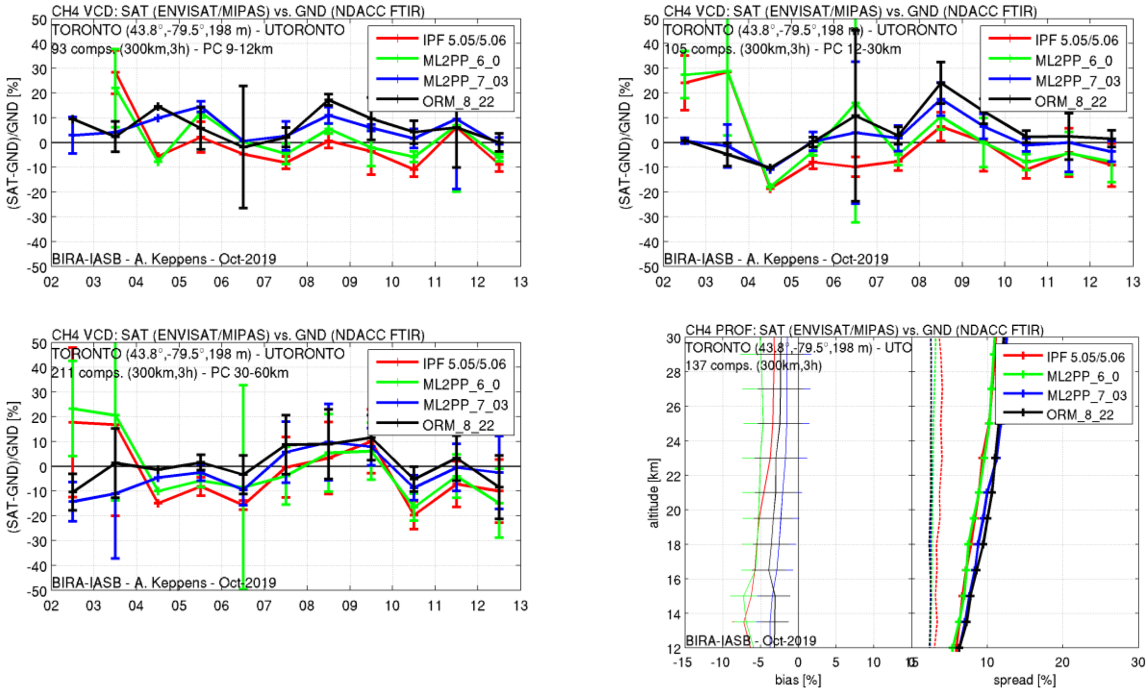
CH4 VCD: SAT (ENVISAT/MIPAS) vs. GND (NDACC FTIR)
TORONTO (43.8°,-79.5°,198 m) - UTORONTO
93 comps. (300km,3h) - PC 9-12km
105 comps. (300km,3h) - PC 12-30km
211 comps. (300km,3h) - PC 30-60km
CH4 PROF: SAT (ENVISAT/MIPAS) vs. GND (NDACC FTIR)
137 comps. (300km,3h)
IPF 5.05/5.06
ML2PP_6_0
ML2PP_7_03
ORM_8_22
(SAT-GND)/GND [%]
altitude [km]
bias [%]
spread [%]
BIRA-IASB - A. Keppens - Oct-2019
BIRA-IASB - Oct-2019

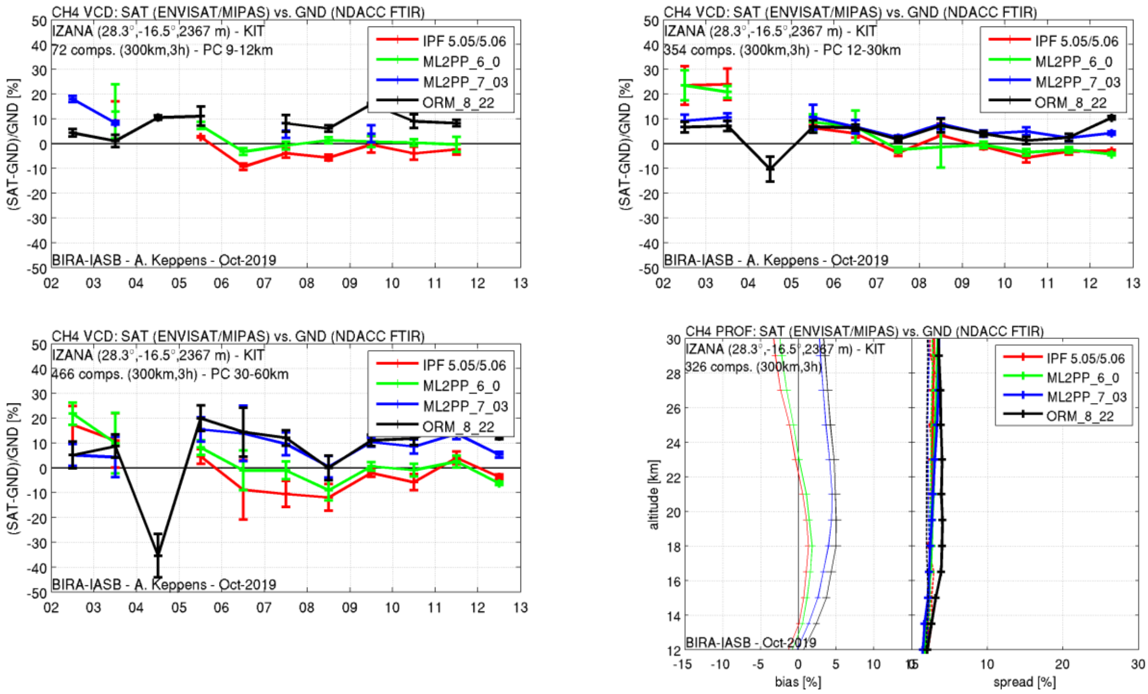
CH4 VCD: SAT (ENVISAT/MIPAS) vs. GND (NDACC FTIR)
IZANA (28.3°,-16.5°,2367 m) - KIT
72 comps. (300km,3h) - PC 9-12km
354 comps. (300km,3h) - PC 12-30km
466 comps. (300km,3h) - PC 30-60km
CH4 PROF: SAT (ENVISAT/MIPAS) vs. GND (NDACC FTIR)
326 comps. (300km,3h)
IPF 5.05/5.06
ML2PP_6_0
ML2PP_7_03
ORM_8_22
(SAT-GND)/GND [%]
altitude [km]
bias [%]
spread [%]
BIRA-IASB - A. Keppens - Oct-2019
BIRA-IASB - Oct-2019

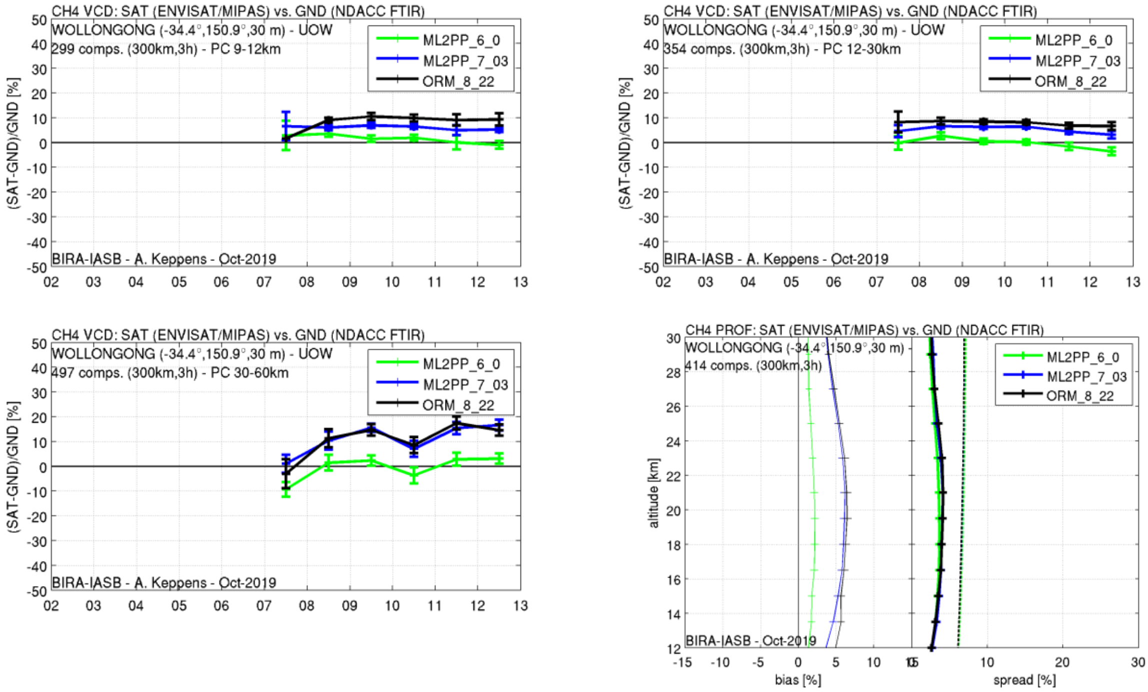

Figure 22: Comparison of four versions of operational MIPAS CH4 data to FTIR measurements at nine locations sorted north to south. Time series (2002-2012) show yearly medians (as relative bias) and 68 % interpercentiles (as vertical error bars) for three partial columns (9-12 km, 12-30 km, 30-60 km). The vertical profile plot shows the median (bias) and 68 % interpercentile (spread) of the 12-30 km profile differences for all co-locations combined. Horizontal error bars in the bias profile plots indicate 3σ standard errors on the means, while dashed lines represent to ex-ante satellite retrieval uncertainties. The MIPAS profiles are vertically smoothed using the coincident FTIR averaging kernel matrices. Positive values indicate too high MIPAS CH4 relative to the correlative data.

III.5 Nitric acid

Using co-location criteria of 300 km and 3 hours, 2508 unique HNO3 profile measurements from nine FTIR stations have been found to coincide with the MIPAS L2 V5 to V8 observations (note that the number of subcolumn comparisons can be different because of vertical integration constraints). Time series of the yearly relative MIPAS HNO3 bias and spread with respect to these FTIR measurements are plotted in Figure 23. The bias is calculated as the weighted median relative difference, while the spread equals the 68 % interpercentile of the set of relative differences. For each FTIR instrument, these difference statistics are shown for the subcolumn integrated between 12 and 30 km, which contains roughly one degree of freedom in the retrieval. The median (bias) and 68 % interpercentile (spread) of the corresponding 12-30 km profile differences are added as well, whereby the MIPAS profiles have been vertically smoothed using the coincident FTIR averaging kernel matrices. The four MIPAS HNO3 retrieval versions under consideration are overplotted in each plot for intercomparison. Moreover, the subcolumn difference statistics for HNO3 V8 at all nine FTIR stations, subdivided over five latitude bands, are collected in Table 12. The following observations can be made:

- The comparison results overall show a less than 5 % negative V8 bias (no Southern hemisphere data), which is smaller than for previous retrieval versions, and an order of 10 % dispersion, which is well within the typical FTIR spectrometer uncertainty.
- The comparisons show a significant vertical dependence, with a strong negative MIPAS HNO3 bias above 16-26 km, reaching a minimum at roughly 22 km in the Arctic or higher towards the equator, and spreads between 5 and 50 %, with a minimum around the altitude of the most negative bias. This vertical dependence is also seen in the MIPAS balloon comparisons at Kiruna., However, the MIPAS balloon results have an altitude-independent offset with respect to those reported here (different overall bias, see MIPAS QWG, 2020).
- A significant seasonal bias dependence is also observed, with values that are more negative in local winter times around the bias minimum (not shown).
- The time series plots show that no (significant) drifts can be observed for the 12 to 30 km profiles, also due to the occasional occurrence of relative difference outliers that might be due to the FTIR validation instruments.

Table 12: HNO3 12-30 km subcolumn difference statistics for MIPAS ORM 8.22 retrievals versus coincident FTIR measurements, subdivided over five latitude bands.

ORM 8.22	# stations	# comps.	bias [%]	spread [%]
			12-30 km	
60N-90N	4	2042	-4.1	8.1
30N-60N	3	220	-4.8	9.2
30N-30S	2	246	-2.5	10.9
30S-60S	0	0		
60S-90S	0	0		

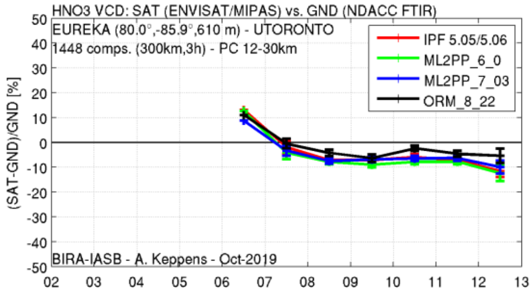
HNO3 VCD: SAT (ENVISAT/MIPAS) vs. GND (NDACC FTIR)
EUREKA (80.0°,-85.9°,610 m) - UTORONTO
1448 comps. (300km,3h) - PC 12-30km
IPF 5.05/5.06
ML2PP_6_0
ML2PP_7_03
ORM_8_22
(SAT-GND)/GND [%]
BIRA-IASB - A. Keppens - Oct-2019

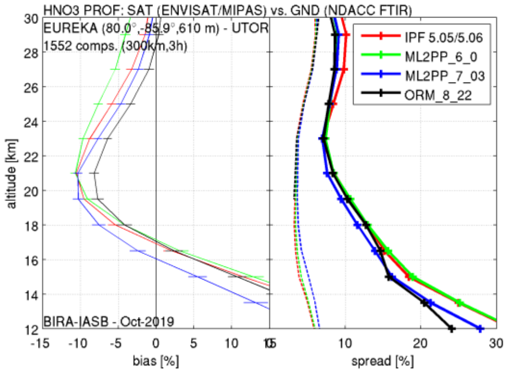
HNO3 PROF: SAT (ENVISAT/MIPAS) vs. GND (NDACC FTIR)
EUREKA (80.0°,-85.9°,610 m) - UTOR
1552 comps. (300km,3h)
IPF 5.05/5.06
ML2PP_6_0
ML2PP_7_03
ORM_8_22
altitude [km]
bias [%]
spread [%]
BIRA-IASB - Oct-2019

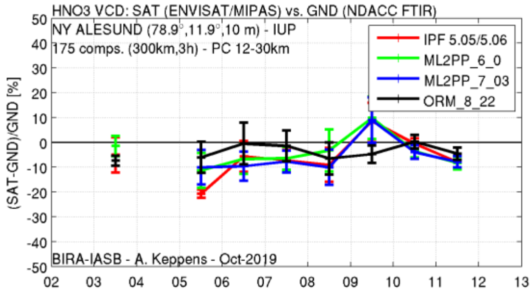
HNO3 VCD: SAT (ENVISAT/MIPAS) vs. GND (NDACC FTIR)
NY ALESUND (78.9°,11.9°,10 m) - IUP
175 comps. (300km,3h) - PC 12-30km
IPF 5.05/5.06
ML2PP_6_0
ML2PP_7_03
ORM_8_22
(SAT-GND)/GND [%]
BIRA-IASB - A. Keppens - Oct-2019

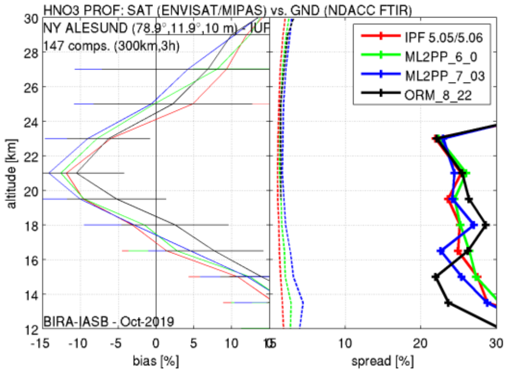
HNO3 PROF: SAT (ENVISAT/MIPAS) vs. GND (NDACC FTIR)
NY ALESUND (78.9°,11.9°,10 m) - IUP
147 comps. (300km,3h)
IPF 5.05/5.06
ML2PP_6_0
ML2PP_7_03
ORM_8_22
altitude [km]
bias [%]
spread [%]
BIRA-IASB - Oct-2019

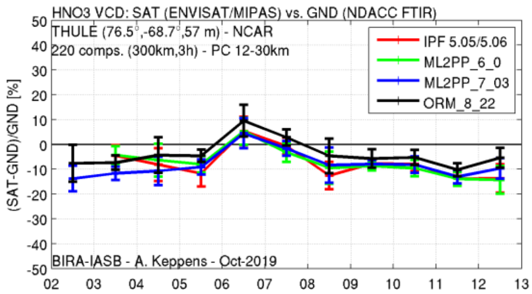
HNO3 VCD: SAT (ENVISAT/MIPAS) vs. GND (NDACC FTIR)
THULE (76.5°,-68.7°,57 m) - NCAR
220 comps. (300km,3h) - PC 12-30km
IPF 5.05/5.06
ML2PP_6_0
ML2PP_7_03
ORM_8_22
(SAT-GND)/GND [%]
BIRA-IASB - A. Keppens - Oct-2019

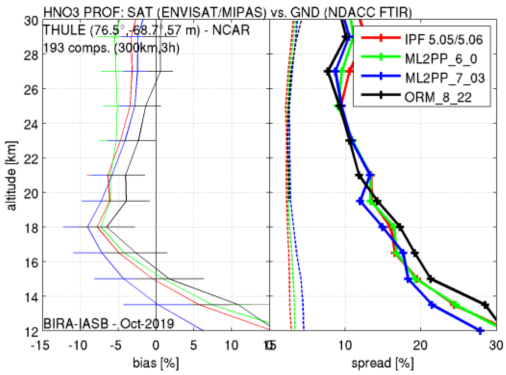
HNO3 PROF: SAT (ENVISAT/MIPAS) vs. GND (NDACC FTIR)
THULE (76.5°,-68.7°,57 m) - NCAR
193 comps. (300km,3h)
IPF 5.05/5.06
ML2PP_6_0
ML2PP_7_03
ORM_8_22
altitude [km]
bias [%]
spread [%]
BIRA-IASB - Oct-2019

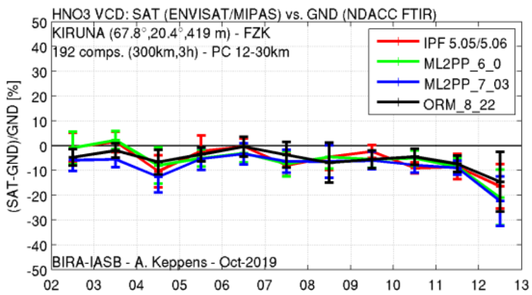
HNO3 VCD: SAT (ENVISAT/MIPAS) vs. GND (NDACC FTIR)
KIRUNA (67.8°,20.4°,419 m) - FZK
192 comps. (300km,3h) - PC 12-30km
IPF 5.05/5.06
ML2PP_6_0
ML2PP_7_03
ORM_8_22
(SAT-GND)/GND [%]
BIRA-IASB - A. Keppens - Oct-2019

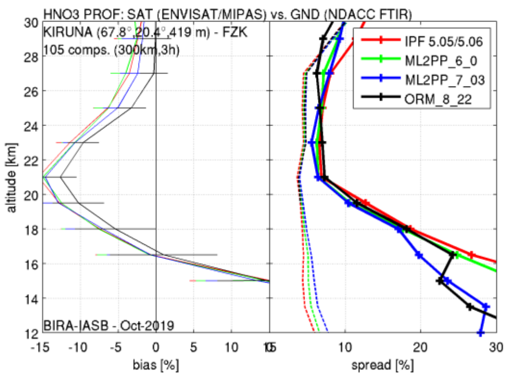
HNO3 PROF: SAT (ENVISAT/MIPAS) vs. GND (NDACC FTIR)
KIRUNA (67.8°,20.4°,419 m) - FZK
105 comps. (300km,3h)
IPF 5.05/5.06
ML2PP_6_0
ML2PP_7_03
ORM_8_22
altitude [km]
bias [%]
spread [%]
BIRA-IASB - Oct-2019

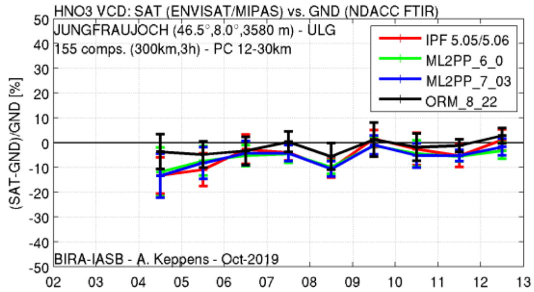
HNO3 VCD: SAT (ENVISAT/MIPAS) vs. GND (NDACC FTIR)
JUNGFRAUJOCH (46.5°,8.0°,3580 m) - ULG
155 comps. (300km,3h) - PC 12-30km
IPF 5.05/5.06
ML2PP_6_0
ML2PP_7_03
ORM_8_22
(SAT-GND)/GND [%]
BIRA-IASB - A. Keppens - Oct-2019

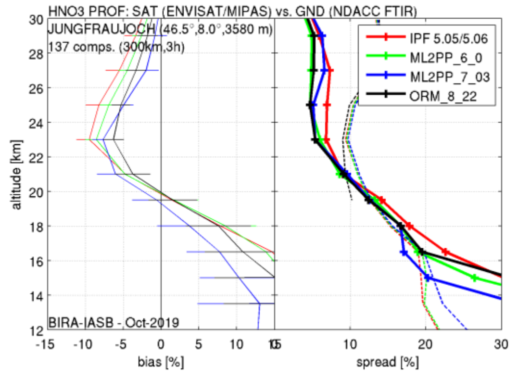
HNO3 PROF: SAT (ENVISAT/MIPAS) vs. GND (NDACC FTIR)
JUNGFRAUJOCH (46.5°,8.0°,3580 m)
137 comps. (300km,3h)
IPF 5.05/5.06
ML2PP_6_0
ML2PP_7_03
ORM_8_22
altitude [km]
bias [%]
spread [%]
BIRA-IASB - Oct-2019

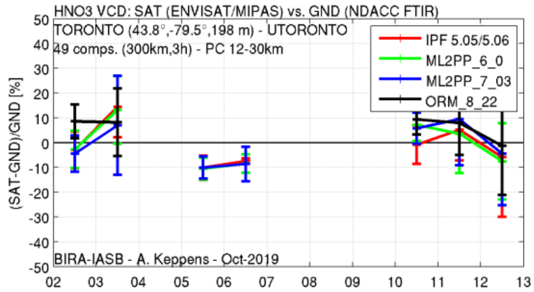
HNO3 VCD: SAT (ENVISAT/MIPAS) vs. GND (NDACC FTIR)
TORONTO (43.8°,-79.5°,198 m) - UTORONTO
49 comps. (300km,3h) - PC 12-30km
IPF 5.05/5.06
ML2PP_6_0
ML2PP_7_03
ORM_8_22
(SAT-GND)/GND [%]
BIRA-IASB - A. Keppens - Oct-2019

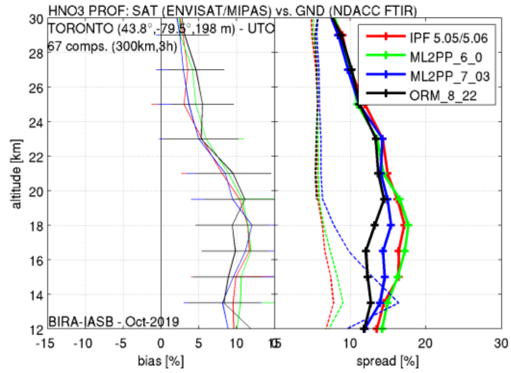
HNO3 PROF: SAT (ENVISAT/MIPAS) vs. GND (NDACC FTIR)
TORONTO (43.8°,-79.5°,198 m) - UTO
67 comps. (300km,3h)
IPF 5.05/5.06
ML2PP_6_0
ML2PP_7_03
ORM_8_22
altitude [km]
bias [%]
spread [%]
BIRA-IASB - Oct-2019

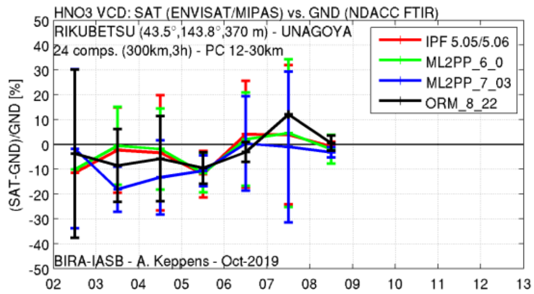
HNO3 VCD: SAT (ENVISAT/MIPAS) vs. GND (NDACC FTIR)
RIKUBETSU (43.5°,143.8°,370 m) - UNAGOYA
24 comps. (300km,3h) - PC 12-30km
IPF 5.05/5.06
ML2PP_6_0
ML2PP_7_03
ORM_8_22
(SAT-GND)/GND [%]
BIRA-IASB - A. Keppens - Oct-2019

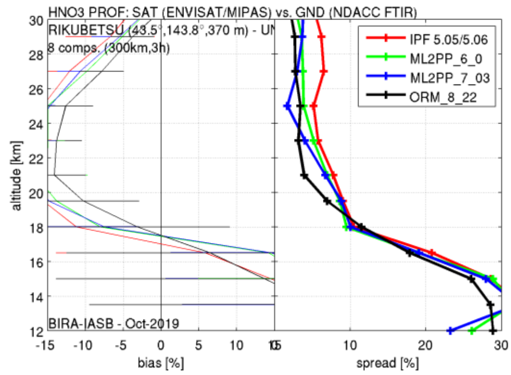
HNO3 PROF: SAT (ENVISAT/MIPAS) vs. GND (NDACC FTIR)
RIKUBETSU (43.5°,143.8°,370 m) - UN
8 comps. (300km,3h)
IPF 5.05/5.06
ML2PP_6_0
ML2PP_7_03
ORM_8_22
altitude [km]
bias [%]
spread [%]
BIRA-IASB - Oct-2019

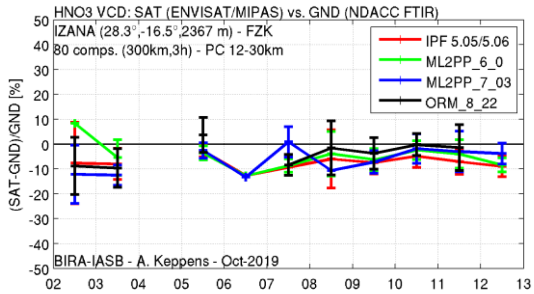
HNO3 VCD: SAT (ENVISAT/MIPAS) vs. GND (NDACC FTIR)
IZANA (28.3°,-16.5°,2367 m) - FZK
80 comps. (300km,3h) - PC 12-30km
IPF 5.05/5.06
ML2PP_6_0
ML2PP_7_03
ORM_8_22
(SAT-GND)/GND [%]
BIRA-IASB - A. Keppens - Oct-2019

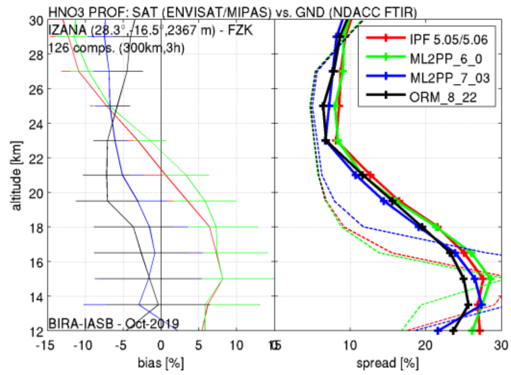
HNO3 PROF: SAT (ENVISAT/MIPAS) vs. GND (NDACC FTIR)
IZANA (28.3°,-16.5°,2367 m) - FZK
126 comps. (300km,3h)
IPF 5.05/5.06
ML2PP_6_0
ML2PP_7_03
ORM_8_22
altitude [km]
bias [%]
spread [%]
BIRA-IASB - Oct-2019

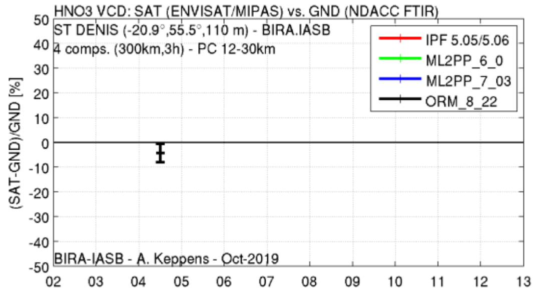

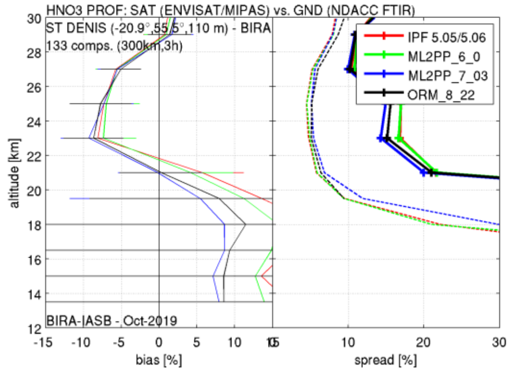

Figure 23: Comparison of four versions of MIPAS HNO3 data to FTIR measurements at nine locations sorted north to south. Time series (2002-2012) show yearly medians (as relative bias) and 68 % interpercentiles (as vertical error bars) for the 12-30 km partial column. The vertical profile plot shows the median (bias) and 68 % interpercentile (spread) of the 12-30 km profile differences for all co-locations combined. Horizontal error bars in the bias profile plots indicate 3σ standard errors on the means, while dashed lines represent to ex-ante satellite retrieval uncertainties. The MIPAS profiles are vertically smoothed using the coincident FTIR averaging kernel matrices. Positive values indicate too high MIPAS HNO3 relative to the correlative data.

III.6 Nitrous oxide

Using co-location criteria of 300 km and 3 hours, 3055 unique N_2O profile measurements from eight FTIR stations have been found to coincide with the MIPAS L2 V5 to V8 observations (note that the number of subcolumn comparisons can be different because of vertical integration constraints). Time series of the yearly relative MIPAS N2O bias and spread with respect to these FTIR measurements are plotted in Figure 24. The bias is calculated as the weighted median relative difference, while the spread equals the 68 % interpercentile of the set of relative differences. For each FTIR instrument, these difference statistics are shown for two subcolumns integrated between 9 and 12 km and between 12 and 30 km, which each contain roughly one degree of freedom in the retrieval. The median (bias) and 68 % interpercentile (spread) of the 12-30 km profile differences are added as well, whereby the MIPAS profiles have been vertically smoothed using the coincident FTIR averaging kernel matrices. Four MIPAS N2O retrieval products are overplotted here for intercomparison. The subcolumn difference statistics for all eight FTIR stations, subdivided over five latitude bands, are collected in Table 13. The following observations can be made:

- For all four product versions, a globally (without the Antarctic) and temporally consistent 5 to 10 % positive bias and a similar spread are observed, meaning that median differences are at the edge of being significant.
- Despite the typically smaller number of comparisons for the lowest subcolumn (9-12 km), which is due to the FTIR instrument measurement range not always reaching below 9 km, these comparison statistics are very similar for both subcolumns under consideration. This indicates that the bias and spread values are also vertically consistent (although a smaller number of comparisons typically increases the dispersion). This can also be seen from the smoothed vertical profile comparisons, which show little vertical dependence, except for the measurements at Zugspitze and Toronto. The latter is due to the FTIR kernels at these stations, and the occurrence of questionable measurements at Toronto between 2005 and 2008, as can also be seen in the yearly averaged subcolumn comparisons.
- The smoothed difference profile shape does not seem to be in agreement with the MIPAS balloon comparisons at Kiruna (MIPAS QWG, 2020), which show higher bias results than the few percent obtained here.
- The V8 (and V7) N2O bias is slightly reduced with respect to the V5 and V6 bias results in the full resolution period, yet at the cost of a small bias increase in the optimised resolution period. The order of 5 % per decade negative drift for the N2O subcolumns that was suggested by the ML2PP V7 processing, although statistically insignificant, as a result is reduced in V8.
- The large comparison uncertainties make it difficult to detect seasonal dependences or trends.

Table 13: N2O subcolumn difference statistics for MIPAS ORM 8.22 retrievals versus coincident FTIR measurements, subdivided over five latitude bands.

ORM 8.22	# stations	# comps.	bias [%]	spread [%]	bias [%]	spread [%]
			9-12 km		12-30 km	
60N-90N	3	1394	+6.7	6.2	+6.3	5.6
30N-60N	3	1109	+6.5	5.8	+4.5	4.7
30N-30S	1	179	+4.5	6.3	+3.5	3.3
30S-60S	1	373	+8.5	4.5	+4.0	4.0
60S-90S	0	0				

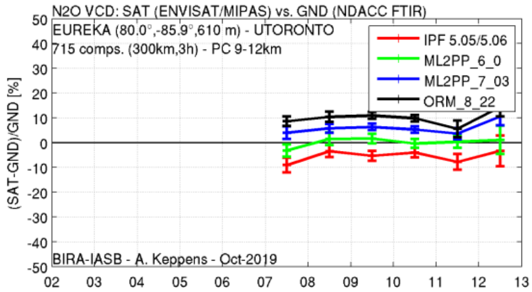
N2O VCD: SAT (ENVISAT/MIPAS) vs. GND (NDACC FTIR)
EUREKA (80.0°,-85.9°,610 m) - UTORONTO
715 comps. (300km,3h) - PC 9-12km
IPF 5.05/5.06
ML2PP_6_0
ML2PP_7_03
ORM_8_22
(SAT-GND)/GND [%]
BIRA-IASB - A. Keppens - Oct-2019

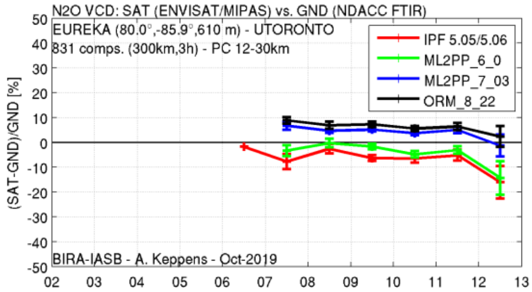
N2O VCD: SAT (ENVISAT/MIPAS) vs. GND (NDACC FTIR)
EUREKA (80.0°,-85.9°,610 m) - UTORONTO
831 comps. (300km,3h) - PC 12-30km
IPF 5.05/5.06
ML2PP_6_0
ML2PP_7_03
ORM_8_22
(SAT-GND)/GND [%]
BIRA-IASB - A. Keppens - Oct-2019

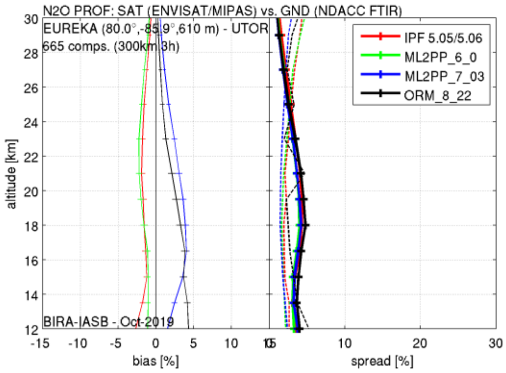
N2O PROF: SAT (ENVISAT/MIPAS) vs. GND (NDACC FTIR)
EUREKA (80.0°,-85.9°,610 m) - UTOR
665 comps. (300km,3h)
IPF 5.05/5.06
ML2PP_6_0
ML2PP_7_03
ORM_8_22
altitude [km]
bias [%]
spread [%]
BIRA-IASB - Oct-2019

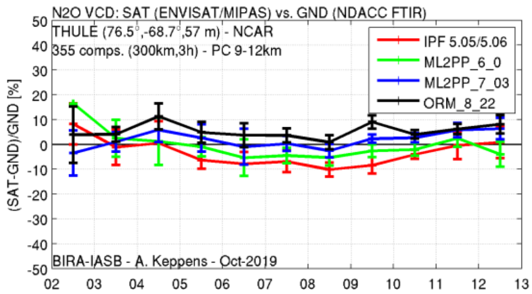
N2O VCD: SAT (ENVISAT/MIPAS) vs. GND (NDACC FTIR)
THULE (76.5°,-68.7°,57 m) - NCAR
355 comps. (300km,3h) - PC 9-12km
IPF 5.05/5.06
ML2PP_6_0
ML2PP_7_03
ORM_8_22
(SAT-GND)/GND [%]
BIRA-IASB - A. Keppens - Oct-2019

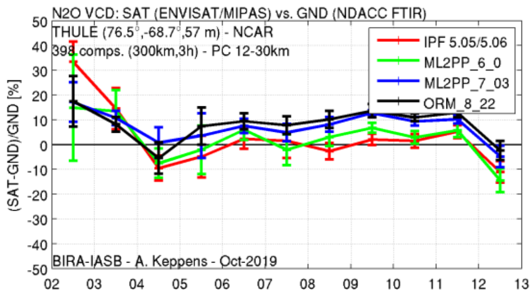
N2O VCD: SAT (ENVISAT/MIPAS) vs. GND (NDACC FTIR)
THULE (76.5°,-68.7°,57 m) - NCAR
398 comps. (300km,3h) - PC 12-30km
IPF 5.05/5.06
ML2PP_6_0
ML2PP_7_03
ORM_8_22
(SAT-GND)/GND [%]
BIRA-IASB - A. Keppens - Oct-2019

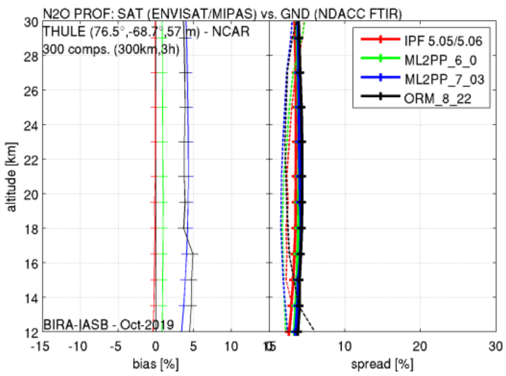
N2O PROF: SAT (ENVISAT/MIPAS) vs. GND (NDACC FTIR)
THULE (76.5°,-68.7°,57 m) - NCAR
300 comps. (300km,3h)
IPF 5.05/5.06
ML2PP_6_0
ML2PP_7_03
ORM_8_22
altitude [km]
bias [%]
spread [%]
BIRA-IASB - Oct-2019

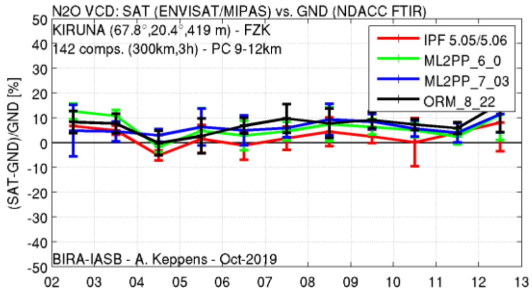
N2O VCD: SAT (ENVISAT/MIPAS) vs. GND (NDACC FTIR)
KIRUNA (67.8°,20.4°,419 m) - FZK
142 comps. (300km,3h) - PC 9-12km
IPF 5.05/5.06
ML2PP_6_0
ML2PP_7_03
ORM_8_22
(SAT-GND)/GND [%]
BIRA-IASB - A. Keppens - Oct-2019

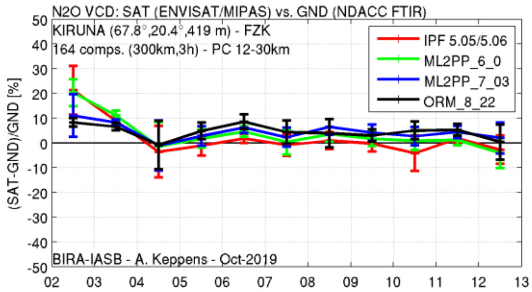
N2O VCD: SAT (ENVISAT/MIPAS) vs. GND (NDACC FTIR)
KIRUNA (67.8°,20.4°,419 m) - FZK
164 comps. (300km,3h) - PC 12-30km
IPF 5.05/5.06
ML2PP_6_0
ML2PP_7_03
ORM_8_22
(SAT-GND)/GND [%]
BIRA-IASB - A. Keppens - Oct-2019

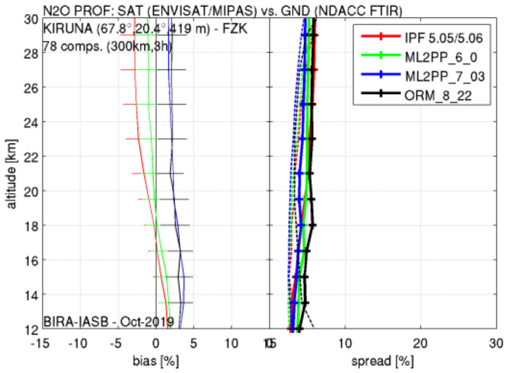
N2O PROF: SAT (ENVISAT/MIPAS) vs. GND (NDACC FTIR)
KIRUNA (67.8°,20.4°,419 m) - FZK
78 comps. (300km,3h)
IPF 5.05/5.06
ML2PP_6_0
ML2PP_7_03
ORM_8_22
altitude [km]
bias [%]
spread [%]
BIRA-IASB - Oct-2019

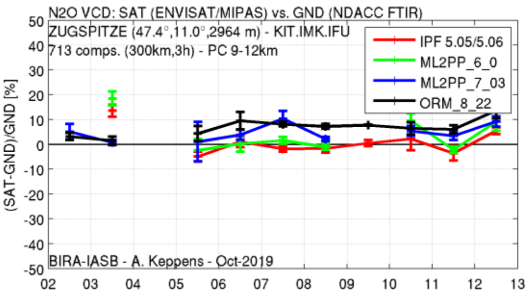
N2O VCD: SAT (ENVISAT/MIPAS) vs. GND (NDACC FTIR)
ZUGSPITZE (47.4°,11.0°,2964 m) - KIT.IMK.IFU
713 comps. (300km,3h) - PC 9-12km
IPF 5.05/5.06
ML2PP_6_0
ML2PP_7_03
ORM_8_22
(SAT-GND)/GND [%]
BIRA-IASB - A. Keppens - Oct-2019

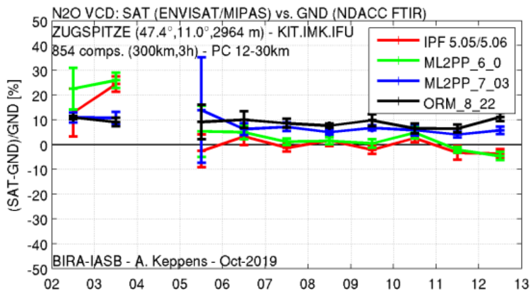
N2O VCD: SAT (ENVISAT/MIPAS) vs. GND (NDACC FTIR)
ZUGSPITZE (47.4°,11.0°,2964 m) - KIT.IMK.IFU
854 comps. (300km,3h) - PC 12-30km
IPF 5.05/5.06
ML2PP_6_0
ML2PP_7_03
ORM_8_22
(SAT-GND)/GND [%]
BIRA-IASB - A. Keppens - Oct-2019

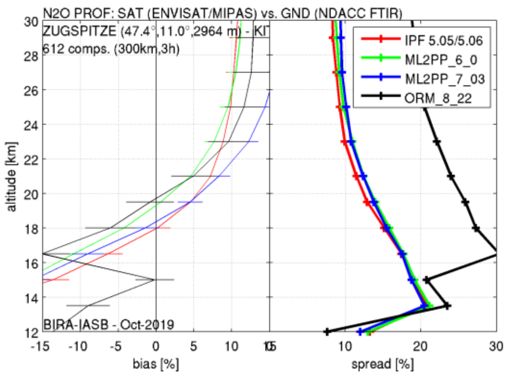
N2O PROF: SAT (ENVISAT/MIPAS) vs. GND (NDACC FTIR)
ZUGSPITZE (47.4°,11.0°,2964 m) - KI
612 comps. (300km,3h)
IPF 5.05/5.06
ML2PP_6_0
ML2PP_7_03
ORM_8_22
altitude [km]
bias [%]
spread [%]
BIRA-IASB - Oct-2019

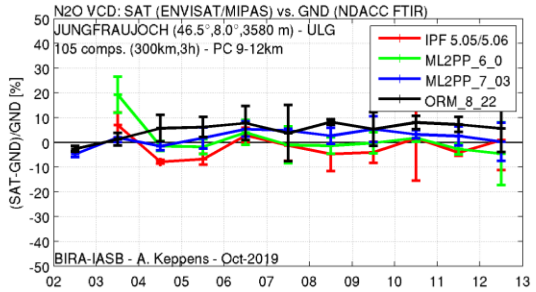
N2O VCD: SAT (ENVISAT/MIPAS) vs. GND (NDACC FTIR)
JUNGFRAUJOCH (46.5°,8.0°,3580 m) - ULG
105 comps. (300km,3h) - PC 9-12km
IPF 5.05/5.06
ML2PP_6_0
ML2PP_7_03
ORM_8_22
(SAT-GND)/GND [%]
BIRA-IASB - A. Keppens - Oct-2019

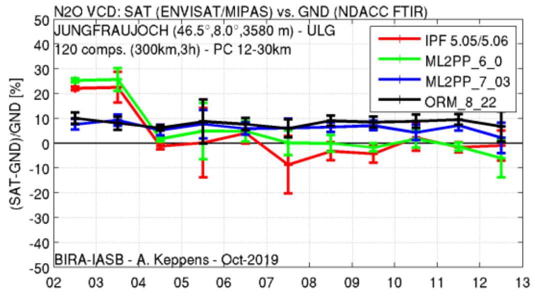
N2O VCD: SAT (ENVISAT/MIPAS) vs. GND (NDACC FTIR)
JUNGFRAUJOCH (46.5°,8.0°,3580 m) - ULG
120 comps. (300km,3h) - PC 12-30km
IPF 5.05/5.06
ML2PP_6_0
ML2PP_7_03
ORM_8_22
(SAT-GND)/GND [%]
BIRA-IASB - A. Keppens - Oct-2019

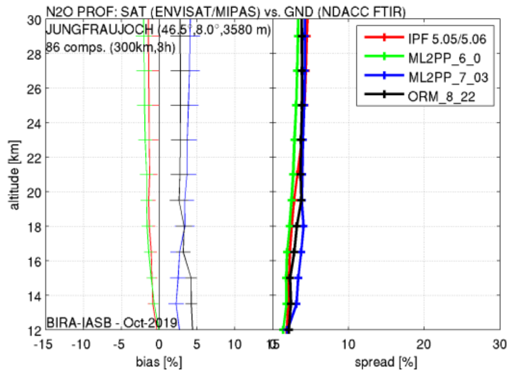
N2O PROF: SAT (ENVISAT/MIPAS) vs. GND (NDACC FTIR)
JUNGFRAUJOCH (46.5°,8.0°,3580 m)
86 comps. (300km,3h)
IPF 5.05/5.06
ML2PP_6_0
ML2PP_7_03
ORM_8_22
altitude [km]
bias [%]
spread [%]
BIRA-IASB - Oct-2019

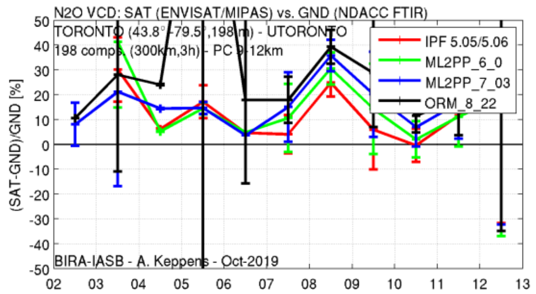
N2O VCD: SAT (ENVISAT/MIPAS) vs. GND (NDACC FTIR)
TORONTO (43.8°,-79.5°,198 m) - UTORONTO
198 comps. (300km,3h) - PC 9-12km
IPF 5.05/5.06
ML2PP_6_0
ML2PP_7_03
ORM_8_22
(SAT-GND)/GND [%]
BIRA-IASB - A. Keppens - Oct-2019

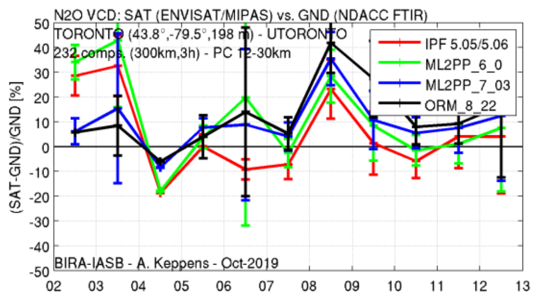
N2O VCD: SAT (ENVISAT/MIPAS) vs. GND (NDACC FTIR)
TORONTO (43.8°,-79.5°,198 m) - UTORONTO
232 comps. (300km,3h) - PC 12-30km
IPF 5.05/5.06
ML2PP_6_0
ML2PP_7_03
ORM_8_22
(SAT-GND)/GND [%]
BIRA-IASB - A. Keppens - Oct-2019

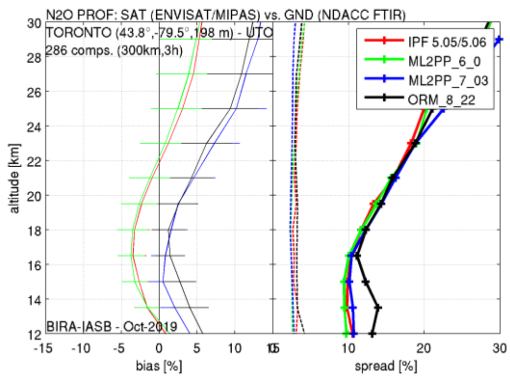
N2O PROF: SAT (ENVISAT/MIPAS) vs. GND (NDACC FTIR)
TORONTO (43.8°,-79.5°,198 m) - UTO
286 comps. (300km,3h)
IPF 5.05/5.06
ML2PP_6_0
ML2PP_7_03
ORM_8_22
altitude [km]
bias [%]
spread [%]
BIRA-IASB - Oct-2019

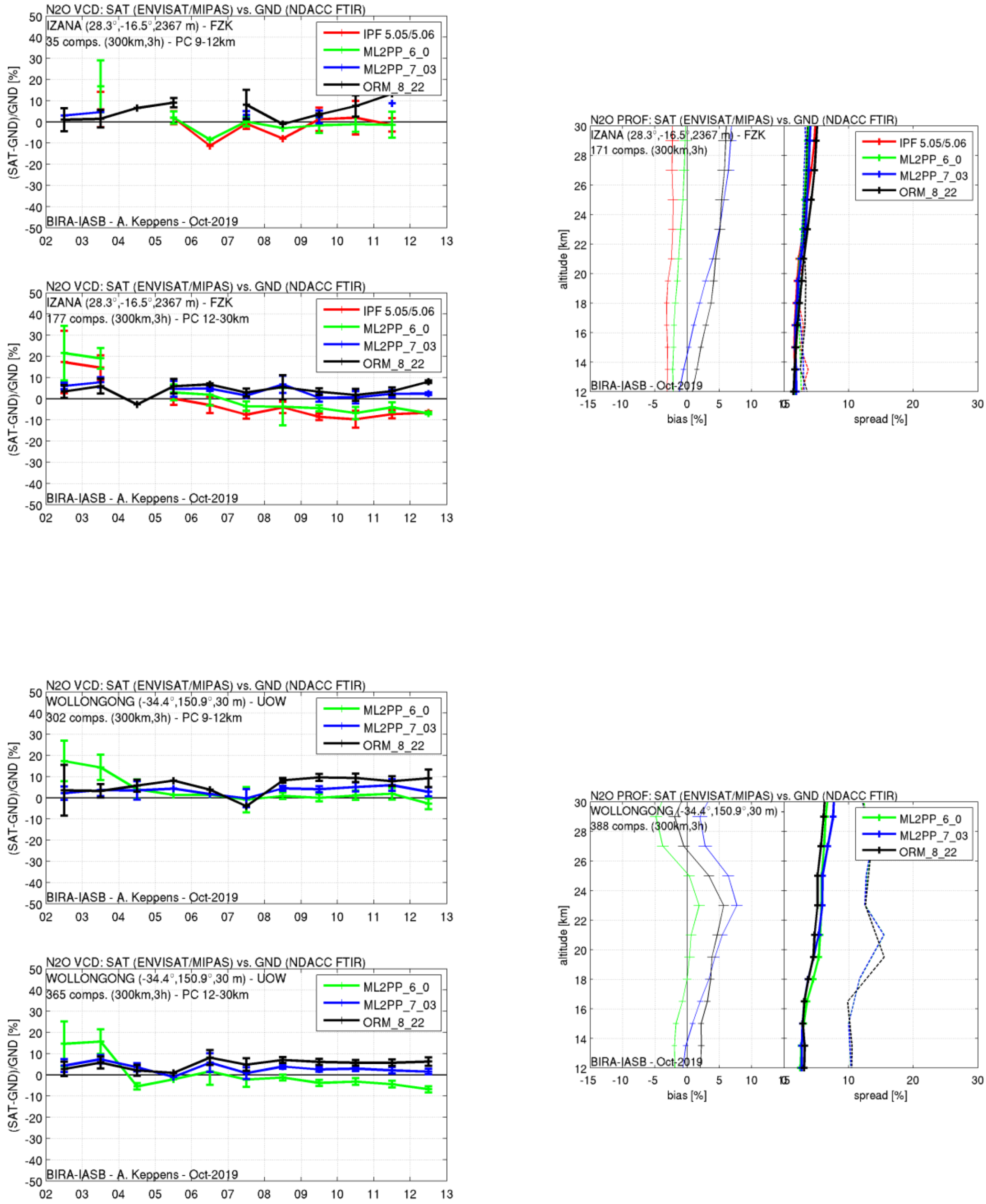

Figure 24: Comparison of four versions of MIPAS N2O data to FTIR measurements at eight locations sorted north to south. Time series (2002-2012) show yearly medians (as relative bias) and 68 % interpercentiles (as vertical error bars) for two partial columns (9-12 km, 12-30 km). The vertical profile plot shows the median (bias) and 68 % interpercentile (spread) of the 12-30 km profile differences for all co-locations combined. Horizontal error bars in the bias profile plots indicate 3σ standard errors on the means, while dashed lines represent to ex-ante satellite retrieval uncertainties. The MIPAS profiles are vertically smoothed using the coincident FTIR averaging kernel matrices. Positive values indicate too high MIPAS N2O relative to the correlative data.

IV Acknowledgements

This work was funded by ESA contract 4000112093/14/I/LG, CCN-1 and CCN-2, in support to the MIPAS Quality Working Group activities. The ground-based data used in this report has been obtained as part of the World Ozone and Ultraviolet Radiation Data Centre, the Network for the Detection of Atmospheric Composition Change (NDACC) and NASA's Southern Hemisphere Additional Ozonesonde programme and is publicly available (https://woudc.org, https://ndacc.org, https://tropo.gsfc.nasa.gov/shadoz). The PIs and staff at the stations are warmly thanked for their sustained effort on maintaining high quality measurements and for valuable scientific discussions. Special thanks go to the responsible for the FTIR measurements and/or data analysis at the different NDACC stations: Christian Hermans, Nicolas Kumps, and Minqiang Zhou from BIRA-IASB; Luciana Gatti from INPE; Uwe Raffalski from IRF Kiruna; Omaira García and Eliezer Sepulveda from AEMet; Cornelis Becker from SAHO; John Robinson from NIWA; Anatoly Poberovskii, Hamud Imkhasin, and Sergey Osipov from SPbU; Alejandro Bezanilla and César Guarín from UNAM; Pascal Jeseck from Sorbonne Université; Markus Rettinger from IMK-IFU; Hideaki Nakajima from NIES; and Christian Servais from Université de Liège.

V Bibliography

Calisesi, Y., Soebijanta, V. T., and van Oss, R.: *Regridding of remote soundings: Formulation and application to ozone profile comparison*, J. Geophys. Res., 110, D23306, doi:10.1029/2005JD006122, 2005.

Hubert, D., N. Kalb, J.-C. Lambert *et al*, *Multi-TASTE: Technical Assistance to Multi-mission Validation by Sounders, Spectrometers and Radiometers*, TN-BIRA-IASB-MultiTASTE-FR, Multi-TASTE Final Report / October 2008 – October 2011, 157 pp., http://earth.eo.esa.int/pcs/envisat/calval_res/2012/TN-BIRA-IASB-MultiTASTE-FR-iss1revC-Oct2012.pdf, 8 October 2012.

Hubert, D. et al.: *Ground-based assessment of the bias and long-term stability of 14 limb and occultation ozone profile data records*, Atmos. Meas. Tech., 9, 2497-2534, , doi:10.5194/amt-9-2497-2016, 2016a.

Hubert, D., A. Keppens, J. Granville, F. Hendrick, J.-C. Lambert, A. van Gijsel and P. Stammes, *Multi-TASTE Phase-F : Final Report (October 2013 – December 2015)*, TN-BIRA-IASB-MultiTASTE-Phase-F-FR-Iss2-RevA, Issue 2 / Rev. A, 79pp., https://earth.esa.int/documents/700255/702251/TN-BIRA-IASB-MultiTASTE-Phase-F-FR-Iss2-RevA.pdf, 1 February 2016b.

Hubert, D. et al.: *MIPAS ML2PP 7.03 profiles of T, altitude, O3, CH4, HNO3 and N2O*, TN-BIRA-IASB-MultiTASTE-Phase-F-MIPAS-ML2PP7-Iss1-RevB, https://earth.esa.int/documents/700255/2621625/TN-BIRA-IASB-MultiTASTE-Phase-F-MIPAS-ML2PP7-Iss1-RevB/34f7f395-75ef-46c4-855e-a0f9d225e7c2, 25 August 2016c.

Keppens, A., D. Hubert and J.-C. Lambert, *MIPAS Technical Note: Methodology for switching among MIPAS vertical averaging kernel matrix representations*, TN_BIRA-IASB_MIPAS-AKM-conversions_Keppens, Issue 1 / Rev. 2, 7 pp., 16 Oct 2014.

Keppens, A., Compernolle, S., Verhoelst, T., Hubert, D., and Lambert, J.-C.: *Harmonization and comparison of vertically resolved atmospheric state observations: methods, effects, and uncertainty budget*, Atmos. Meas. Tech., 12, 4379–4391, https://doi.org/10.5194/amt-12-4379-2019, 2019.

MIPAS Quality Working Group: *MIPAS Level 2 IPF 5.06 Readme*, ENVI-GSOP-EOGD-QD-11-0111, issue 2.0, https://envisat.esa.int/handbooks/availability/disclaimers/MIP_NL_2P_README_V5.pdf, 18 Oct 2011b.

MIPAS Quality Working Group: *MIPAS Level 2 ML2PP Version 6 Readme*, ENVI-GSOP-EOGD-QD-12-0116, issue 1.1, https://earth.esa.int/documents/700255/707722/ MIP_NL_2P_README_V6.0.pdf/1a6c6de8-35f3-400b-abd0-8ca8c0640453, 5 Jun 2012.

MIPAS Quality Working Group: *Product Quality Readme File for MIPAS Level 2 version 7.03 products*, ENVI-GSOP-EOGD-QD-16-0141, issue 1.0, https://earth.esa.int/documents/700255/2635669/RMF_0141+MIP_NL__2P_issue1.pdf/59beb833-5ad4-4301-8422-f41001da36d4, 7 Sep 2016.

MIPAS Quality Working Group: *Product Quality Readme File for MIPAS Level 2 version 8.2 products*, ESA-EOPG-EBA-TN-5, issue 1.0, 2020.

Payan, S., Camy-Peyret, C., Oelhaf, H., Wetzel, G., Maucher, G., Keim, C., Pirre, M., Huret, N., Engel, A., Volk, M. C., Kuellmann, H., Kuttippurath, J., Cortesi, U., Bianchini, G., Mencaraglia, F., Raspollini, P., Redaelli, G., Vigouroux, C., De Mazière, M., Mikuteit, S., Blumenstock, T., Velazco, V., Notholt, J., Mahieu, E., Duchatelet, P., Smale, D., Wood, S., Jones, N., Piccolo, C., Payne, V., Bracher, A., Glatthor, N., Stiller, G., Grunow, K., Jeseck, P., Te, Y., and Butz, A.: *Validation of version-4.61 methane and nitrous oxide observed by MIPAS*, Atmos. Chem. Phys., 9, 413-442, doi:10.5194/acp-9-413-2009, 2009.

Raspollini, P., Carli, B., Carlotti, M., Ceccherini, S., Dehn, A., Dinelli, B. M., Dudhia, A., Flaud, J.-M., López-Puertas, M., Niro, F., Remedios, J. J., Ridolfi, M., Sembhi, H., Sgheri, L., and von Clarmann, T.: *Ten years of MIPAS measurements with ESA Level 2 processor V6 – Part 1: Retrieval algorithm and diagnostics of the products*, Atmos. Meas. Tech., 6, 2419-2439, doi:10.5194/amt-6-2419-2013, 2013.

Rodgers, C. D. and Connor, B. J.: *Intercomparison of remote sounding instruments*, J. Geophys. Res., 108, D3, 4116, doi:10.1029/2002JD002299, 2003.

Stauffer, R. M., Morris, G. A., Thompson, A. M., Joseph, E., Coetzee, G. J. R., and Nalli, N. R.: *Propagation of radiosonde pressure sensor errors to ozonesonde measurements*, Atmos. Meas. Tech., 7, 65-79, doi:10.5194/amt-7-65-2014, 2014.

Vigouroux, C., De Mazière, M., Errera, Q., Chabrillat, S., Mahieu, E., Duchatelet, P., Wood, S., Smale, D., Mikuteit, S., Blumenstock, T., Hase, F., and Jones, N.: *Comparisons between ground-based FTIR and MIPAS N_2O and HNO_3 profiles before and after assimilation in BASCOE*, Atmos. Chem. Phys., 7, 377-396, doi:10.5194/acp-7-377-2007, 2007.

VI Acronyms and abbreviations

AK	Averaging Kernel
BIRA-IASB	Koninklijk Belgisch Instituut voor Ruimte-Aeronomie / Institut royal d'Aéronomie Spatiale de Belgique (Royal Belgian Institute for Space Aeronomy)
CF	Climate and Forecast (metadata conventions)
DIAL	Differential Absorption Lidar
Envisat	ESA's Environmental Satellite
ESA	European Space Agency / Agence spatiale européenne
FR	Full Resolution period (2002-2004)
FTIR	Fourier Transform Infrared Spectroscopy
GAW	WMO's Global Atmospheric Watch
HDF	Hierarchical Data Format
IPF	Instrument Processing Facility
JJA	June-July-August
Lidar	Light Detection and Ranging
LM	Lower Mesosphere
LS	Lower Stratosphere
MIPAS	Michelson Interferometer for Passive Atmospheric Sounding
ML2PP	MIPAS Level-2 Prototype Processor
MS	Middle Stratosphere
Multi-TASTE	Technical Assistance to Multi-mission Validation by Sounders, Spectrometers and Radiometers
MWR	MicroWave Radiometer
NDACC	Network for the Detection of Atmospheric Composition Change (formerly NDSC)
netCDF	Network Common Data Form
NH	Northern Hemisphere
OR	Optimised Resolution period (2005-2012)
ORM	Optimised Retrieval Model (processor)
pT retrieval	Pressure-temperature retrieval
QSWG	Quality Working Group
SH	Southern Hemisphere
SHADOZ	Southern Hemisphere ADditional Ozonesondes
SON	September-October-November
TASTE	Technical Assistance to Envisat validation by Soundings, Spectrometers and Radiometers
US	Upper Stratosphere
UT	Upper Troposphere
UV	Ultra Violet
VMR	Volume Mixing Ratio
WMO	World Meteorological Organization

VII Appendix: Evolution data quality operational MIPAS products

VII.1 Temperature

VII.1.1 Seasonal cycle

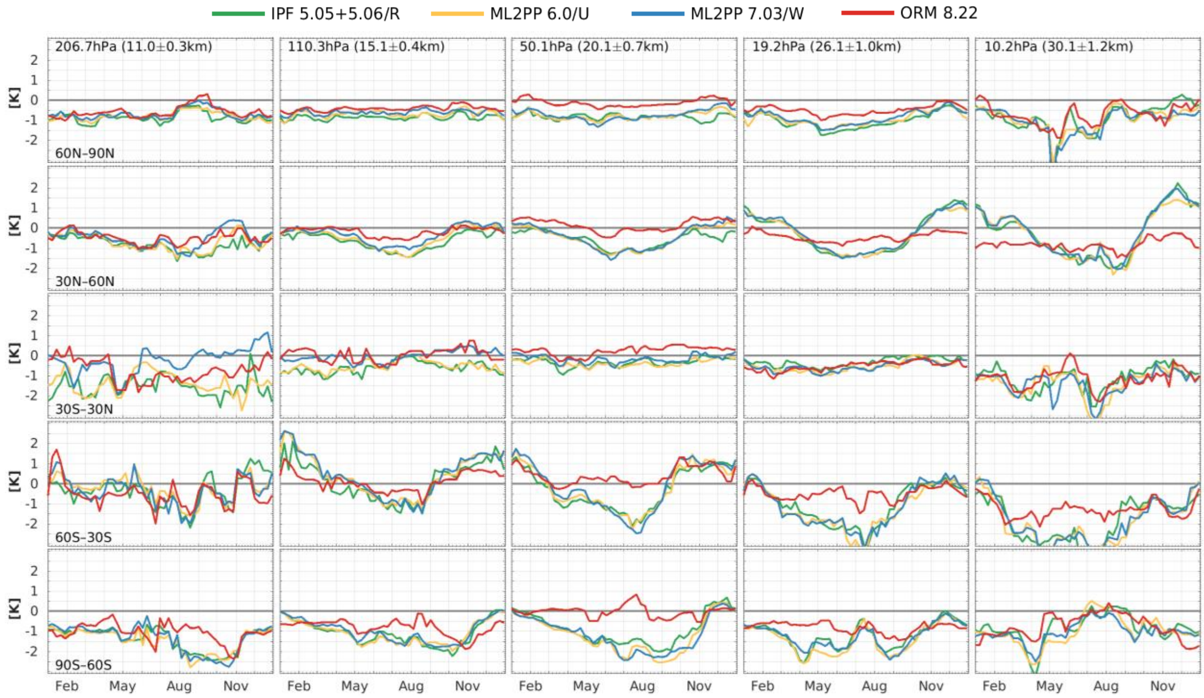

Figure 25: Seasonal dependence of the absolute difference of co-located MIPAS and radiosonde temperature profiles in different latitude zones and at different pressure levels. Colours represent different versions of the MIPAS operational data product. Curves show the median value in one-month moving windows. Positive values indicate too warm MIPAS temperature relative to correlative data. This complements Figure 4 in the main report.

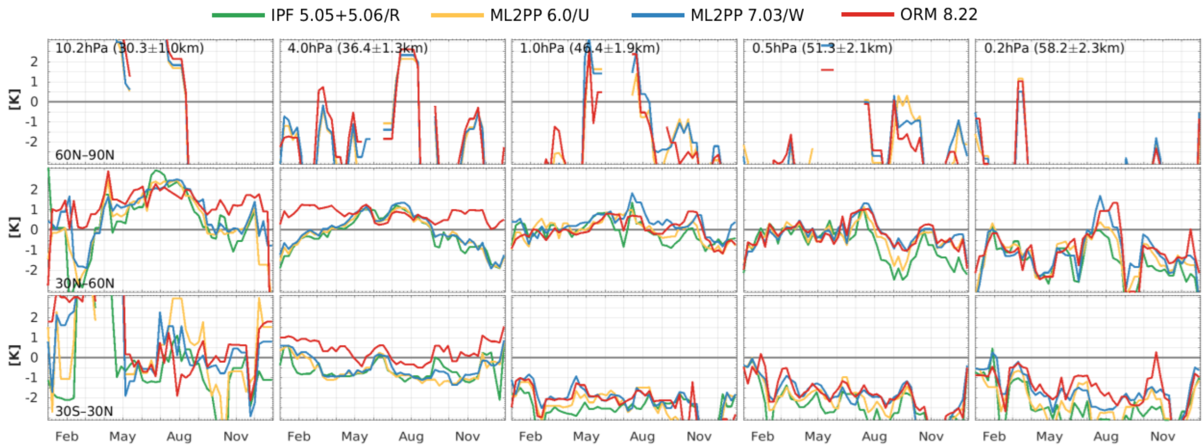

Figure 26: As in Figure 25, but for the comparisons to temperature lidar. This complements Figure 5 in the main report.

VII.1.2 Seasonal cycle : change w.r.t. MIPAS V7

This section shows time series of

$$(T_{MIPAS\_VX} - T_{GROUNDBASED}) - (T_{MIPAS\_V7} - T_{GROUNDBASED}),$$

where VX can be V5, V6 or V8.

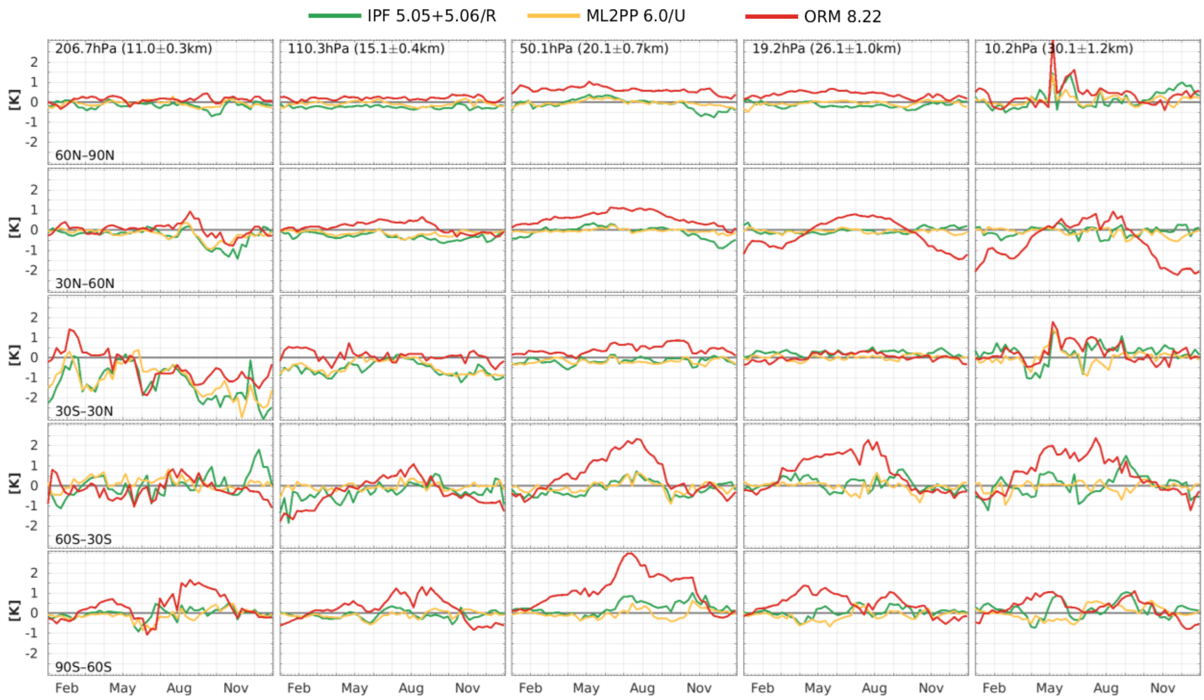

Figure 27: Difference between MIPAS minus radiosonde temperature comparison annual cycle for V5, V6 and V8 versus the comparison annual cycle of MIPAS V7 (see Figure 25).

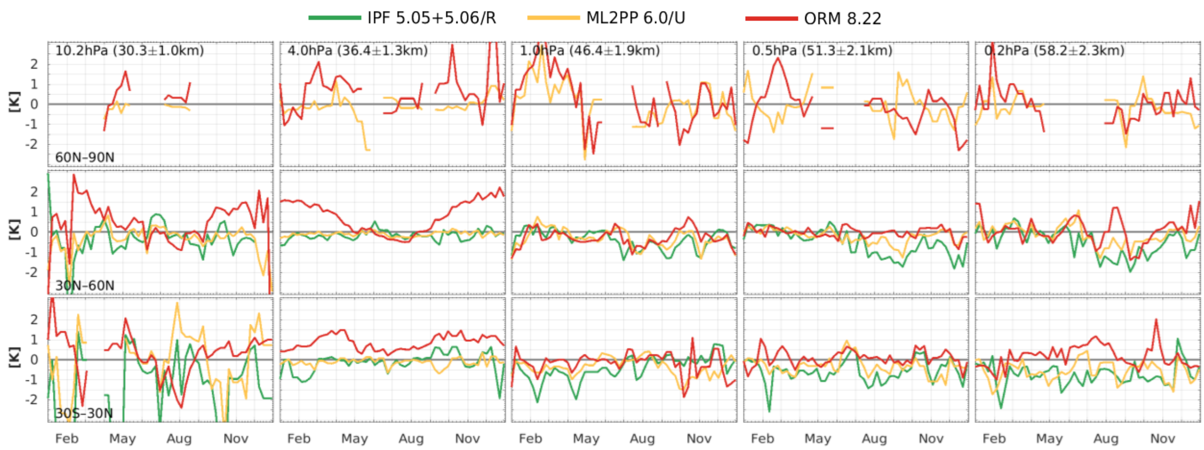

Figure 28: As in Figure 27, but for the comparisons to temperature lidar.

VII.1.3 Time series

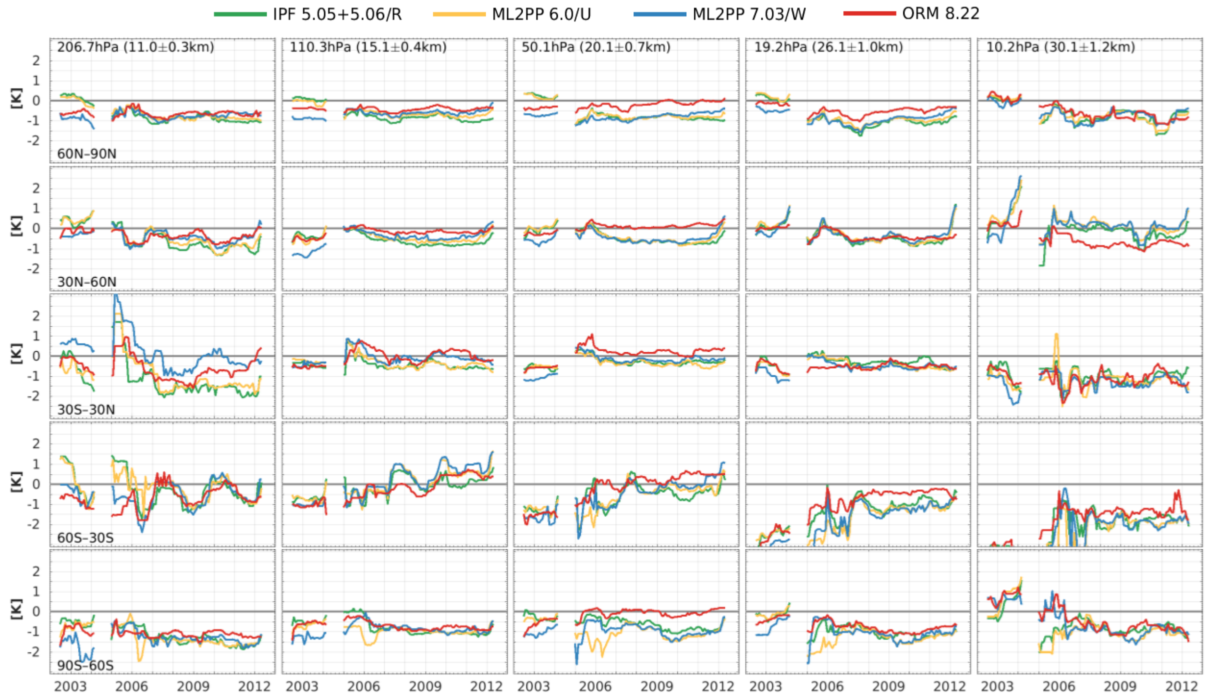

Figure 29: Absolute difference time series of co-located MIPAS and radiosonde temperature profiles in different latitude zones and at different pressure levels. Colours represent different versions of the MIPAS operational data product. Curves show the median value in 12-month moving windows. Positive values indicate too warm MIPAS temperature relative to correlative data. This complements Figure 2 in the main report.

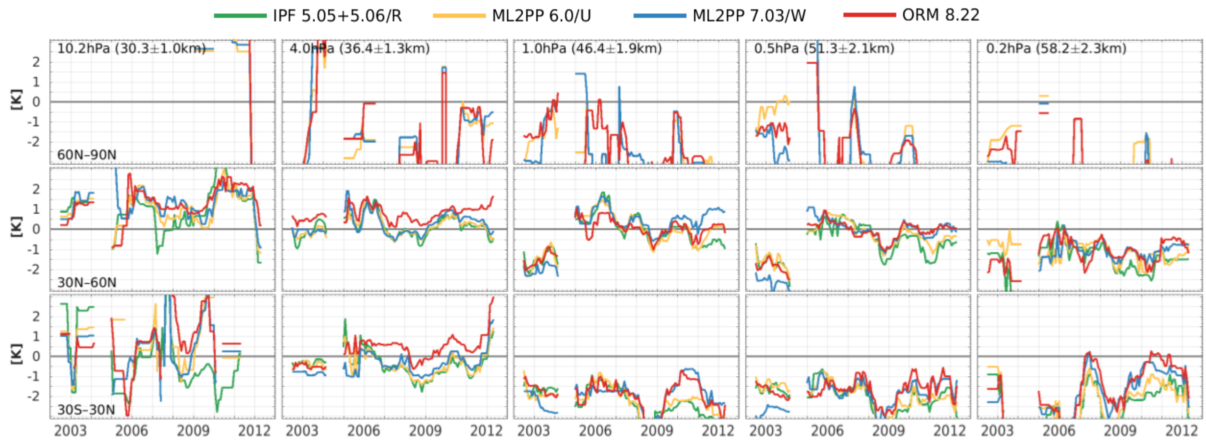

Figure 30: As in Figure 29, but for the comparisons to temperature lidar. This complements Figure 3 in the main report.

VII.1.4 Time series : change w.r.t. MIPAS V7

This section shows time series of

$$(T_{MIPAS\_VX} - T_{GROUNDBASED}) - (T_{MIPAS\_V7} - T_{GROUNDBASED}),$$

where VX can be V5, V6 or V8.

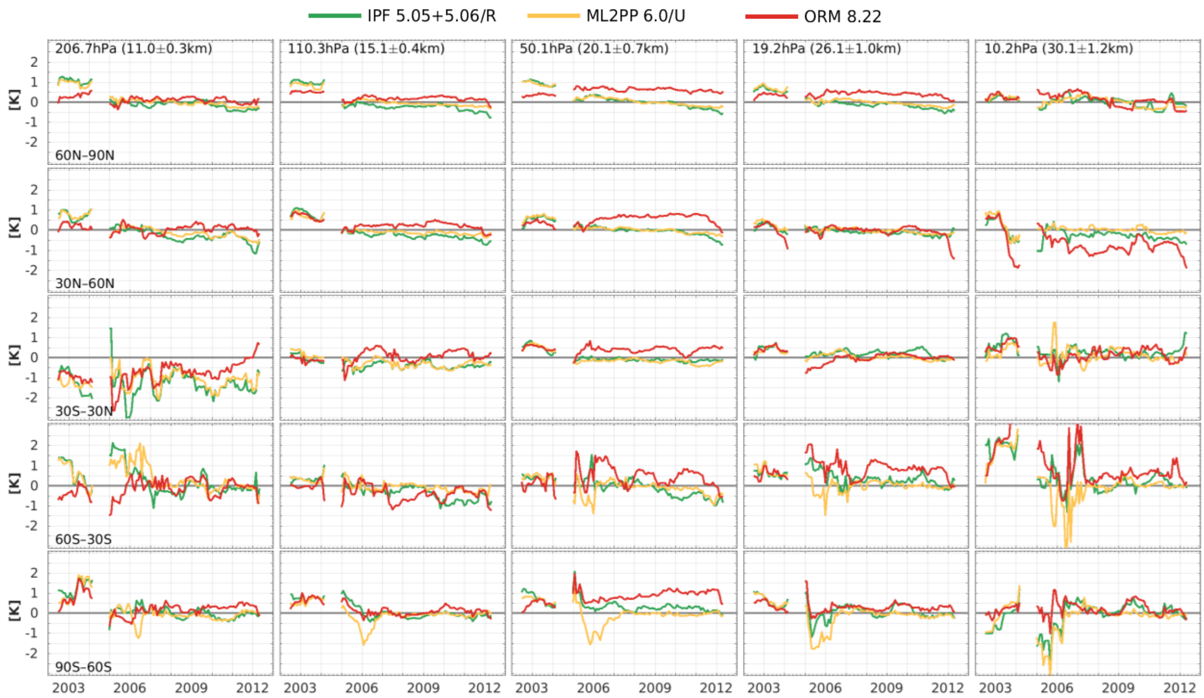

Figure 31: Difference between MIPAS minus radiosonde temperature comparison time series for V5, V6 and V8 versus the comparison time series of MIPAS V7 (see Figure 29).

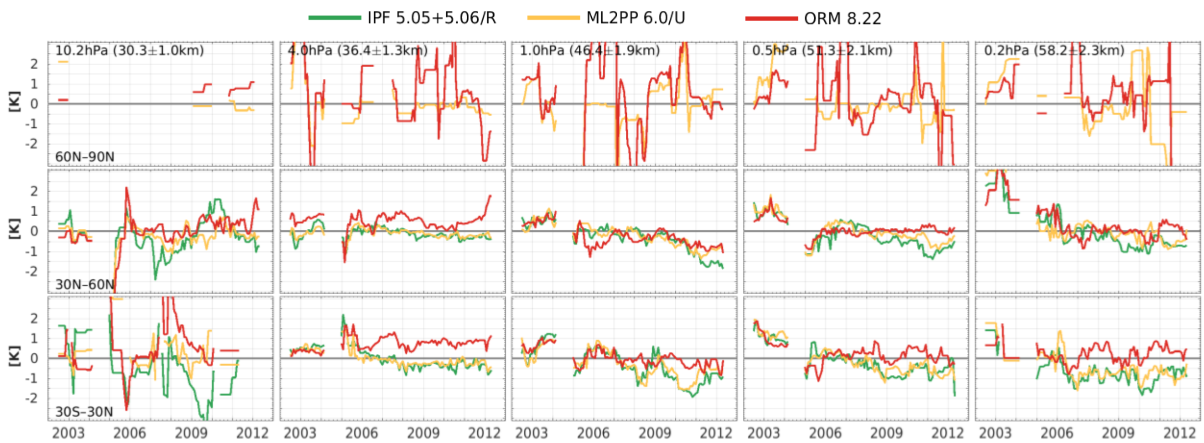

Figure 32: As in Figure 31, but for the comparisons to temperature lidar.

VII.1.5 Long-term drift

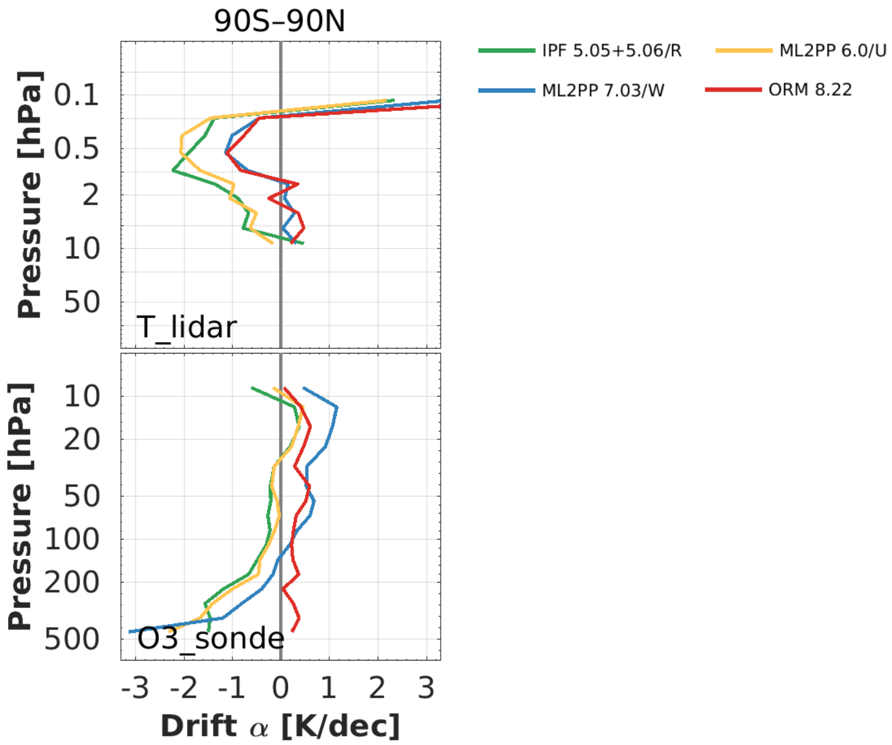

Figure 33: Ground-network averaged linear drift (K per decade) during the 2005-2012 period of MIPAS temperature relative to radiosonde (bottom) and lidar (top). Colours represent different versions of the MIPAS operational data product. Positive values indicate that MIPAS T increases relative to correlative data. The shaded areas represent the 95% confidence interval for the drift estimates. This complements Figure 6 in the main report.

VII.1.6 Dispersion and bias

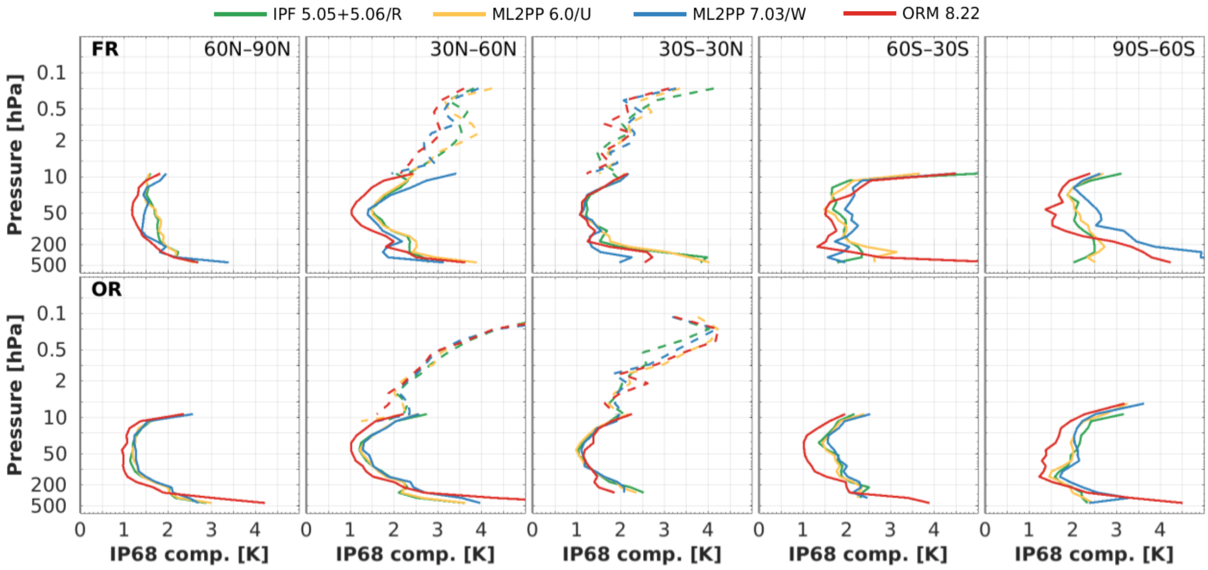

Figure 34: Dependence on MIPAS spectral resolution scanning mode of the spread in the comparisons of MIPAS temperature to lidar (dashed line) and radiosonde (solid line). FR stands for Full Resolution (2002-2004), OR for Optimised Resolution (2005-2012). Colours represent different versions of the MIPAS operational data product. This complements Figure 7 in the main report.

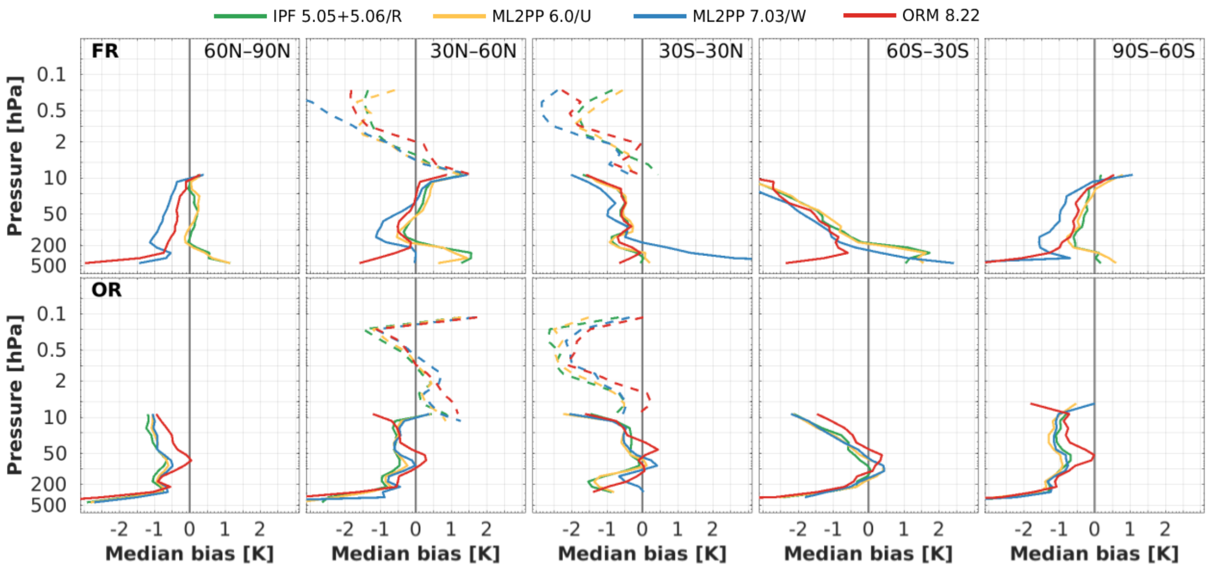

Figure 35: As in Figure 34, but for the median of the absolute differences. Positive values indicate that MIPAS retrievals overestimate correlative measurements. This complements Figure 8 in the main report.

VII.2 Altitude

VII.2.1 Seasonal cycle

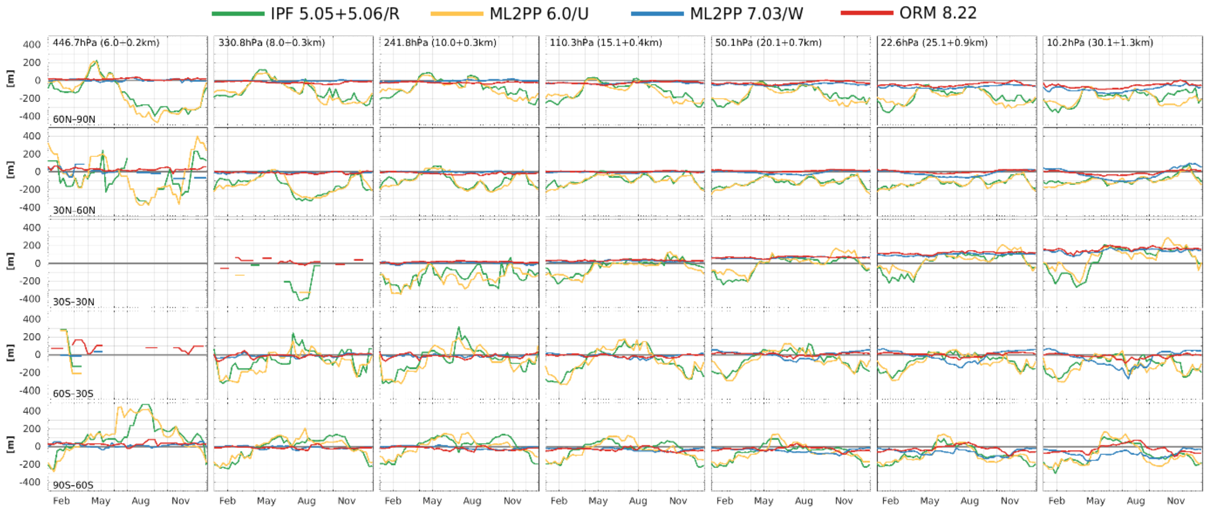

Figure 36: Seasonal dependence of the absolute difference of co-located MIPAS and radiosonde altitude profiles in different latitude zones and at different pressure levels. Colours represent different versions of the MIPAS operational data product. Curves show the median value in one-month moving windows. Positive values indicate too high MIPAS altitude relative to correlative data. This complements Figure 10 in the main report.

VII.2.2 Seasonal cycle : change w.r.t. MIPAS V7

This section shows time series of

$$(z_{\mathrm{MIPAS\_VX}} - z_{\mathrm{GROUNDBASED}}) - (z_{\mathrm{MIPAS\_V7}} - z_{\mathrm{GROUNDBASED}}),$$

where VX can be V5, V6 or V8.

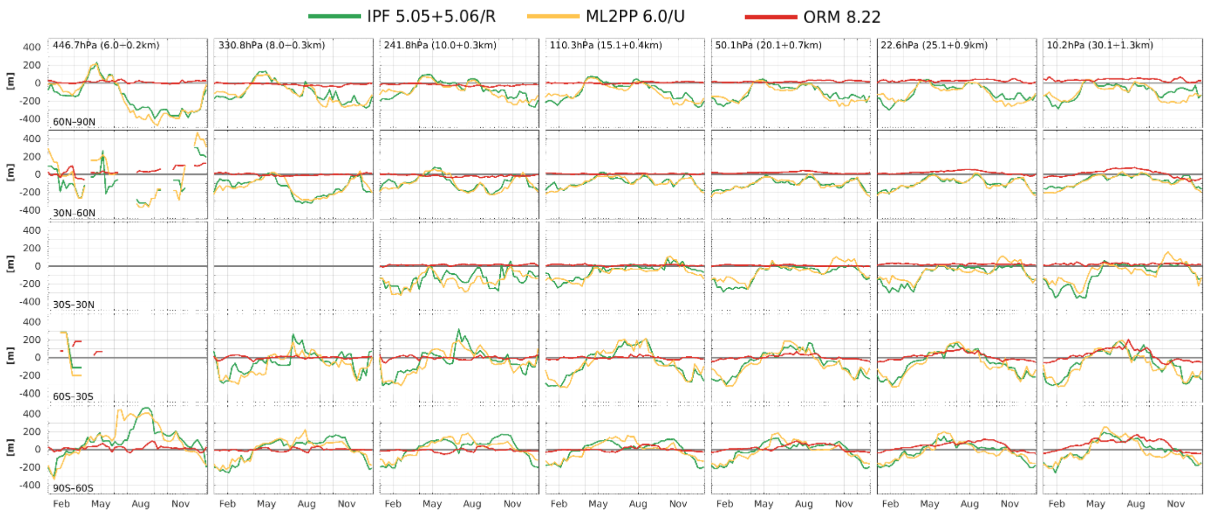

Figure 37: Difference between MIPAS minus radiosonde altitude comparison annual cycle for V5, V6 and V8 versus the comparison annual cycle of MIPAS V7 (see Figure 36).

VII.2.3 Time series

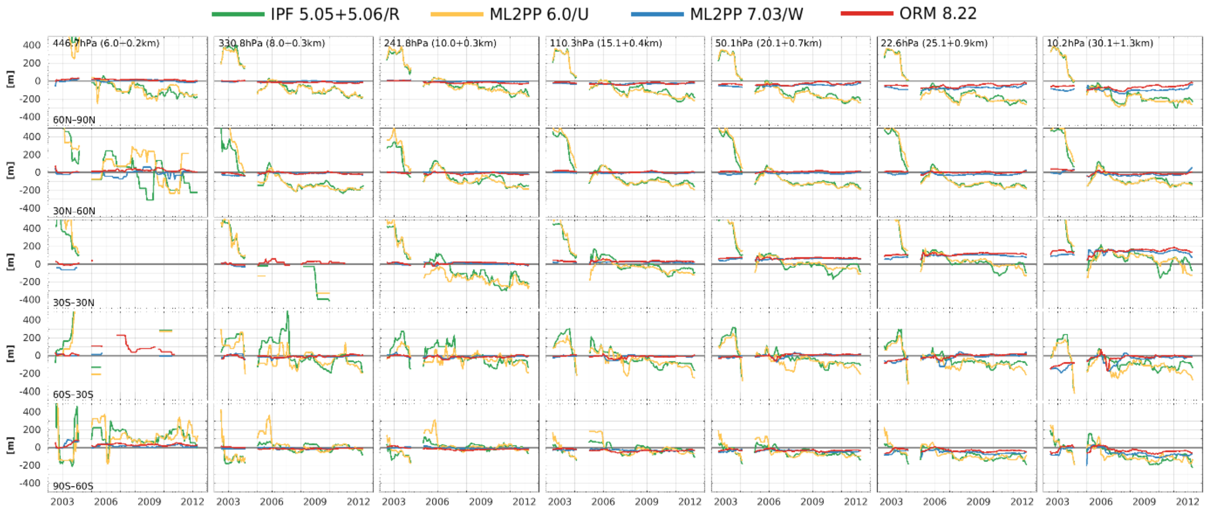

Figure 38: Absolute difference time series of co-located MIPAS and radiosonde altitude profiles in different latitude zones and at different pressure levels. Colours represent different versions of the MIPAS operational data product. Curves show the median value in 12-month moving windows. Positive values indicate too high MIPAS altitude relative to correlative data. This complements Figure 9 in the main report.

VII.2.4 Time series : change w.r.t. MIPAS V7

This section shows time series of

$$(z_{MIPAS\_VX} - z_{GROUNDBASED}) - (z_{MIPAS\_V7} - z_{GROUNDBASED}),$$

where VX can be V5, V6 or V8.

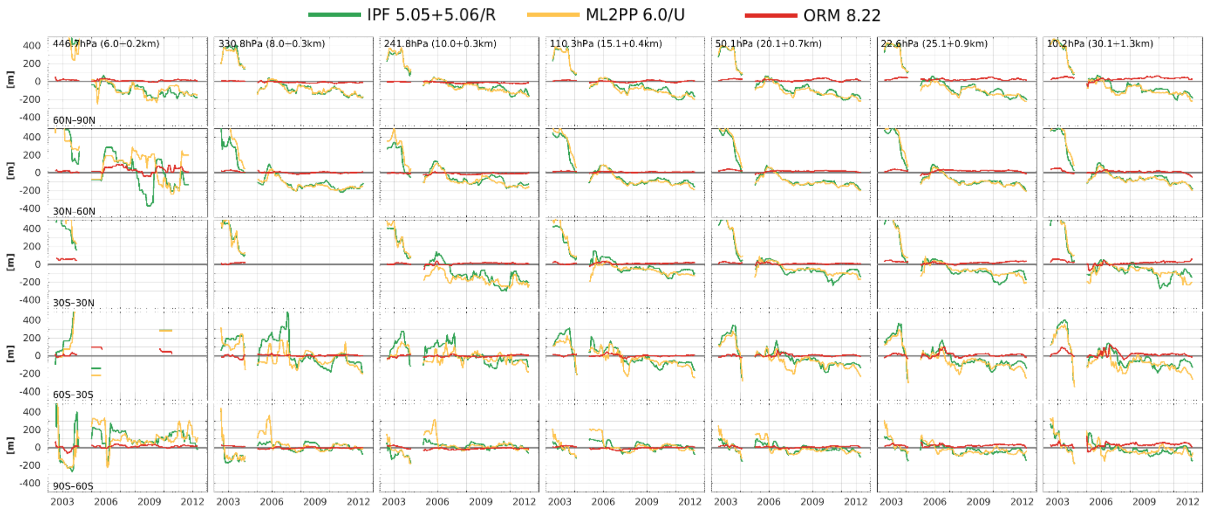

Figure 39: Difference between MIPAS minus radiosonde altitude comparison time series for V5, V6 and V8 versus the comparison time series of MIPAS V7 (see Figure 38).

VII.2.5 Dispersion and bias

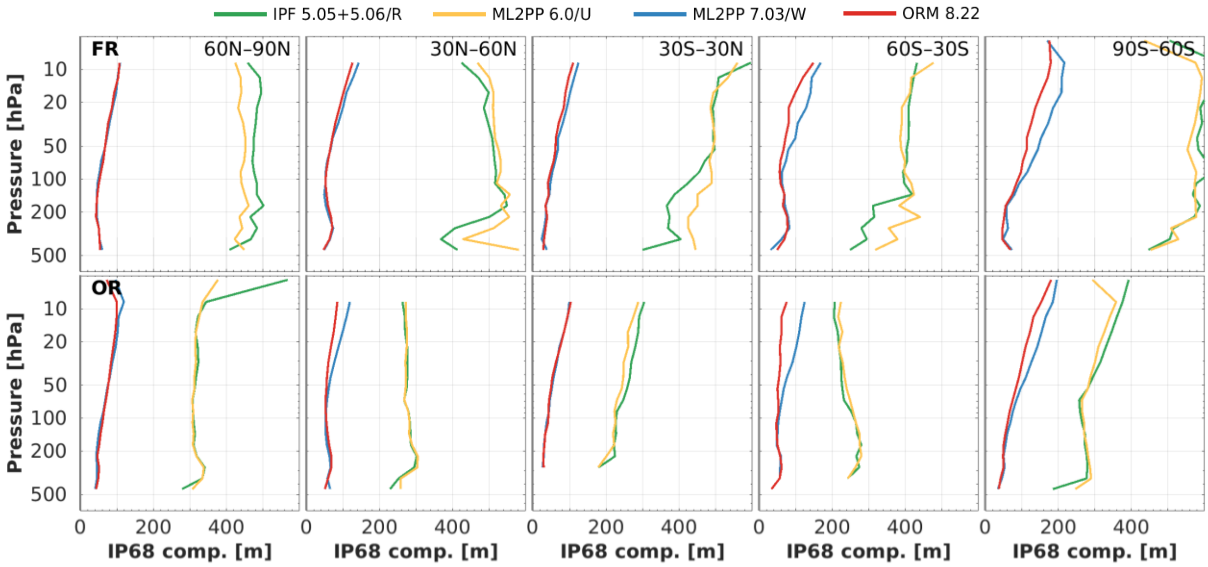

Figure 40: Dependence on MIPAS spectral resolution scanning mode of the spread in the comparisons of MIPAS altitude to radiosonde. FR stands for Full Resolution (2002-2004), OR for Optimised Resolution (2005-2012). Colours represent different versions of the MIPAS operational data product. This complements Figure 11 in the main report.

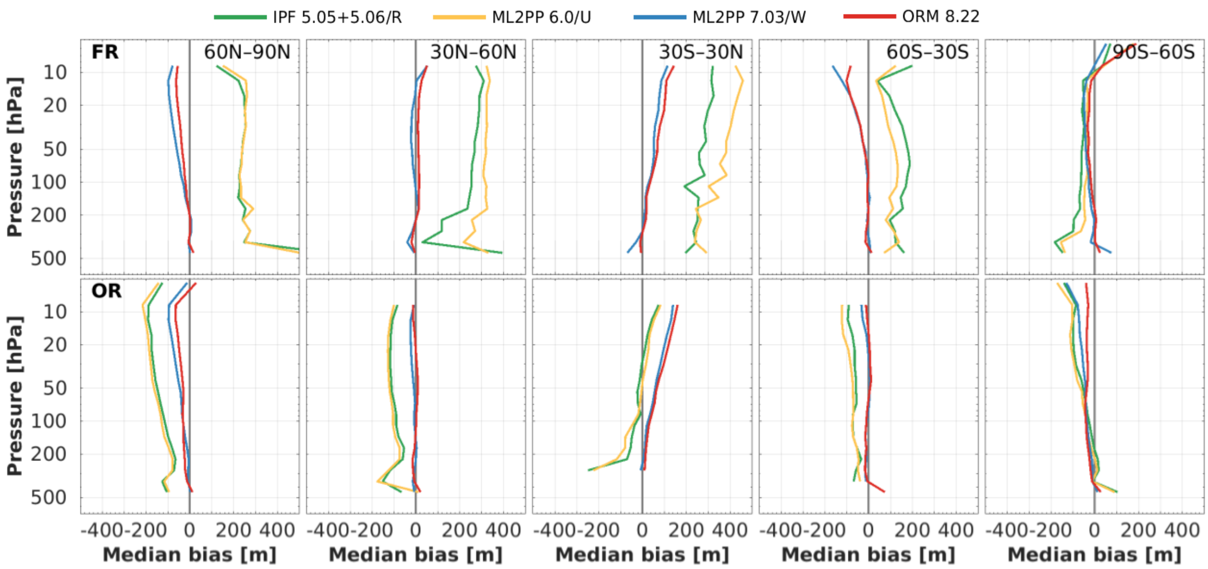

Figure 41: As in Figure 40, but for the median of the absolute differences. Positive values indicate that MIPAS retrievals overestimate correlative measurements. This complements Figure 12 in the main report.

VII.3 Ozone

VII.3.1 Seasonal cycle

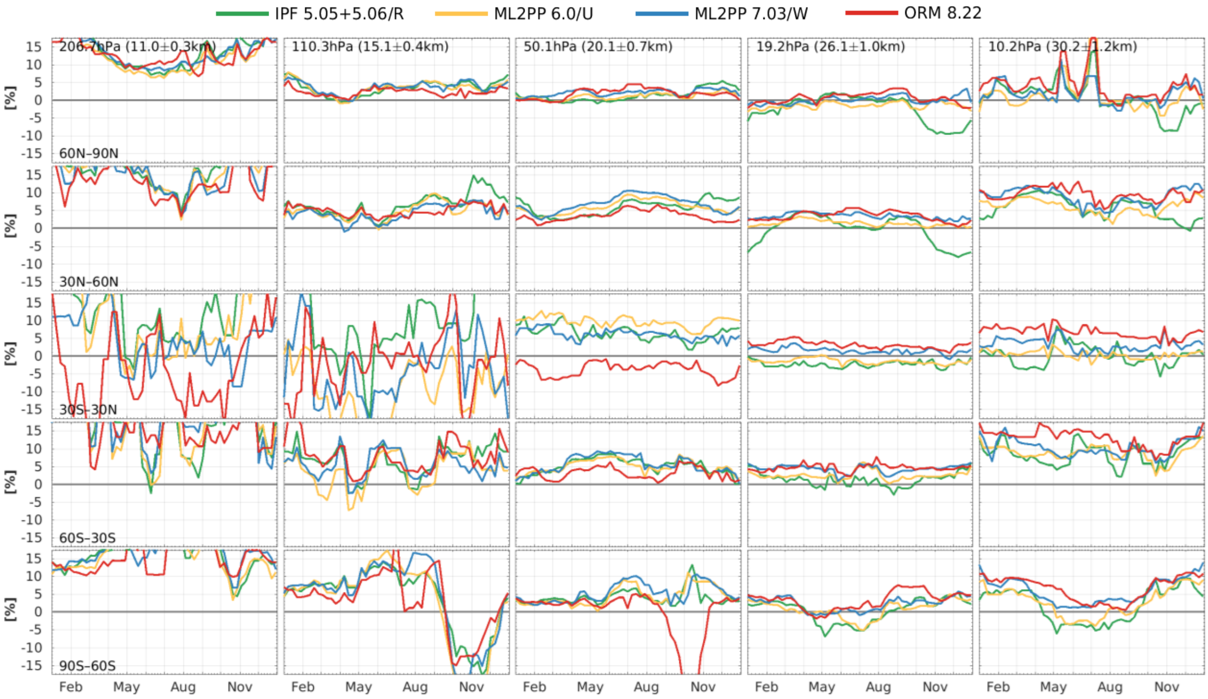

Figure 42: Seasonal dependence of the relative difference of co-located MIPAS and ozonesonde ozone profiles in different latitude zones and at different pressure levels. Colours represent different versions of the MIPAS operational data product. Curves show the median value in one-month moving windows. Positive values indicate too high MIPAS ozone relative to correlative data. This complements Figure 16 in the main report.

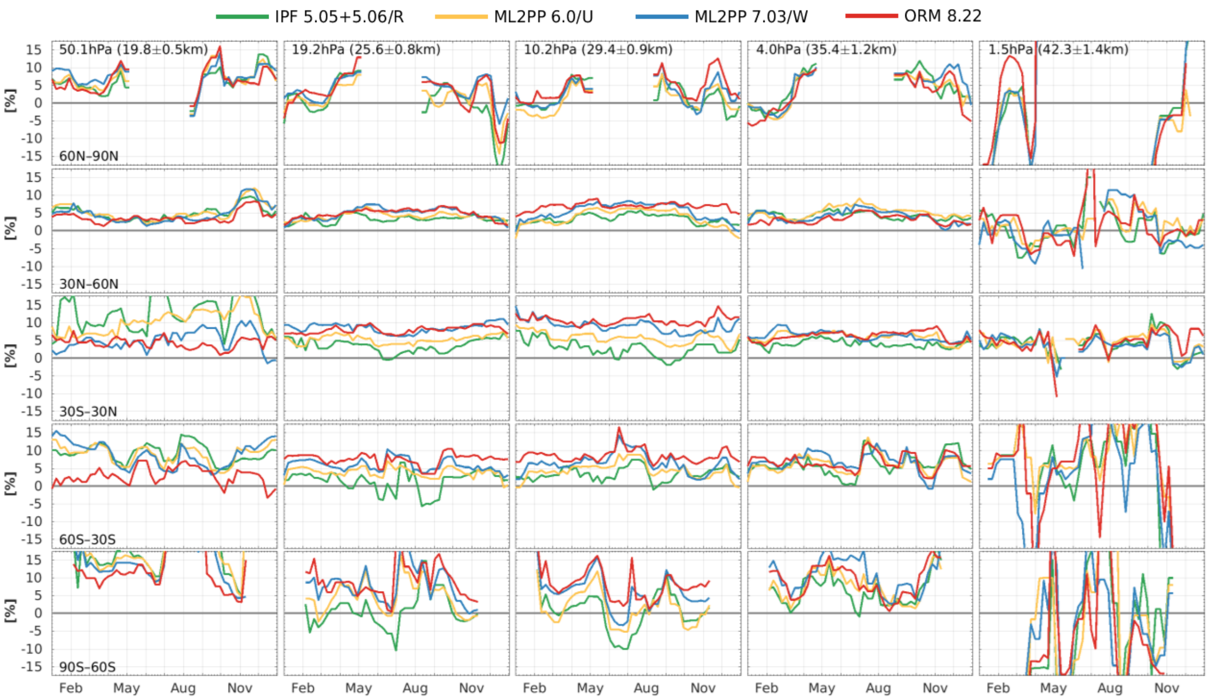

Figure 43: As in Figure 42, but for the comparisons to ozone lidar. This complements Figure 17 in the main report.

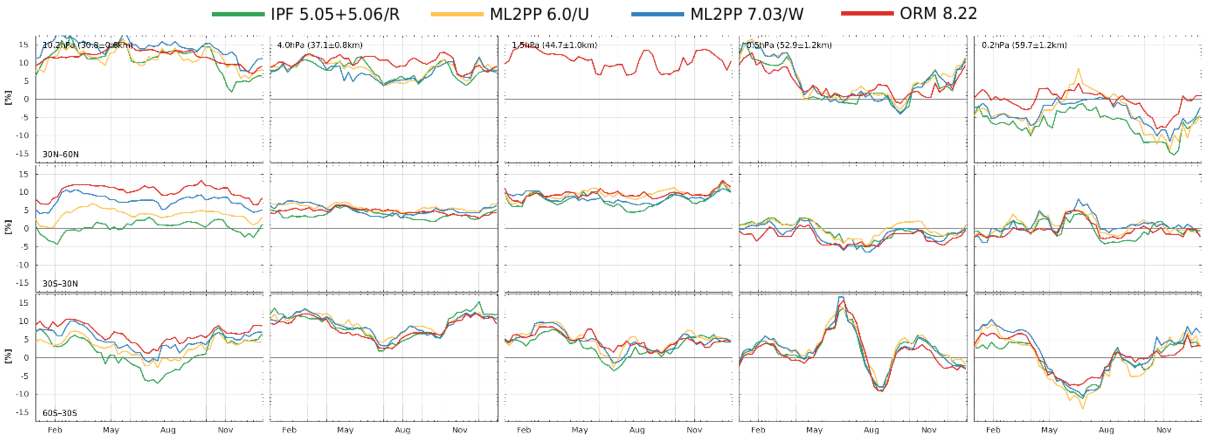

Figure 44: As in Figure 42, but for the comparisons to ozone microwave radiometer. This complements Figure 18 in the main report.

VII.3.2 Seasonal cycle : change w.r.t. MIPAS V7

This section shows time series of

$$(O3_{MIPAS\_VX} - O3_{GROUNDBASED})/O3_{GROUNDBASED} - (O3_{MIPAS\_V7} - O3_{GROUNDBASED})/O3_{GROUNDBASED},$$

where VX can be V5, V6 or V8.

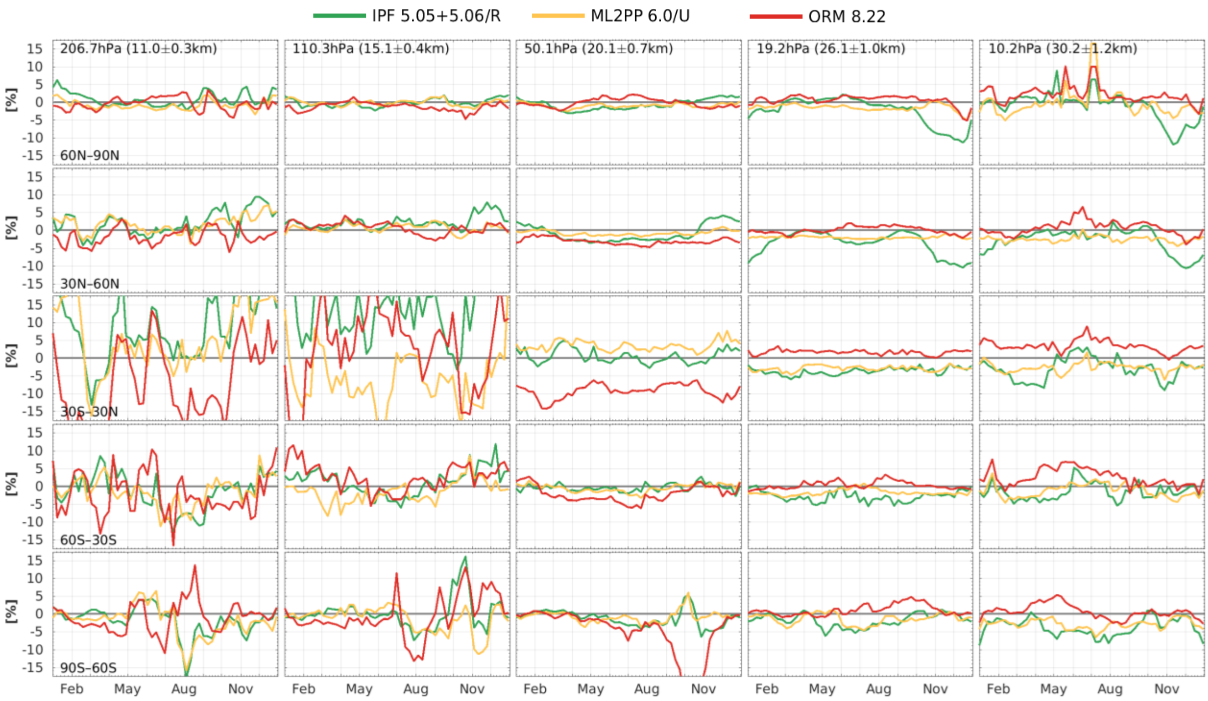

Figure 45: Difference between MIPAS minus ozonesonde ozone comparison annual cycle for V5, V6 and V8 versus the comparison annual cycle of MIPAS V7 (see Figure 42).

Figure 46: As in Figure 45, but for the comparisons to ozone lidar.

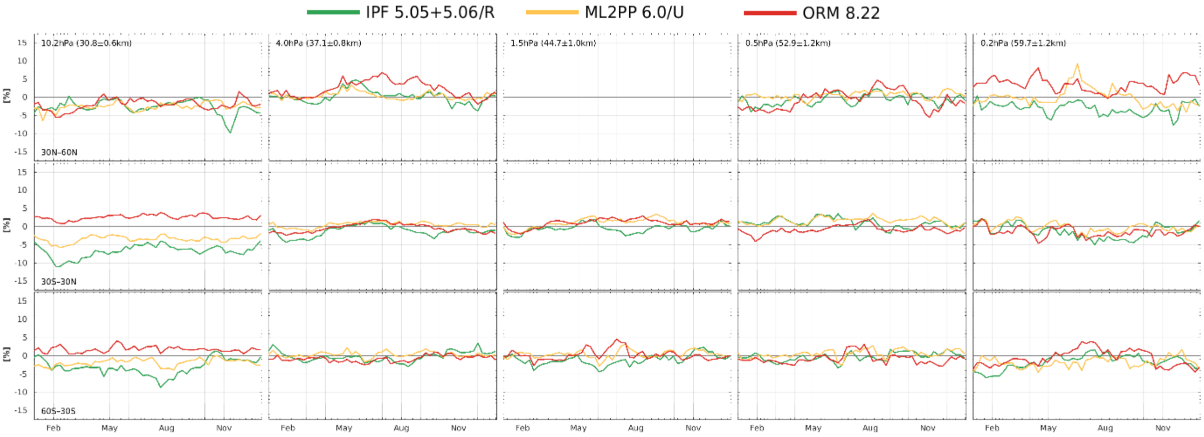

Figure 47: As in Figure 45, but for the comparisons to ozone microwave radiometer.

VII.3.3 Time series

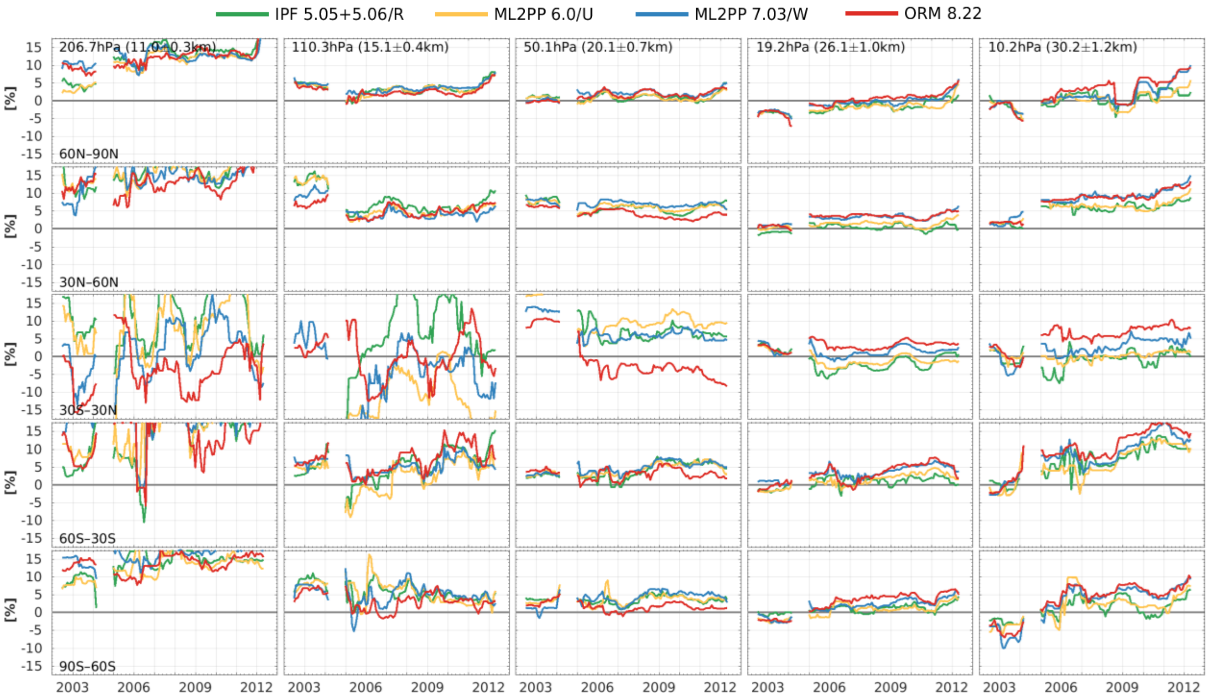

Figure 48: Relative difference time series of co-located MIPAS and ozonesonde ozone profiles in different latitude zones and at different pressure levels. Colours represent different versions of the MIPAS operational data product. Curves show the median value in 12-month moving windows. Positive values indicate too high MIPAS ozone relative to correlative data. This complements Figure 13 in the main report.

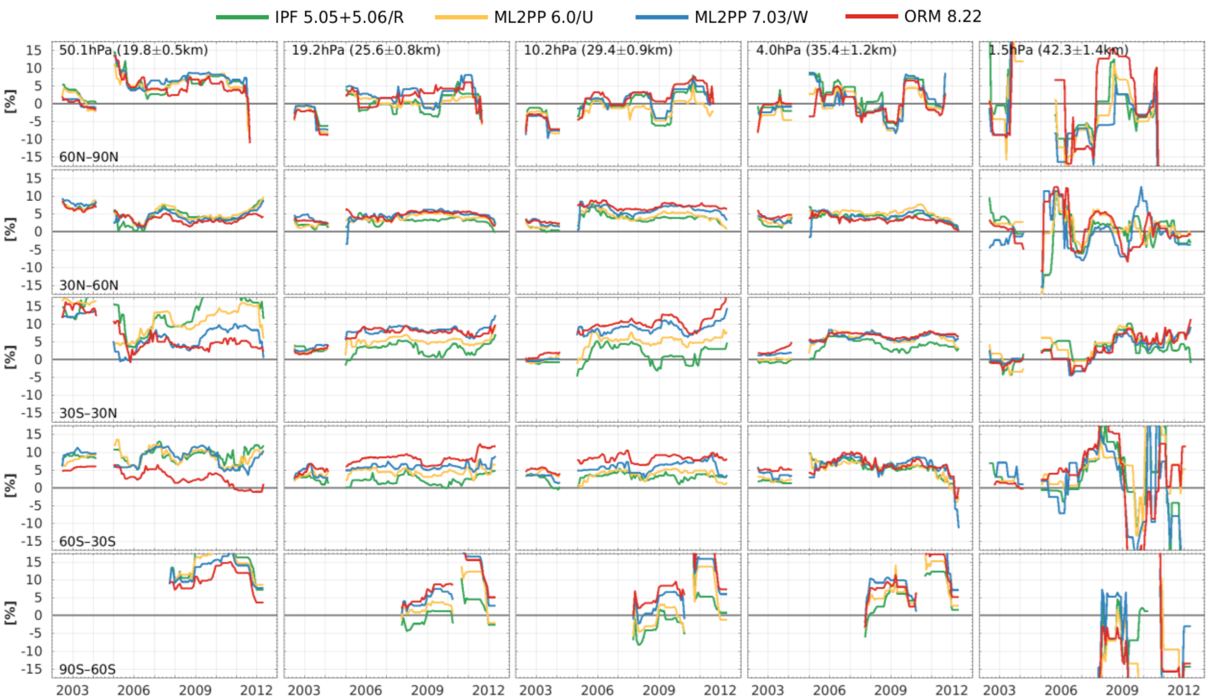

Figure 49: As in Figure 48, but for the comparisons to ozone lidar. This complements Figure 14 in the main report.

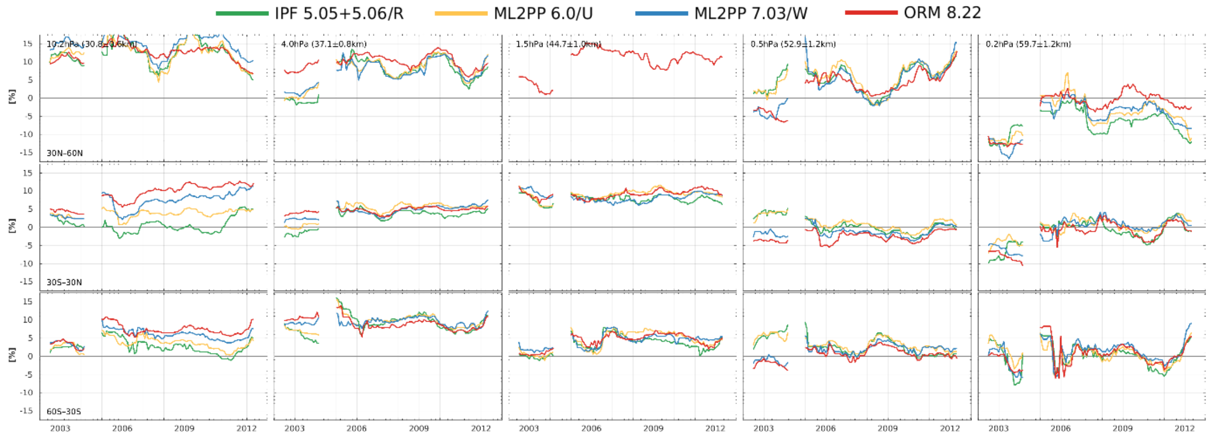

Figure 50: As in Figure 48, but for the comparisons to ozone microwave radiometer. This complements Figure 15 in the main report.

VII.3.4 Time series : change w.r.t. MIPAS V7

This section shows time series of

$$(O3_{MIPAS\_VX} - O3_{GROUNDBASED})/O3_{GROUNDBASED} - (O3_{MIPAS\_V7} - O3_{GROUNDBASED})/O3_{GROUNDBASED},$$

where VX can be V5, V6 or V8.

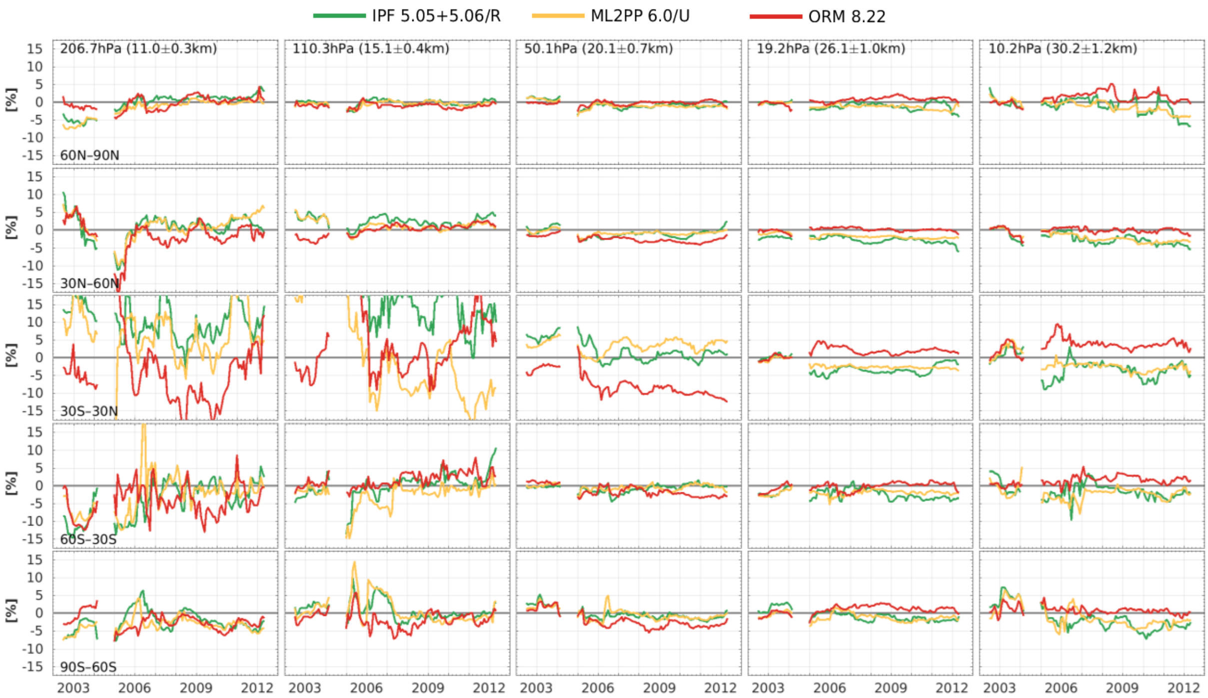

Figure 51: Difference between MIPAS minus ozonesonde ozone comparison time series for V5, V6 and V8 versus the comparison time series of MIPAS V7 (see Figure 48).

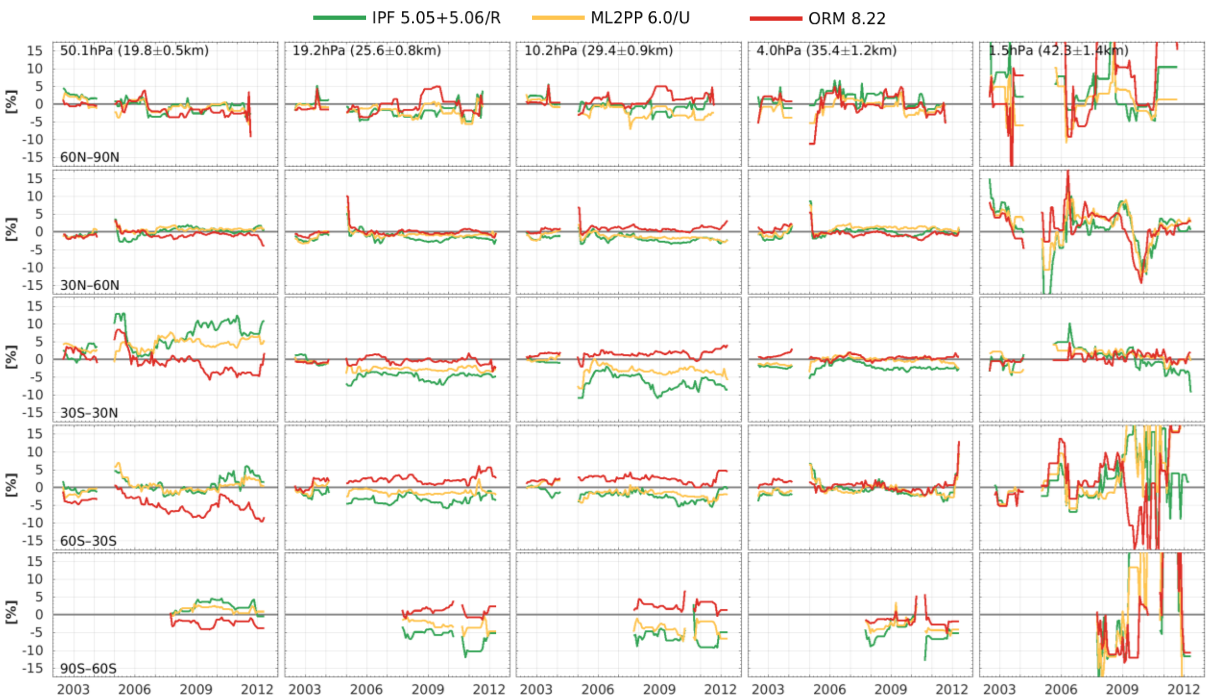

Figure 52: As in Figure 51, but for the comparisons to ozone lidar.

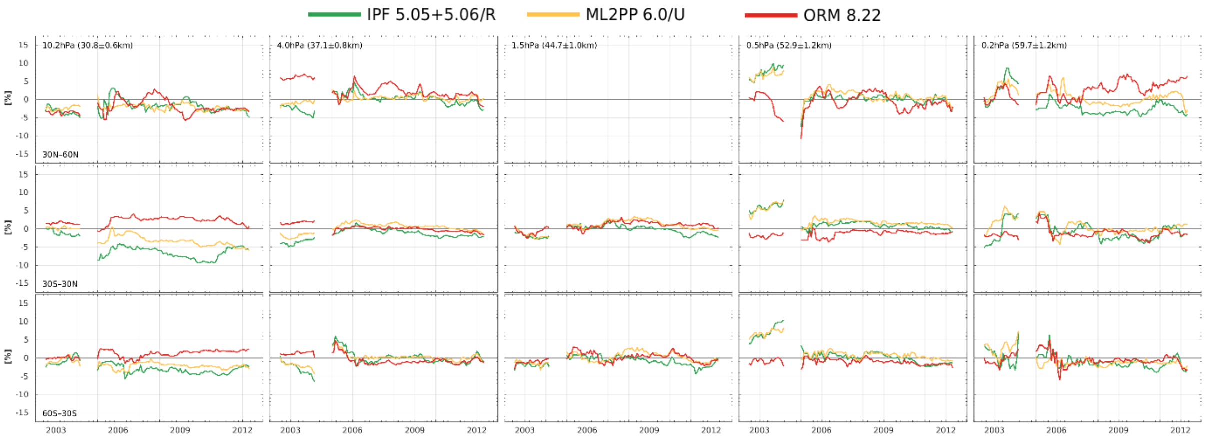

Figure 53: As in Figure 51, but for the comparisons to ozone microwave radiometer.

VII.3.5 Long-term drift

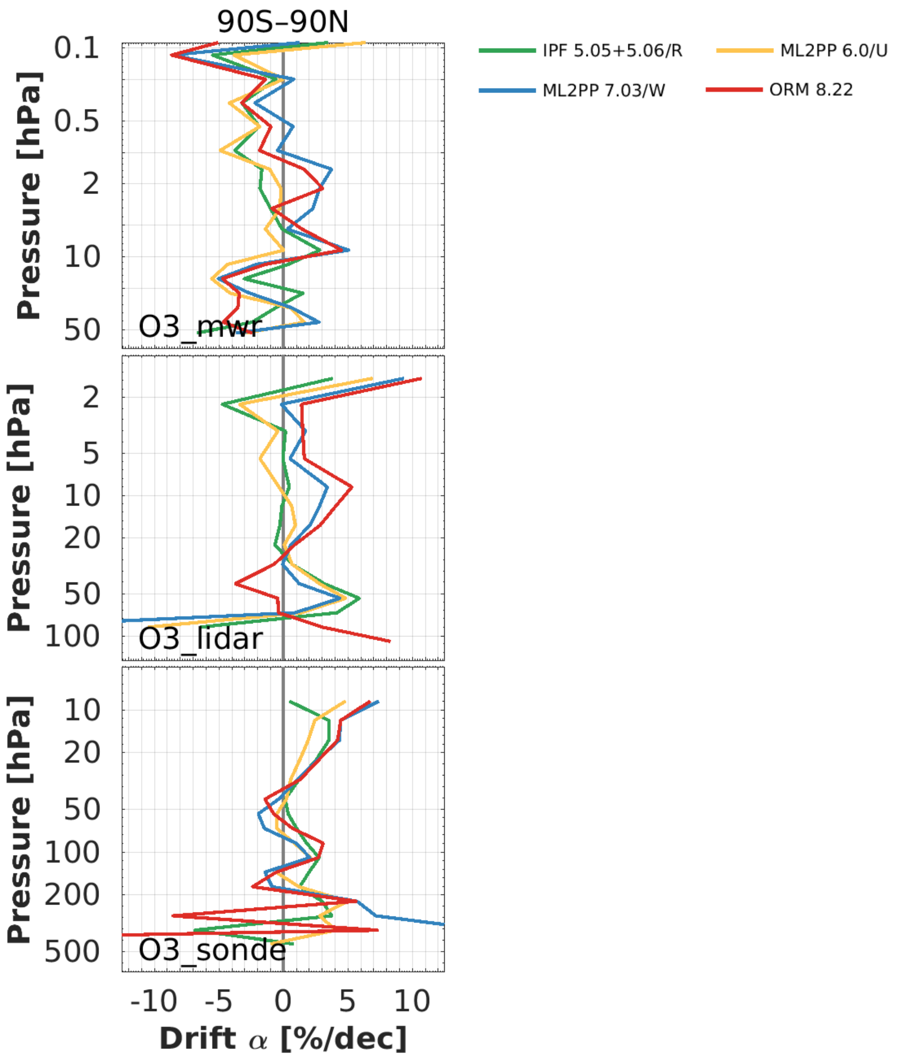

Figure 54: Ground-network averaged linear drift (% per decade) during the 2005-2012 period of MIPAS ozone relative to ozonesonde (bottom), lidar (centre) and microwave radiometer (top). Colours represent different versions of the MIPAS operational data product. Positive values indicate that MIPAS O3 increases relative to correlative data. The shaded areas represent the 95% confidence interval for the drift estimates. This complements Figure 19 in the main report.

VII.3.6 Dispersion and bias

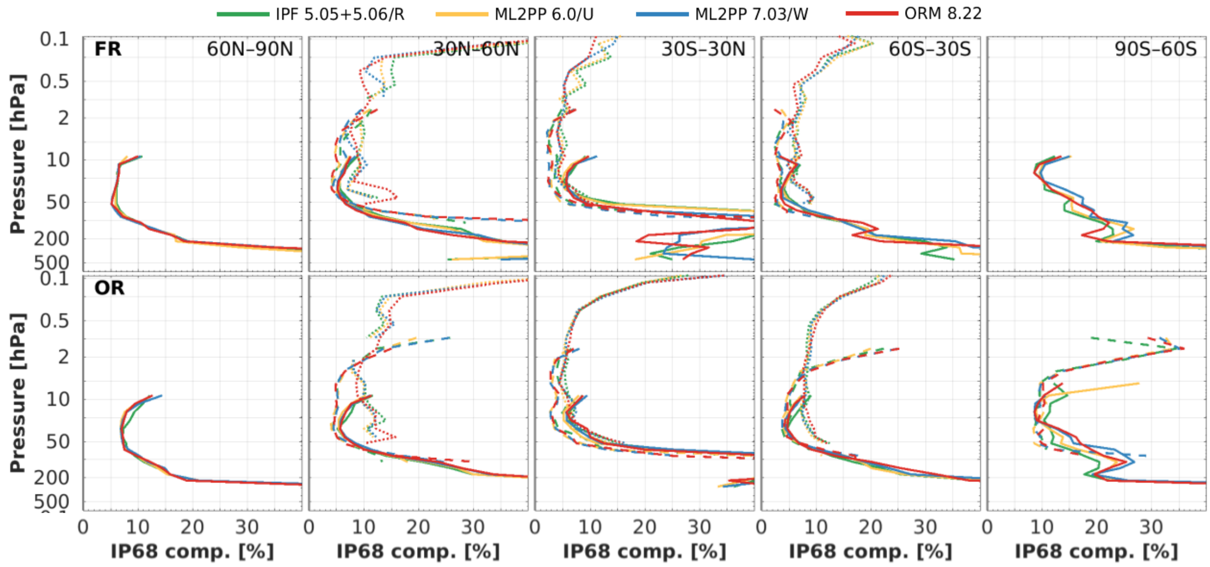

Figure 55: Dependence on MIPAS spectral resolution scanning mode of the spread in the comparisons of MIPAS ozone to microwave radiometer (dash-dotted line), lidar (dashed line) and radiosonde (solid line). FR stands for Full Resolution (2002-2004), OR for Optimised Resolution (2005-2012). Colours represent different versions of the MIPAS operational data product. This complements Figure 20 in the main report.

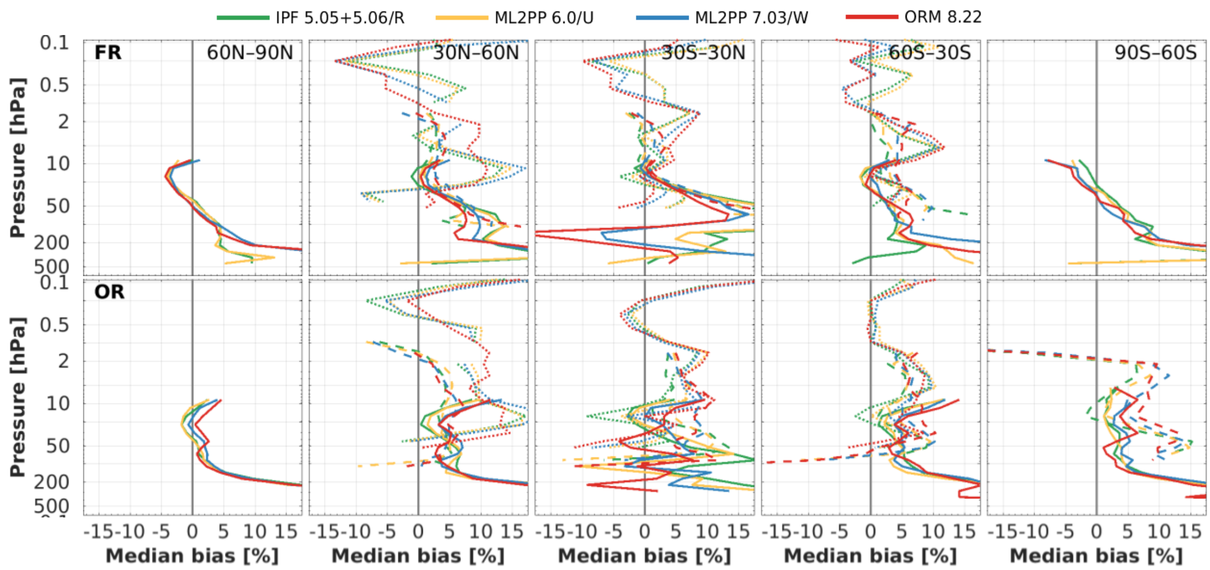

Figure 56: As in Figure 55, but for the median of the absolute differences. Positive values indicate that MIPAS retrievals overestimate correlative measurements. This complements Figure 21 in the main report.